

1 Ecological facilitation hinders adaptation to climate change in a  
2 stressful environment

3 Raphaël Scherrer<sup>1,\*</sup>, Megan Korte<sup>1,2</sup>, G. Sander van Doorn<sup>1</sup>, and Rampal S. Etienne<sup>1</sup>

4 <sup>1</sup>Groningen Institute for Evolutionary Life Sciences, University of Groningen, Groningen, the  
5 Netherlands

6 <sup>2</sup>Center for Conservation Biology, University of California, Riverside, California, USA

7 \*Corresponding author: raphael.scherrer@evobio.eu

8 **Abstract**

9 Many plants, in (semi-)arid ecosystems in particular, rely on so-called nurse plants for  
10 protection and growth, in a species interaction called ecological facilitation. However, it  
11 is not clear whether facilitation will protect the facilitated plant from extinction if the  
12 environmental conditions change, for example due to climate change. Here, we use an  
13 evolutionary model to study the impact of ecological facilitation on the adaptive potential  
14 of an annual plant facilitated by nurse shrubs under a changing climate, specifically, when  
15 the landscape becomes more arid. We find that two alternative strategies can arise: a stress-  
16 tolerant strategy, capable of surviving outside the facilitated patches as well as underneath  
17 shrubs, but at a fecundity cost; and a stress-sensitive strategy, with a higher reproductive  
18 output but confined to the facilitated patches. Under some conditions, these two strategies  
19 can coexist. The presence of the stress-tolerant strategy is key to preventing extinction  
20 when the climate causes more stress (drought). By running three different climate change  
21 scenarios (stress increase under the shrubs, whole-landscape deterioration and shrub-cover  
22 shrinkage), we find that a trade-off between fecundity and stress tolerance usually traps  
23 an initially stress-sensitive population into staying sensitive even as the facilitated patches  
24 recede under climate change. The population then continues to rely on facilitation, and  
25 is unable to evolve stress tolerance before it is too late and extinction is unavoidable. By  
26 contrast, an increase in stress in the facilitated areas, with or without an increase in stress  
27 outside of the facilitated areas, readily promotes adaptation to increasingly severe aridity.  
28 Thus, persistence of sheltered areas in a patchy landscape may prevent adaptation to the  
29 harsher surroundings, putting the population at risk of extinction in a changing climate.

30 **Keywords** — stress tolerance, evolutionary rescue, extinction, habitat heterogeneity, adaptive dynamics, metapopulation

## 32 **Introduction**

33 Global climate change is threatening to increase the degradation of ecosystems worldwide, and  
34 has far-reaching consequences on populations of organisms, particularly in plant communities  
35 (Franklin et al., 2016). Ecosystems that already endure stressful environmental conditions are  
36 especially susceptible to adverse manifestations of climate change, such as amplification of heat  
37 waves and water shortages in arid and semi-arid regions, which are at high risk of desertification  
38 over the next decades (D'Odorico et al., 2013; Vicente-Serrano et al., 2014). It is thus crucial  
39 to examine the mechanisms promoting community resilience that could alleviate stressors on  
40 plant communities to prevent further decline.

41

42 Interspecific facilitation is a widespread type of ecological interaction in many of the world's  
43 ecosystems, and one particularly known to play a key role in plant community structure. In in-  
44 terspecific facilitation, a nurse or benefactor species (which is adapted to local environmentally  
45 stressful conditions) positively affects a spatially associated beneficiary species (which is then  
46 better able to survive and/or reproduce in this environment; Bruno et al., 2003). This allows  
47 many species to cope with stressful climates where their potential to thrive would otherwise  
48 be seriously impacted (Bertness & Callaway, 1994; Callaway, 2007a, 2007b). For example, the  
49 observation that in some plant communities 90% of the species are found only beneath the  
50 canopies of perennial plants has led authors to propose facilitation as a key force maintaining  
51 biodiversity in those ecosystems (Valiente-Banuet & Verdú, 2007).

52

53 Facilitated patches of vegetation provide buffered microclimates for many populations that  
54 struggle to survive environmental stressors and as such, contribute to environmental heterogene-  
55 ity in harsh habitats (Armas et al., 2008; Pugnaire et al., 2011; Hannah et al., 2014; Suggitt  
56 et al., 2018). This, in turn, can have profound consequences for evolutionary processes and local  
57 adaptation in the beneficiary species (O'Brien et al., 2020), sometimes at the microgeographic  
58 scale (Richardson et al., 2014; O'Brien et al., 2020; Verdú et al., 2021). Typical facilitated  
59 microhabitats are characterized by milder and/or more enriched conditions with respect to  
60 temperature, humidity or nutrients, in contrast to the open landscape (Armas & Pugnaire,  
61 2005; Wright et al., 2005; Prieto et al., 2010). They may also be the theater of more intense  
62 competition (Adler et al., 2018), but that is not necessarily always the case (Raath-Krüger et  
63 al., 2021). By affecting habitat heterogeneity in this way, facilitation in harsh landscapes may  
64 have profound consequences on the eco-evolutionary dynamics of beneficiary species, especially  
65 in the face of a changing climate. How exactly the environmental heterogeneity brought about  
66 by ecological facilitation affects the adaptive potential of the beneficiary populations is less well  
67 understood, however, and the idea that facilitation always positively affects adaptation in the  
68 beneficiary species has been subject to debate.

69

70 The idea that facilitation may foster adaptation comes from several lines of evidence. First,  
71 facilitation can expand the geographical range over which a species can occur and therefore  
72 can give it a head start, in the form of a higher global population size, in the race to avoid  
73 extinction (Bruno et al., 2003; Armas et al., 2011; Soliveres et al., 2011). This was proposed

74 for the alga *Mazzaella laminarioides*, whose establishment probability is increased in harsher  
75 environments at the edge of its range, thanks to benefactor barnacles (Aguilera et al., 2015).  
76 Alternatively, as a form of niche construction, facilitation may play a similar role to phenotypic  
77 plasticity in exposing organisms to environments they would otherwise not experience, setting  
78 up the stage for genetic assimilation and adaptation (Day et al., 2003; Flatt, 2005; Chevin &  
79 Lande, 2011; Laland et al., 2016; Chevin & Hoffmann, 2017). Relaxed selection in sheltered  
80 environments may also contribute to the accumulation of cryptic genetic variation, which may  
81 become adaptive in the context of a changing environment (Gibson & Dworkin, 2004; Badyaev,  
82 2005; Ledón-Rettig et al., 2014; Paaby & Rockman, 2014). Finally, facilitation may promote  
83 survival in the face of a changing climate in the absence of adaptation, by allowing benefi-  
84 ciary species to keep their ancestral niche through associations with benefactor species. This  
85 has been suggested as an explanation for the observation that many mesophilic Tertiary plant  
86 lineages that survived the transition to the drier Quaternary climate are now found in facilita-  
87 tive associations with benefactor xerophilic species in semi-arid and Mediterranean ecosystems  
88 (Valiente-Banuet et al., 2006; Valiente-Banuet & Verdú, 2007; Hampe & Jump, 2011).

89

90 In contrast, facilitation may also hamper adaptation. Gene flow among populations adapted  
91 to different microhabitats in a heterogeneous landscape is known to curb local adaptation, of-  
92 fering one powerful explanation for why species are restricted in space (e.g. García-Ramos and  
93 Kirkpatrick, 1997; Kirkpatrick and Barton, 1997; Lenormand, 2002). Facilitation could play  
94 a similar inhibitory role in the emergence of ecotypes adapted to new, harsher environments  
95 (Liancourt et al., 2012), not only because of maladaptive gene flow but also hybrid rescue (which  
96 would prevent the full divergence and speciation of a new ecotype by providing shelter to oth-  
97 erwise maladapted hybrids). Furthermore, adaptation to harsh habitats is restricted by the  
98 amount of genetic variation for adaptive traits (Lande & Shannon, 1996; Barton, 2001; Tufto,  
99 2001; Gilbert & Whitlock, 2017), and new adaptive alleles are unlikely to arise in marginal  
100 habitats with low population densities (Orr & Unckless, 2008). Moreover, harsh environments  
101 close to the limits of the fundamental niche of a species (demographic ‘sinks’) are thought to  
102 be notoriously difficult to adapt to, because the strength of selection is lower where fitness (and  
103 density) is lower (Brown & Pavlovic, 1992; Holt & Gaines, 1992; Kawecki, 1995; Kawecki &  
104 Holt, 2002; Holt et al., 2003).

105

106 A resolution of the debate about the role of facilitation in adaptation may be aided by  
107 turning to the general theoretical literature on local adaptation in heterogeneous landscapes  
108 (Holt, 2003; Kawecki, 2004; Holt et al., 2005; Bridle & Vines, 2007; Kawecki, 2008; Holt &  
109 Barfield, 2011; Angert et al., 2020). This literature is vast and has shown that adaptation is  
110 complicated by many factors, such as stochastic effects in small demes (Glémén et al., 2003;  
111 Alleaume-Benharira et al., 2006; Lopez et al., 2009; Bridle et al., 2010; Polechová, 2018), the  
112 type of density regulation (Holt, 1996, 1997; Gomulkiewicz et al., 1999; Filin et al., 2008),  
113 species interactions (Case & Taper, 2000; Tufto, 2001; Gandon & Michalakis, 2002; Nuismer  
114 & Kirkpatrick, 2003; Case et al., 2005; Nuismer, 2006; García-Ramos & Huang, 2013; Urban  
115 et al., 2019), phenotypic plasticity (Sasaki & de Jong, 1999; Chevin & Lande, 2011), the genetic

116 architecture of adaptive traits (Kawecki, 2000; Kimbrell & Holt, 2007; Schiffrers et al., 2014;  
117 Gilbert & Whitlock, 2017) or dispersal (Ronce & Kirkpatrick, 2001; Kawecki, 2003; Aguilée  
118 et al., 2016). How populations living in such landscapes will, on top of that, respond to a  
119 progressive deterioration of their environment, may be even more difficult to predict.

120

121 There has been an appreciation in the past two decades that eco-evolutionary dynamics can  
122 unfold on short, ecological time scales (Kinnison & Hairston, 2007; Hendry, 2017), thus begging  
123 the question of the potential of natural populations for evolutionary rescue (the phenomenon  
124 by which a population or species avoids extinction through genetic adaptation, Kinnison and  
125 Hairston, 2007; Bell and Collins, 2008; Gonzalez et al., 2013; Bell, 2017) in the face of climate  
126 change. Earlier work focusing on simple scenarios of environmental change highlighted the now  
127 well-accepted roles of genetic variation, speed of environmental change, population size and  
128 stochastic demographic effects in adaptation to a changing climate (Levins, 1974; Pease et al.,  
129 1989; Holt, 1990; Bürger & Lynch, 1995; Gomulkiewicz & Holt, 1995; Boulding & Hay, 2001;  
130 Gomulkiewicz & Houle, 2009; Willi & Hoffmann, 2009; Holt & Barfield, 2011; Arenas et al.,  
131 2012; Polechová & Barton, 2015). Moreover, theoretical models have confirmed that many of  
132 the factors influencing local adaptation should also impact evolutionary rescue, such as genetic  
133 architecture (Orr & Unckless, 2008; Gomulkiewicz et al., 2010; Duputié et al., 2012; Schif-  
134 fers et al., 2014), recombination (Uecker & Hermisson, 2016), dispersal (Alfaro et al., 2017) or  
135 species interactions (Case & Taper, 2000; Mellard et al., 2015). Yet, most of the studies done  
136 so far do not consider adaptation to a changing climate in conjunction with a population that  
137 already inhabits a heterogeneous landscape, such as a plant community subject to interspecific  
138 ecological facilitation.

139

140 Here, we aim to address this gap with a theoretical study of adaptation to climate change  
141 in a facilitated sessile species living in a stressful, heterogeneous environment, with (facilitated)  
142 sheltered and (unfacilitated) hostile patches, as the conditions in this environment deteriorate.  
143 Our study is inspired by the case of *Brachypodium distachyon*, an annual grass species found in  
144 semi-arid ecosystems across the Mediterranean basin, and often found in natural populations in  
145 a facilitative association with nurse shrubs, underneath which *B. distachyon* plants are found to  
146 be taller and have higher seed production than grasses growing in the open landscape (Korte et  
147 al., 2025). These phenotypic differences between plants growing in facilitated and unfacilitated  
148 environments were also found to be retained over several generations in greenhouse experiments  
149 (Korte, 2024), indicating that nurse shrubs do affect fitness traits in spatially associated *B. dis-*  
150 *tachyon* and could play a role in local adaptation in this species. While our modeling is inspired  
151 by plants, the results of our study could in principle extend more generally to other organisms  
152 experiencing ecological facilitation, as long as they are sessile (e.g. in marine systems, Bulleri,  
153 2009, or soil mycorrhizal networks, van der Heijden and Horton, 2009).

154

155 We developed a model where our focal species lives and evolves in a heterogeneous landscape  
156 composed of facilitated and unfacilitated patches (mimicking a semi-arid ecosystem with areas  
157 covered by nurse shrubs and open landscape). Note that unfacilitated patches are not just

158 another niche in this landscape, where fitness can be optimized to the same level as in the  
159 facilitated patches through some locally optimum phenotype. Instead, the conditions in the  
160 harsh matrix outside of the shrubs are inherently limiting and close to the physiological limits  
161 of the organism (similar to sinks *sensu* Kawecki, 2008; Chevin and Hoffmann, 2017). Survival in  
162 these patches requires (genetically determined) investment in stress tolerance, which comes at  
163 a fecundity cost, and the carrying capacity (i.e. the population density that can be sustained)  
164 is low compared to the less limiting facilitated patches, for an area of the same surface. Using a  
165 combination of individual-based simulations and adaptive dynamics analyses (Metz et al., 1992;  
166 Metz et al., 1996; Geritz et al., 1998), we study the eco-evolutionary dynamics and equilibrium  
167 states reached by our facilitated population in such a landscape, as well as its resilience and  
168 potential for adaptation to different scenarios of habitat deterioration driven by climate change.  
169 We expand our results to different numbers of heterogeneous demes in a metapopulation setting,  
170 and to various levels of outcrossing (an important modulator of the effects of recombination in  
171 annual plants, Pannell, 2016) versus selfing (i.e. self-fertilization).

172 **Methods**

173 **The model**

174 We consider a landscape consisting of  $n_D$  demes, or *sites*, each containing two habitat *patches*  
175 (Fig. 1A) — a facilitated patch (F), and an unfacilitated patch (UF). The facilitated patch  
176 represents the total area of the site that is covered by nurse shrubs. The unfacilitated patch  
177 represents the area that is not protected. Although facilitated patches would typically corre-  
178 spond to individual shrubs in a semi-arid landscape and therefore be patchy, here we clumped  
179 all shrubs together within each site. We assume this is a reasonable simplification, reflecting  
180 that shrub locations may be labile on an evolutionary time scale, and may be more accurately  
181 described as a general cover that applies to the whole site. Hence, each site  $k$  is characterized  
182 by its fractional cover  $c_k$  in facilitated patches (the area of the site that is unfacilitated is  $1 - c_k$ ).  
183

184 A population of individual grasses dwells in this landscape. Every generation, each adult  
185 plant produces a number of seeds, or offspring, sampled from a Poisson distribution with a  
186 mean that is equal to the expected reproductive output of that parent plant. The reproductive  
187 output of a plant is a function of its stress tolerance, which may be regarded as its resistance to  
188 aridity, and of local density dependence arising from competition with other plants living in the  
189 same local patch. For a plant living in patch  $j$  (UF or F) of deme  $k$  and with stress tolerance  
190 level  $x$ , we assume that this reproductive output is given by

$$r_{jk}(x) = \exp \left[ y(x) \left( 1 - \frac{N_{jk}}{C_{jk} K_j} \right) \right] \quad (1)$$

191 where  $N_{jk}$  is the number of plants in patch  $j$  of site  $k$ ,  $C_{jk}$  is the shrub cover in that patch  
192 (equal to  $c_k$  if  $j = F$  and  $1 - c_k$  if  $j = UF$ ),  $K_j$  is the per-area carrying capacity of patch  $j$  (the  
193 same across all demes, as it roughly represents the number of individuals that a given surface  
194 of bare or covered soil can sustain), and  $y$  is the fecundity, given by

$$y(x) = r_{\max} - \epsilon x (x/x_{\max})^{\nu-1} \quad (2)$$

195 where  $r_{\max}$  is the maximum achievable population growth rate,  $x_{\max}$  is the maximum achievable  
196 stress tolerance level,  $\epsilon$  is a trade-off parameter incurring a fecundity cost to higher stress  
197 tolerance, and  $\nu$  is a non-linearity parameter modifying the shape (convex for  $\nu < 1$ , linear  
198 for  $\nu = 1$  or concave for  $\nu > 1$ ) of the trade-off relationship between stress tolerance and  
199 fecundity (Fig. 1B) — an aspect which may have important consequences on the dynamics of  
200 an evolving system under selection (e.g. de Mazancourt and Dieckmann, 2004). Note here that  
201 stress tolerance  $x$  not only affects the (density-independent) fecundity  $y(x)$ , it also indirectly  
202 affects the density-dependent part of the reproductive output  $r_{jk}(x)$  because of its effect on the  
203 number of individuals,  $N_{jk}$ , able to coexist given the local carrying capacity.

204 **Fertilization** Many plants can self-pollinate as well as outcross. In the annual grass *Brachypodium*  
205 *distachyon*, for example, the rate of outcrossing is thought to be about 5% (Vogel et al., 2009).  
206 In the model, each seed produced by an adult plant can either result from fertilization by pollen

207 from another plant with outcrossing probability  $g$ , or from selfing, with probability  $1-g$ . If a seed  
 208 is the result of outcrossing, one plant is chosen at random from the entire population (i.e. from  
 209 any deme) to be the provider of the fertilizing pollen grain (all plants being hermaphrodites).  
 210 This reflects the assumption that pollen is small enough that long-range dispersal is readily  
 211 achieved.

212 **Dispersal** Once fully formed, each seed can disperse to another site with probability  $m$ ,  
 213 the migration rate (Fig. 1A). Within a site, each seed lands into a patch with probability  
 214 proportional to the surface of that patch in that site ( $c_k$  for F or  $1 - c_k$  for UF). This free  
 215 dispersal of seeds within sites, but not between sites, reflects the assumption that seeds are  
 216 more likely to land meters away from their parent plant (possibly in a different microhabitat),  
 217 while long-range dispersal to far away sites is less likely (Korte, 2024).

218 **Germination** Upon landing, the survival and successful germination of each seedling is sam-  
 219 pled with a probability that depends on the level of stress tolerance  $x$  of that seedling, relative  
 220 to the intensity of the stress it encounters in its local patch. The survival probability of a  
 221 seedling in patch  $j$  and in site  $k$  is assumed to be given by the decreasing sigmoid function,

$$s_{jk}(x) = \frac{1}{1 + \exp[a(\theta_{jk} - x)]} \quad (3)$$

222 in which the probability of survival decays from one to zero as the stress level of the environment  
 223  $\theta_{jk}$  increases relative to the tolerance level  $x$  of the plant,  $a$  being the magnitude of the downward  
 224 slope of the sigmoid at its inflection point (where  $\theta_{jk} = x$  in Fig. 1C). This means that stress  
 225 tolerance  $x$  must be somewhat larger than environmental stress  $\theta_{jk}$  for the seedling to have  
 226 somewhat decent chances of survival (Fig. 1C).

227 **Genetics** Stress tolerance is encoded by a number of separate loci in the genome. We assume  
 228 that each plant has a haploid genome consisting of  $n_L = 100$  loci, uniformly distributed along a  
 229 single chromosome (the genomic position of each locus is the same for all individuals, and is ran-  
 230 domly sampled at the start of a simulation). Within an individual, each locus can harbor either  
 231 of two alternative alleles, a *stress-sensitive* allele (0) and a *stress-tolerant* allele (1) (Fig. 1D).  
 232 The level of tolerance (i.e. the phenotype) of a plant is equal to the sum of the contributions  
 233 of all alleles in its genome, where each tolerance allele contributes a quantity  $\eta$ , the locus effect  
 234 size (which is the same for all loci unless stated otherwise) to the final tolerance value (Fig. 1D).

235  
 236 Once a seed is fertilized, genetic recombination occurs between the two parental genomes.  
 237 Upon recombination, the genome of the offspring is a haploid result of a series of crossovers  
 238 between the two parental haplotypes, where crossover points are sampled at an exponentially  
 239 distributed distance from each other with rate  $\rho$ , the recombination rate. The genome of the  
 240 seed is randomly picked among the recombinant haplotypes produced by this meiosis process.  
 241 Because the genome is haploid, self-fertilization is equivalent to asexual (i.e. clonal) repro-  
 242 duction. Hence, in the model, if a seed is not the result of outcrossing, it simply inherits the  
 243 haplotype of its (maternal) parent plant. Each locus within the offspring then mutates with

<sup>244</sup> probability  $\mu$ , the mutation rate, which flips the allele present at that locus to its opposite (0  
<sup>245</sup> becomes 1 and vice versa).

<sup>246</sup>

<sup>247</sup> At the end of each discrete generation, all adult plants die (the species is an annual) and  
<sup>248</sup> the seedlings that have survived become the adults of the next generation. Every simulation  
<sup>249</sup> is initialized with a population of  $N_0$  individuals whose genomes are randomly generated with  
<sup>250</sup> initial frequency  $p_0$  for the tolerance allele. All founder individuals are randomly scattered  
<sup>251</sup> across the landscape, with equal probability to land in each site, but landing in each patch with  
<sup>252</sup> probability proportional to the relative surface of that patch ( $c_k$  or  $1 - c_k$ ) in the local site.  
<sup>253</sup> Table 1 summarizes the model parameters and their default values.

## <sup>254</sup> Simulations

<sup>255</sup> We ran individual-based stochastic simulations of our model, first to understand its dynam-  
<sup>256</sup> ics and evolutionary outcomes across parameter combinations, and subsequently to study the  
<sup>257</sup> potential for evolutionary rescue of a facilitated population in the face of climate change. For  
<sup>258</sup> that latter purpose, we designed a digital ‘climate change experiment’ in which we subjected  
<sup>259</sup> the population to different scenarios of environmental deterioration (by means of progressively  
<sup>260</sup> changing environmental parameters through time, see below).

<sup>261</sup> **Null scenario** In what follows, we first examine the dynamics and evolutionary steady states  
<sup>262</sup> of the model, in conditions most relevant to our study system (facilitation by nurse shrubs in a  
<sup>263</sup> harsh matrix). These conditions are: higher stress levels in unfacilitated compared to facilitated  
<sup>264</sup> patches ( $\theta_{UF} > \theta_F$ ), and much lower carrying capacities per surface area ( $K_{UF} \ll K_F$ ).

<sup>265</sup> **Climate change experiment** Each simulation in the experiment started with 10 000 genera-  
<sup>266</sup> tions of evolution in a constant environment resembling typical semi-arid, facilitated-landscape  
<sup>267</sup> conditions. We then subjected the population to one of three climate change scenarios. In the  
<sup>268</sup> first scenario (stress increase under the shrubs), we increased the level of stress  $\theta_F$  and decreased  
<sup>269</sup> the carrying capacity  $K_F$  of the facilitated patch until these two parameters reached the values  
<sup>270</sup> of the unfacilitated patch ( $\theta_{UF}$  and  $K_{UF}$ , respectively). In the second scenario (whole-landscape  
<sup>271</sup> deterioration), we increased the stress level and decreased the carrying capacity of the facili-  
<sup>272</sup> tated patches ( $\theta_F$  and  $K_F$ ) as well as of the unfacilitated patches ( $\theta_{UF}$  and  $K_{UF}$ ). In the third  
<sup>273</sup> scenario (shrub-cover shrinkage), stress level and carrying capacity remained unchanged but we  
<sup>274</sup> reduced the shrub cover  $c$ . The exact values of the varied parameters are given in Table 2.  
<sup>275</sup> All changes in parameters were gradual and linear through time (Fig. 2). The three scenarios  
<sup>276</sup> correspond to different ways in which global warming may affect the system. For each scenario,  
<sup>277</sup> we explore the effect of various rates of environmental change  $\Delta t_W$  (or warming period, i.e. the  
<sup>278</sup> number of generations needed for environmental parameters to reach their final value).

## <sup>279</sup> Adaptive dynamics

<sup>280</sup> Separately from the stochastic simulations, we developed a deterministic approximation of the  
<sup>281</sup> model, which we study here using adaptive dynamics theory (Metz et al., 1992; Metz et al.,

1996; Geritz et al., 1998), to tease apart the role of selection from that of genetics or stochasticity in simulation outcomes. These analyses and accompanying derivations are detailed in the Appendix, and notably allow to determine whether and under which conditions plants of different morphs (i.e. with different tolerance strategies) can diversify within the model. However, because coexistence does not rely exclusively on evolutionary diversification *in situ*, the scope for the maintenance of polymorphism is wider than for sympatric divergence only. In this study, to map the portions of parameter space where such coexistence of two morphs is permitted, we perform *mutual invasibility analyses* based on our adaptive dynamics approximation (Geritz et al., 1998). These analyses consist in establishing first, for a given parameter combination, which pairs of strategies are capable of mutually invading each other (therefore, of coexisting as part of a protected polymorphism). Once pairs of morphs are found that can potentially coexist, we ask, for each pair, whether evolution will maintain this coexistence (if so, they form a *stable coalition*). To perform this type of analysis, we derived equations for the selection dynamics in a system with two morphs (see Appendix). We then use these equations to predict, for all putative pairs of coexisting morphs, which would evolve towards a stable equilibrium coalition where two morphs are still present (i.e. where none has outcompeted the other), and what their phenotypes would be. Figure S2 illustrates the analysis graphically.

## 299 Specifications

300 The simulation code in this study was written in the programming language C++20 using  
301 standard libraries. Analyses of the simulations were performed in the R computing language,  
302 version 4.3.3 (R Core Team, 2025). Adaptive dynamics calculations were performed in R and  
303 in C++. See accompanying code for details.

304 **Results**

305 *Constant climate*

306

307 Under stable semi-arid conditions, either of two possible alternative strategies can generally  
308 evolve in our simulations. The first strategy is a *stress-sensitive* strategy, whose stress tolerance  
309 value is just above the level of stress occurring in facilitated patches, but well below that of the  
310 unfacilitated patches (Fig. 3A, red circle). Consequently, plants with this strategy can only  
311 survive in the facilitated patches (Fig. 3C). The second strategy is a *stress-tolerant* strategy,  
312 whose stress tolerance is just above the level of stress of the unfacilitated patch (Fig. 3A, blue  
313 circle). This strategy can survive in both the unfacilitated and the facilitated patches (Fig. 3C).

314

315 These two alternative outcomes result from a balance between selection favoring adaptation  
316 to the stressful conditions of the unfacilitated patches, and the fecundity costs of increased  
317 stress tolerance (which trades off with reproductive output, see Eq. 2). On the one hand, if  
318 we remove stress in the unfacilitated patches, only a sensitive morph is predicted to evolve  
319 (see e.g. Fig. S3,  $\theta_{UF} = 0$ ). On the other hand, if we remove the fecundity cost to stress  
320 tolerance ( $\epsilon = 0$ ), selection favors ever-increasing adaptation to stress (see e.g. Fig. S4). Shrub  
321 cover plays a role too, as the tolerant strategy remains the only possible outcome if the shrub  
322 cover is too low to support a viable population of the sensitive morph (see e.g. Fig. S5,  $c = 0.1$ ).

323

324 Under the aforementioned conditions, the stress-sensitive and stress-tolerant strategy rep-  
325 resent alternative stable states of the system: both are stable attractors of the evolutionary  
326 dynamics, but with distinct and exclusive basins of attraction. Which strategy the popula-  
327 tion evolves towards depends on its starting stress tolerance (determined by the initial allele  
328 frequency  $p_0$ ). If the starting stress tolerance value is below a certain threshold (the border  
329 between basins of attraction in Fig. 3A), the population evolves towards the sensitive strategy,  
330 and therefore only establishes underneath the nurse shrubs (low  $p_0$  in Fig. 3B–C). If the initial  
331 stress tolerance is above that point, the population evolves into a stress-tolerant morph capable  
332 of establishing inside and outside the shrubs (high  $p_0$  in Fig. 3B–C).

333

334 The survival of a facilitated population in a harsh environment that can no longer sustain  
335 a stress-sensitive strategy depends on the evolution of a stress-tolerant strategy that no longer  
336 relies on facilitation from nurse shrubs. A population starting off as highly stress sensitive will  
337 rapidly go extinct, for example, in an environment where the shrub cover is too low for this  
338 population to be viable (e.g.  $c = 0.1$  in Fig. S6). Increasing the rate of outcrossing  $g$  does not  
339 rescue the population from extinction in such environment (Fig. S6B).

340 **Outcrossing** In some cases, outcrossing can make the difference between survival and extinc-  
341 tion of a stress-sensitive population in a constant climate. This happens in conditions that are  
342 not so harsh that the sensitive strategy is totally nonviable, but harsh enough that only low  
343 densities of sensitive plants can be sustained, which would otherwise go extinct due to stochastic  
344 demographic fluctuations if only selfing occurs ( $g = 0$ , Fig. S7). The rescue effect of outcrossing

345 is likely due to an increase in genetic variance through recombination, improving the efficiency  
346 of selection in homogenizing phenotypic values around the sensitive equilibrium strategy, and  
347 avoiding genetic drift into neighboring areas of phenotype space with dangerously low equilib-  
348 rium densities (which causes extinction in selfing populations, Fig. S7E–G). Note that because  
349 of demographic stochasticity, this effect of outcrossing is only visible when the total population  
350 size is high enough (e.g.  $n_D = 5$  in Fig. S7B).

351

352 *Climate change experiment*

353

354 In our climate change experiment, we first evolved an initially stress-sensitive population in  
355 similar conditions as described above, i.e. resembling a patchy semi-arid landscape, for 1 000  
356 generations. We then changed certain environmental parameters, gradually and at different  
357 paces, according to three different scenarios (see Methods).

358 **Scenario 1: stress increase under the shrubs** In this scenario, the level of stress  $\theta_F$  and  
359 the carrying capacity  $K_F$  of the facilitated patch were increased and decreased, respectively,  
360 until these two parameters reached their corresponding values  $\theta_{UF}$  and  $K_{UF}$  in the unfacilitated  
361 patch. We find that a population readily survives the changing climate (as long as the pace  
362 of climate change is not too fast) by evolving a higher stress tolerance, thus adapting to the  
363 conditions in the open landscape as the environment underneath the shrubs becomes more and  
364 more similar to that on the outside (Fig. S8A, S9A). A look at the adaptive dynamics of this  
365 scenario shows that out of the two possible evolutionary equilibria, the stress-sensitive strategy  
366 quickly becomes nonviable as the climate deteriorates (i.e. as  $\theta_F$  and  $K_F$  change throughout  
367 the experiment), and only the stress-tolerant equilibrium strategy remains, as sole attractor of  
368 the evolutionary dynamics, for the rest of the simulation (Fig. 4A).

369 **Scenario 2: whole-landscape deterioration** In this scenario, the stress level was increased,  
370 and the carrying capacity decreased, in both the facilitated and unfacilitated patches. Here  
371 we often find extinction (Fig. S8B, S9B) where the population initially evolves higher stress  
372 tolerance (Fig. S9B), but eventually becomes extinct nonetheless, regardless of the pace of  
373 environmental change. The adaptive dynamics of this scenario reveal that as the stress tolerance  
374 of the population increases, so does the minimum level of stress tolerance needed to survive  
375 outside the shrubs (Fig. 4B). Limiting the change in conditions outside of the shrubs (the final  
376 values of  $\theta_{UF}$  and  $K_{UF}$ , thus bringing the simulation closer to the first scenario, Fig. S10),  
377 as well as increasing the mutation rate  $\mu$  (Fig. S11A), both help rescue the population from  
378 extinction. Furthermore, the slower the deterioration of the unfacilitated patches, the lower  
379 the minimum mutation rate needed to rescue the population (Fig. S12). This suggests that  
380 extinction has more to do with the distance to the viable stress-tolerant strategy in phenotype  
381 space than with the speed of environmental change per se.

382 **Scenario 3: shrub-cover shrinkage** In this scenario, stress level and carrying capacity  
383 stayed constant and the shrub cover  $c$  (i.e. the surface occupied by the facilitated patches)  
384 was reduced instead. Here we invariably find extinction, irrespective of the pace of shrub

385 cover loss (Fig. S8C, S9C). However, contrary to the second scenario, in this scenario the  
386 population does not evolve higher stress tolerance before going extinct. Instead, its stress  
387 tolerance remains more-or-less stable (Fig. S9C). Using adaptive dynamics analysis, we find  
388 that the population is trapped in a portion of phenotype space, centered around the stress-  
389 sensitive strategy that is viable under the shrubs, but shrinking in phenotypic width, and from  
390 which the population is unable to escape once that window closes and low stress tolerance  
391 becomes nonviable (Fig. 4C). Population survival in this portion of phenotype space depends  
392 on the shrub cover being just high enough to maintain a viable population of plants without  
393 stress tolerance, and remains possible as long as the stress level in the facilitated patch is low  
394 (which it is in our scenario, Fig. S13). A population trapped in this portion of phenotype space  
395 cannot escape extinction, however, because at the moment when the shrub cover has become  
396 too low to support a population of stress-sensitive plants, the boundary of extinction (i.e. the  
397 lowest stress tolerance allowing to survive in the unfacilitated patches) has gone up so far that  
398 it has now become unreachable through small mutational steps from a sensitive strategy (Fig.  
399 4C). Consistent with that, allowing for a few macromutations (giving some loci in the genome  
400 particularly high effect sizes, Fig. S8D and S9D) or simply increasing the mutation rate (Fig.  
401 S11B), both allow to rescue the population from shrinking shrub cover.

402 **Outcrossing** Outcrossed populations generally evolve a stress-tolerant strategy slightly ear-  
403 lier than selfing populations in the scenario with stress increase under the shrubs (Fig. S14,  
404 left panel). Moreover, outcrossing can also rescue populations from extinction in the whole-  
405 landscape deterioration scenario (middle panel) and in the shrub-cover shrinkage scenario (right  
406 panel), but only when the rate of climate change  $\Delta t_W$  is slow and outcrossing is high (e.g. from  
407  $g = 0.3$  in the whole-landscape deterioration scenario, and from  $g = 1$  in the shrub-cover shrink-  
408 age scenario in Fig. S14). This can be explained by the increase in phenotypic variance brought  
409 about by recombination when plants reproduce sexually (see e.g. Fig. S7E), which increases  
410 the probability that the population escapes its evolutionary attractor and falls within the phe-  
411 notypic vicinity of the stress-tolerant equilibrium strategy (similar to the effect of introducing  
412 macromutations, Fig. S9D, or increasing the mutation rate, Fig. S11).

413 **Number of demes** Because of its effect on total population size, increasing the number  
414 of demes in the metapopulation delays extinction by thousands of generations in the whole-  
415 landscape deterioration and shrub-cover shrinkage scenarios, and prevents rapid extinction in  
416 the scenario with stress increase only under the shrubs, when climate change is otherwise too  
417 fast for a single deme to adapt (Fig. S15). In contrast, more demes in the specific case of the  
418 shrub-cover shrinkage scenario with maximum outcrossing ( $g = 1$ ) actually accelerate extinc-  
419 tion, where a single deme would otherwise be rescued by outcrossing (Fig. S15, see previous  
420 section on the role of outcrossing and Fig. S14). This suggests that while recombination may  
421 rescue the population from extinction in a single deme when the shrub cover shrinks, in combi-  
422 nation with migration among demes, gene flow may instead homogenize phenotypes, preventing  
423 any one deme from undergoing the relatively rare event of evolving away from the (soon-to-  
424 become nonviable) stress-sensitive equilibrium strategy.

425

426 *Divergence in sympatry*

427

428 In our model, evolution can lead to either a stress-sensitive or a stress-tolerant strategy, and  
429 under some conditions both strategies can coexist. The diversification of both strategies from a  
430 single one occurs when the tolerant strategy becomes an evolutionary *branching point*, allowing  
431 a sensitive morph to diverge and persist alongside it (Fig. S16 and S17). Branching arises  
432 when the carrying capacity of unfacilitated patches is sufficiently low that frequency-dependent  
433 selection favors the evolution of sensitive plants that can enjoy a fecundity advantage under  
434 the shrubs, without outcompeting the tolerant morph that still retains a higher survivability  
435 over the landscape. By contrast, populations starting from a sensitive strategy never branch,  
436 since their higher fecundity prevents tolerant mutants from establishing. Overall, branching  
437 requires facilitated patches to host roughly an order of magnitude more individuals per unit  
438 area than unfacilitated patches (Fig. S18). Figure S19 summarizes the conditions under which  
439 branching may happen. Note that since the climate change experiment always started with  
440 sensitive plants, branching points were never encountered there. See Supplementary Results S1  
441 for a more detailed explanation.

442

443 *Maintenance of diversity*

444

445 Coexistence between sensitive and tolerant strategies does not rely solely on sympatric  
446 branching. It can also arise through secondary contact in a metapopulation ( $n_D > 1$ ), where  
447 strategies that evolved separately become able to persist together (Fig. S20). Using mutual  
448 invasibility analysis (see Methods, Fig. S2), we show that stable coexistence is possible across a  
449 broader parameter space than predicted from branching alone (Fig. S21, S22), suggesting that  
450 migration among sites should play a key role in maintaining local diversity, as in its absence,  
451 it cannot be regained once lost without a branching point. However, sexual reproduction and  
452 gene flow often disrupt this diversity in the long term in the absence of mechanisms like as-  
453 sortative mating or reproductive isolation (Fig. S23). See Supplementary Results S2 for details.

454

455 *Non-linear trade-offs*

456

457 We varied the shape of the trade-off function between survival and fecundity by means of  
458 the non-linearity parameter  $\nu$ , which could make the trade-off curve more convex ( $\nu < 1$ ) or  
459 concave ( $\nu > 1$ ), on top of the main trend imposed by the trade-off strength parameter  $\epsilon$  (the  
460 downward slope of the linear trade-off when  $\nu = 1$ , Eq. 2, Fig. 1C). Changing the shape of  
461 the trade-off curve does not greatly affect the conclusions we derived from a linear version of  
462 the model. Qualitatively, the same kinds of evolutionary steady states are found in the same  
463 portions of parameter space (Fig. S24). The non-linearity parameter mostly acts as a modifier  
464 of the effect of the linear trade-off strength on the adaptive dynamics of the system, increasing  
465 the impact of the trade-off when convex, and dampening it when concave (Fig. S25).

466 **Discussion**

467 Climate change is negatively affecting terrestrial ecosystems worldwide, especially those that  
468 occur in water-restricted regions (IPCC, 2014). Shrub-dominated landscapes, like those found  
469 in the Mediterranean basin, provide habitat heterogeneity which results in buffered refuges for  
470 spatially associated plant species. This relegates facilitation into an integral component of the  
471 adaptation and survival of species in the face of climate change (Tirado & Pugnaire, 2003;  
472 Brooker, 2006; Lortie et al., 2022). Here, we used a modeling approach to gain insights into  
473 the eco-evolutionary consequences of ecological facilitation on resilience to climate change in an  
474 annual grass, inspired by the species *Brachypodium distachyon* (a study system for interspecific  
475 facilitation, Korte et al., 2025), in a semi-arid landscape, or more generally, in a heterogeneous  
476 landscape with mild and harsh patches.

477

478 By performing a digital climate change experiment in which we exposed a population of  
479 individuals experiencing facilitation from nurse shrubs to various scenarios of environmental  
480 degradation, we find the following. First, a population will evolve higher stress tolerance, and  
481 become less dependent on nurse benefactor shrubs, if climate change incurs a change in *qual-*  
482 *ity* of the facilitated areas, that is, an increase in stress (e.g. aridity or reduction in nutrient  
483 content) under the shrubs, making it more difficult for seedlings to germinate and reducing the  
484 carrying capacity (the density of plants that can be sustained per unit area) in those protected  
485 patches. In other words, if biologically feasible, plants will adapt to life outside of the shrubs  
486 if the conditions underneath the shrubs become more similar to those outside. Extinction may  
487 still happen if this change is too fast and/or if the unfacilitated areas deteriorate faster than  
488 the genetic variance of the population allows it to keep up with. Second, a reduction in the  
489 *quantity* of facilitated patches (i.e. shrub cover), without a change in quality of such patches,  
490 almost invariably leads to extinction, as short-term selective advantage traps the population in  
491 a facilitation-dependent state. The population remains restricted to the receding shrubs until  
492 the shrub cover has become too low for a viable population of grasses to be sustained — at  
493 that point the phenotypic jump that would be needed to rescue the population and allow it to  
494 survive in the open landscape has become so large that it will in practice not occur with small  
495 mutational steps (i.e. large-effect mutations or a substantial inflow of genetic variance would  
496 be needed). This is not simply a consequence of the removal of a niche from the landscape, but  
497 a result of selection dynamics that can be explained by frequency dependence. As long as the  
498 shrubs are present, they offer a refuge for plants that do not invest in stress tolerance, which, if  
499 stress tolerance incurs a fecundity cost, outcompete slightly more stress-tolerant mutants (even  
500 though high stress tolerance may be the better option overall), thus preventing them from aris-  
501 ing. Selection for short-term benefit keeps the population in a state in which extinction becomes  
502 unavoidable when shrub cover decreases beyond a certain threshold.

503

504 Studies of the impact of ecological facilitation on evolutionary dynamics are relatively scarce.  
505 Using simulations, Kéfi et al. (2008) showed that a self-facilitating plant may drive itself to ex-  
506 tinction during landscape aridification, if cheaters investing less in facilitation invade the system.  
507 Liancourt et al. (2012) propose that facilitation slows down adaptation to harsh environments

508 because of maladaptive gene flow and hybrid rescue. Yet other modeling studies have focused on  
509 the eco-evolutionary dynamics of the benefactor rather than the beneficiary species (Michalet  
510 et al., 2011). In our study, we show that contrary to Kéfi et al. (2008) where it is the loss  
511 of facilitation that leads to extinction, the maintenance of facilitation from an external bene-  
512 factor species can also prevent a population from adapting to harsher conditions. However,  
513 unlike the argument proposed by Liancourt et al. (2012) and reminiscent of the literature on  
514 adaptation at range edges (e.g. Kirkpatrick and Barton, 1997; Lenormand, 2002; Bridle et al.,  
515 2010; Angert et al., 2020), we show with asexual simulations that maladaptive gene flow is  
516 not necessarily the culprit, and that the dynamics of frequency-dependent selection may be at  
517 play instead (stress-sensitive plants take up some of the carrying capacity of the unfacilitated  
518 patches, thereby outcompeting slightly more stress-tolerant mutants with lower fecundity).

519

520 Another explanation that has been put forward for the difficulty of adaptation to harsh  
521 habitats in heterogeneous landscapes is that of weaker selection in demographic sinks, where  
522 fitness and density are lower (Kawecki, 1995; Kawecki & Holt, 2002; Holt et al., 2003; Kawecki,  
523 2008). However, this stems from the population-genetic argument that a beneficial allele will  
524 increase in frequency more slowly because of a stronger effect of drift. Although this effect  
525 probably occurs in our stochastic individual-based simulations, using adaptive dynamics theory  
526 (which ignores drift and purely evaluates the effect of selection, Metz et al., 1996), we show that  
527 selection itself, independently of drift, will also prevent the invasion of mutants investing slightly  
528 more in stress tolerance. This is because of a frequency-dependent competitive advantage not to  
529 suffer the fecundity cost of investing in more stress tolerance, at least as long as sufficient shrub  
530 cover (i.e. facilitation) remains. Hence, we propose that on top of (1) maladaptive gene flow  
531 and (2) weaker selection relative to drift, (3) frequency-dependent selection arising from the life  
532 history trade-off between survival and fecundity also explains why heterogeneous environments  
533 with facilitated patches may have a deleterious effect on adaptation to harsher conditions. Elu-  
534 cidating the relative importance of these forces may constitute a fruitful avenue for further  
535 research.

536

537 A key parameter that commonly differs among plant species is their rate of outcrossing ver-  
538 sus selfing (Pannell, 2016). The rate of outcrossing is thought to influence the adaptive potential  
539 of a species because of the direct impact of recombination on genetic diversity, and its ability  
540 to bring beneficial alleles onto the same haplotype (Tufto, 2001; Uecker & Hermisson, 2016).  
541 We find that outcrossing can make the difference between life and death in situations where the  
542 population is dangerously close to its extinction boundary, for example, when the environment  
543 favors a stress-sensitive strategy, but one that can only remain at very low densities. In such  
544 cases, outcrossing counteracts the high risk of drift into phenotypes whose survival and/or fe-  
545 cundity bring the population growth rate below one. The opposite effect is found, however, in a  
546 metapopulation setting, where the same homogenizing effect of recombination associated with  
547 gene flow prevents any one deme from stumbling upon a sufficiently stress-tolerant phenotype,  
548 which could eventually rescue the entire metapopulation once facilitation disappears from the  
549 landscape.

550

551 Phenotypic plasticity can be an alternative to genetic adaptation in surviving to a changing  
 552 climate (Chevin et al., 2010; Chevin & Hoffmann, 2017). In our implementation the more stress  
 553 tolerant plants can survive both underneath the shrubs and outside — we do not model how  
 554 this stress tolerance materializes explicitly, but it could well correspond to some plastic change  
 555 in key phenotypes directly related to water uptake, retention and loss (such as leaf area or root  
 556 biomass), depending on where the stress-tolerant plant grows. In contrast, a stress-sensitive  
 557 plant could be seen as a plant unable to plastically modify its metabolism depending on exter-  
 558 nal stress. Hence, our model technically describes the evolution of plasticity, if stress tolerance  
 559 is to be interpreted as a form of genetically encoded plasticity that comes at the cost of fecundity.

560

561 The validity of our results rests on their applicability to the real world. One of our as-  
 562 sumptions was that of implicit space, where we clumped all nurse shrubs together in a single  
 563 facilitated habitat patch per deme, instead of modeling individual nurse shrubs in a spatially  
 564 explicit context (e.g. as in Kéfi et al., 2008; Michalet et al., 2011). This approach has the ad-  
 565 vantage of helping disentangle the impact of habitat heterogeneity brought about by facilitation  
 566 from the dynamics of the benefactor species. However, while it may be a reasonable assumption  
 567 when considering that the specific location of nurse shrubs may be labile over evolutionary time,  
 568 and a general cover may be sufficient to capture the facilitated part of the landscape, studying  
 569 a spatially explicit version of this model, with eco-evolutionary dynamics of the benefactor as  
 570 well as the beneficiary species, seems a logical next step. Additional factors could then be  
 571 explored too, such as specific assumptions about the evolutionary investment into facilitation  
 572 by the benefactor species (e.g. as in Kéfi et al., 2008), the evolution of dispersal (Ronce &  
 573 Kirkpatrick, 2001; Holt et al., 2003; Ronce, 2007), or more complex and evolving genetic archi-  
 574 tectures than the polygenic additive genetics used here (e.g. while capable of harboring cryptic  
 575 genetic variation and generating large mutational steps, Crombach and Hogeweg, 2008; Paaby  
 576 and Rockman, 2014, gene networks can hinder adaptation to new patches in heterogeneous  
 577 landscapes by favoring genetic canalization, Kimbrell and Holt, 2007). Habitat choice and sex-  
 578 ual selection may be factors to consider too (Holt, 1985; Proulx, 2002), although less relevant  
 579 in sessile organisms. Similarly, the effect of hybridization with closely related species could also  
 580 be investigated (as it may affect the potential for local adaptation, Kawecki, 2008), especially  
 581 in the case of *B. distachyon*, which is commonly found to coexist with its more stress-tolerant  
 582 congeneric relative, *Brachypodium hybridum* (Korte, 2024).

583

584 Global climate change is occurring within a relatively short time frame and plant com-  
 585 munities are especially vulnerable. Investigation of the eco-evolutionary dynamics of biotic  
 586 interactions such as facilitation can help gain insight into mechanisms that could drive local  
 587 adaptation and its subsequent effect on plant community dynamics. Bridging the gaps between  
 588 ecological and evolutionary theory can shed light on the conditions that could help mitigate  
 589 the effects of current environmental stressors that could otherwise result in significant declines,  
 590 or even extinction, of certain plant populations. Here, we used theoretical modeling tools to  
 591 help bridge that gap, and show that the evolutionary fate of a species facing the risk of ex-

592 tinction in a facilitated landscape crucially depends on the way in which climate change affects  
593 the environment — with receding facilitated patches almost invariably leading the population  
594 to extinction, while exposing the population to deteriorating conditions in the facilitated areas  
595 readily promotes adaptation. This showcases how theoretical models reveal the mechanisms at  
596 play in the eco-evolutionary dynamics of species facing climate change, and the factors that  
597 may be key in predicting the response of organisms. Future work could use our model to tailor  
598 to specific study systems and produce quantitative predictions for the conservation of species  
599 of particular interest.

## 600 Acknowledgments

601 We thank the Center for Information Technology of the University of Groningen for their support  
602 and for providing access to the Hábrók high performance computing cluster. We also thank  
603 Richèl Bilderbeek for initial developments as well as Hanno Hildenbrandt and Chris Smit for  
604 helpful discussions.

## 605 **Author Contributions**

606 RS and MK conceived the study. RS developed the simulation code, performed the analyses,  
607 and wrote the first draft of the manuscript. MK contributed to study design and interpretation  
608 of the results and, together with GSvD and RSE, provided critical feedback on the manuscript.  
609 GSvD and RSE provided additional feedback on mathematical analyses.

610 **Tables**

Table 1: Parameters used in this study and default values. Unless mentioned otherwise, the values of parameters being kept constant are as per this table. See Appendix for details on the deterministic approximation model.

Symbol	Parameter	Default
$n_D$	Number of demes	1
$c_k$	Shrub cover in site $k$	0.5
$\theta_j$	Environmental stress in habitat $j$	{5, 0}
$K_j$	Carrying capacity per unit area in habitat $j$	{500, 2 000}
$r_{\max}$	Maximum population growth rate	2
$a$	Steepness of the stress tolerance function at inflection	5
$g$	Rate of outcrossing	0
$m$	Rate of dispersal	0.0001
$n_L$	Number of loci	100
$p_0$	Initial allele frequency	0.5
$\mu$	Mutation rate	0.0001
$\eta$	Effect size of a locus	0.1
$\epsilon$	Trade-off between survival and fecundity	0.1
$\nu$	Non-linearity of the trade-off curve	1
$x_{\max}$	Maximum possible stress tolerance	10
<i>Climate change experiment</i>		
$\Delta t_W$	Duration of the warming period	20 000
<i>Deterministic approximation model</i>		
$\mu_x$	Phenotypic mutation rate	0.01
$\sigma_x$	Mutational standard deviation	0.5

Table 2: Change in environmental parameters in our climate change experiment. See Table 1 for details about parameters.

Scenario	Parameter affected	Starting value	End value
Stress increase under the shrubs	$\theta_F$	0	5
	$K_F$	2 000	100
Whole-landscape deterioration	$\theta_F$	0	5
	$\theta_{UF}$	5	7
	$K_F$	2 000	100
	$K_{UF}$	100	50
Shrub-cover shrinkage	$c$	0.3	0.1

611 **Figures**

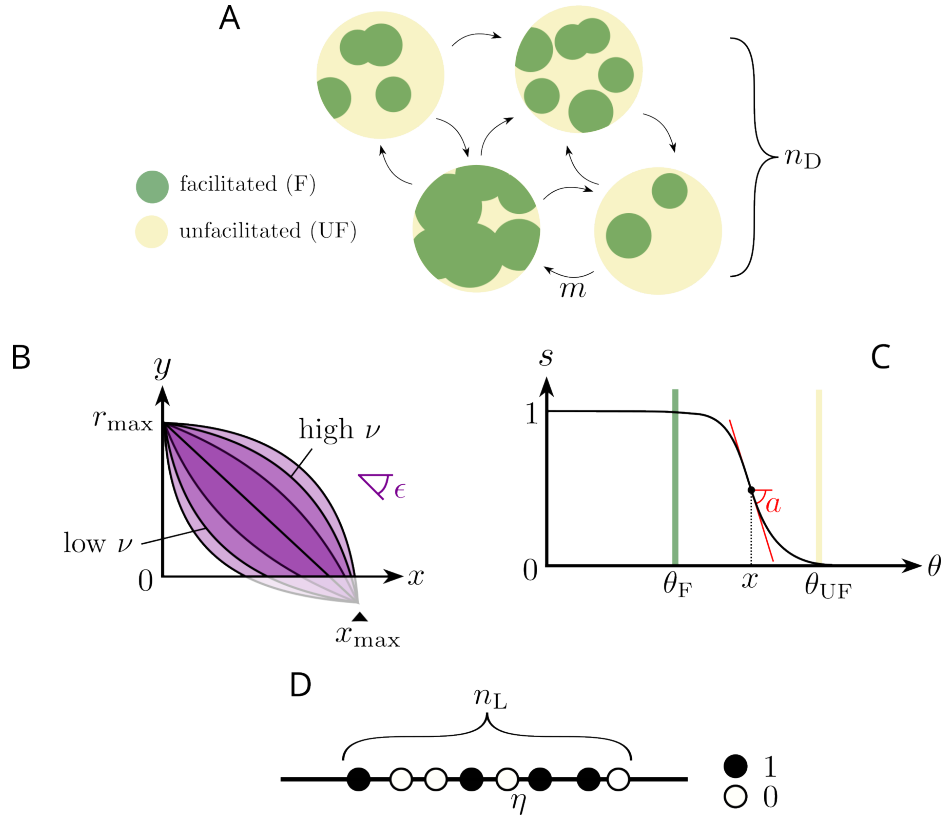


Figure 1: Model overview. (A) Schematic representation of the landscape, consisting of  $n_D$  demes, or sites, each covered by a certain area of shrubs (the *facilitated* patches, or F) and the rest being relatively arid and unsheltered (the *unfacilitated* patches, or UF). Migration occurs at rate  $m$  between the sites. (B) The sigmoid relationship between survival  $s$  and environmental stress  $\theta$ . Once environmental stress goes beyond the tolerance capacity of the plant (the inflection point  $x$ ), the chances of survival are drastically reduced (depending on the steepness  $a$  of the survival curve). In this example, the focal plant is tolerant enough to survive in the facilitated patch ( $x > \theta_F$ ) but is likely to die in the unfacilitated patch ( $x < \theta_{UF}$ ). (C) The trade-off between stress tolerance  $x$  and reproductive output  $y$ . The strength of this trade-off is determined by its slope,  $-\epsilon$ , and its shape by the non-linearity parameter  $\nu$ . (D) The genome consists of  $n_L$  loci in either state (or allele) 0 or 1, where 1-alleles contribute an effect size  $\eta$  to the stress tolerance  $x$  of the individual. See Table 1 for default parameter values.

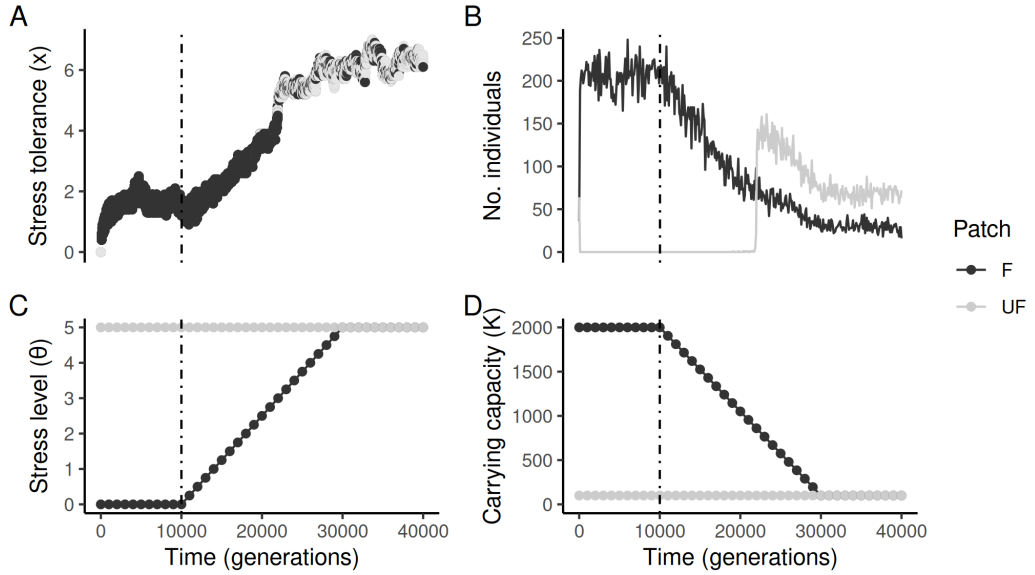


Figure 2: Typical setup for our climate change experiment. In this example, the population first evolves for 10 000 time steps in a stable environment. Relevant climate-dependent parameters (here, the stress level  $\theta_F$  and carrying capacity  $K_F$  in facilitated patches) start changing at time step 10 000, and reach their final value after  $\Delta t_W$  time steps. (A) Stress tolerance values of all individuals through time (colored by patch where the individual lives). (B) Densities of individuals in each patch through time (in this example there is only  $n_D = 1$  deme). (C) Stress levels  $\theta_F$  and  $\theta_{UF}$  through time. (D) Carrying capacities  $K_F$  and  $K_{UF}$  through time. Parameter values in this example are as per Figure 3, except with  $c = 0.3$  to reflect a semi-arid environment in which nurse shrubs occupy less than half of the entire landscape.

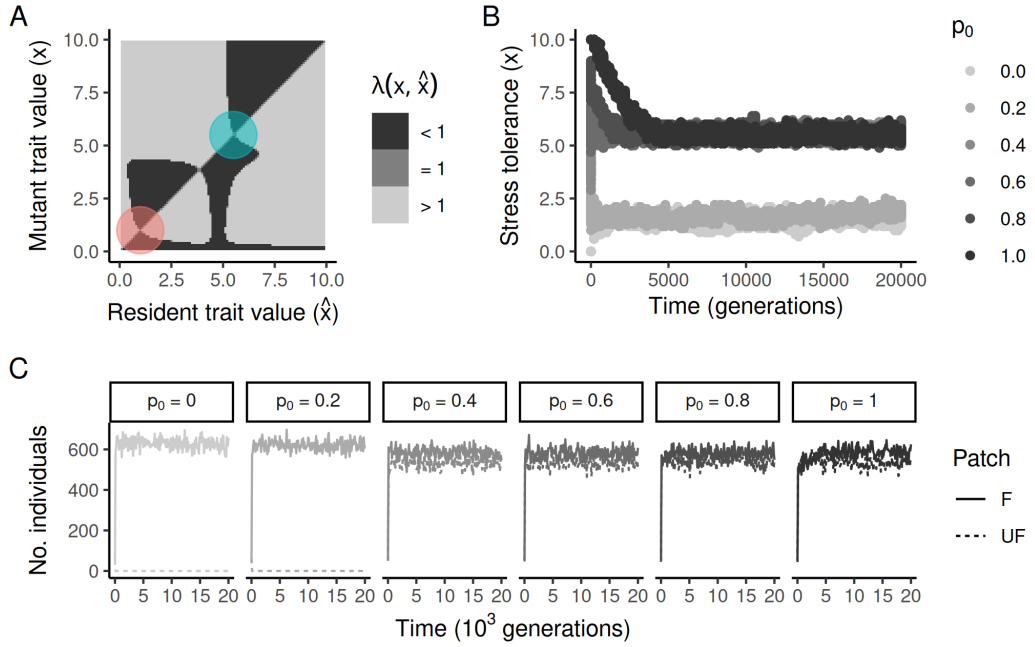


Figure 3: Model behavior in a single site ( $n_D = 1$ ) and under standard parameter values mimicking the conditions in a semi-arid landscape ( $c = 0.5$ ,  $K_{UF} = 500$ ,  $K_F = 2000$ ,  $\theta_{UF} = 5$ ,  $\theta_F = 0$ ), pure selfing ( $g = 0$ ) and a weak trade-off between stress tolerance and fecundity ( $\epsilon = 0.1$ ). Other parameters are as per Table 1. (A) Pairwise invasibility plot (PIP) describing the expected adaptive dynamics of the model under these conditions (see Fig. S1 for how to interpret PIPs, and see Appendix for derivations).  $\lambda(x, \hat{x})$  is the invasion fitness of mutant strategy  $x$  given resident strategy  $\hat{x}$ . Two alternative *continuously stable strategies* (CSS) are predicted: one stress-sensitive equilibrium strategy with stress tolerance too low to survive in the unfacilitated patches ( $x \simeq 1 < \theta_{UF}$ , red circle), and one stress-tolerant equilibrium strategy with a high-enough tolerance to be able to survive in both patches ( $x \simeq 5.5 > \theta_{UF}$ , blue circle). (B) Trait values of individuals through time in multiple simulations that vary in their initial stress tolerance (by way of the frequency  $p_0$  of the tolerance alleles in the genome, see Fig. 1D). Depending on the starting conditions, one of the two equilibrium strategies predicted in A is reached. (C) Densities of individuals through time in both patches across the simulations shown in B. Populations reaching the stress-tolerant equilibrium strategy ( $p_0 \geq 0.4$ ) are able to establish in both patches, while those reaching the stress-sensitive equilibrium strategy ( $p_0 < 0.4$ ) are restricted to the facilitated patches.

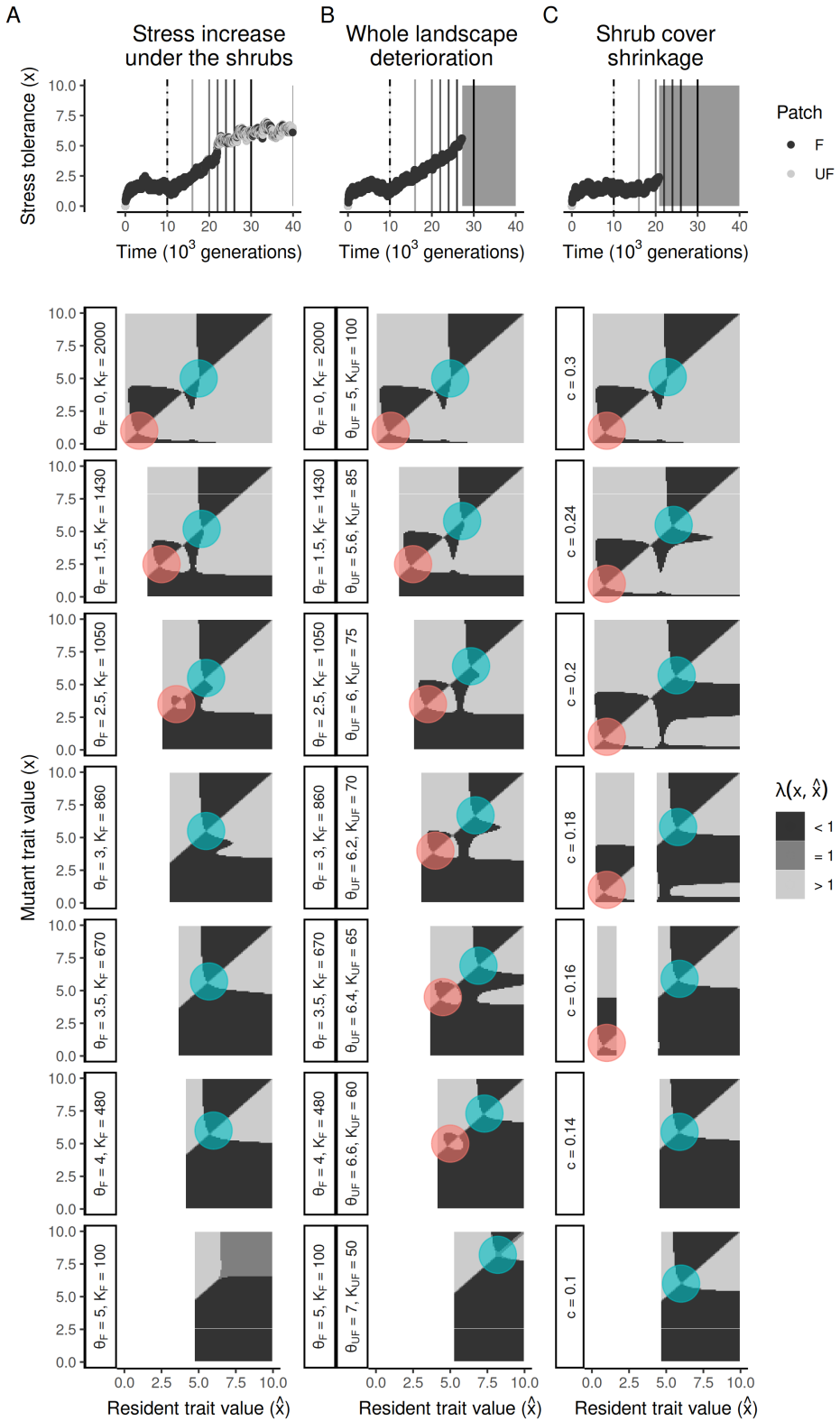


Figure 4: (See next page.)

Figure 4: Adaptive dynamics of the model during climate change. The top row shows three example simulations, each from one of our three climate change scenarios: (A) stress increase only under the shrubs, (B) whole-landscape deterioration, (C) shrinkage of the facilitated patches through time (these examples are taken from Fig. S9 with  $\Delta t_W = 20\,000$ ). Under each simulation, we show how the pairwise invasibility plot (PIP) changes through time, as environmental parameters change. Each PIP in a sequence (from top to bottom) is taken at one of the time steps shown with vertical bars in the corresponding simulation (top row). Red circles show the more stress-sensitive equilibrium. Blue circles show the more stress-resistant one (as in Fig. 3A).

612 **Supplementary Results**

613 **S1 Branching points**

614 Our Results show two possible alternative endpoints of evolution in the model (a sensitive and a  
615 tolerant strategy), in conditions resembling ecological facilitation in a harsh landscape. In some  
616 cases, however, these two strategies are not exclusive, and can both arise and coexist in the same  
617 environment. This happens when a population reaches an evolutionary branching point, i.e. an  
618 attractor of the evolutionary dynamics that becomes evolutionarily unstable, thus promoting  
619 the divergence of two strategies, once reached (see Fig. S1). It also requires a population to  
620 start off with a high stress tolerance, and the carrying capacity of unfacilitated patches to be  
621 sufficiently low (Fig. S16, see e.g.  $K_{UF} \leq 100$ , while  $K_F = 2000$ ). In such cases, the popula-  
622 tion first evolves to the stress-tolerant equilibrium strategy predicted by its adaptive dynamics,  
623 then branches off into two distinct morphs: one that stays stress-tolerant, and one that evolves  
624 to become stress sensitive (Fig. S16). Frequency-dependent selection explains why this happens.

625

626 When the carrying capacity of unfacilitated patches is sufficiently high, the established toler-  
627 ant strategy produces enough propagules across both habitats that no competing strategy (e.g.  
628 a stress-sensitive one with a higher reproductive output underneath the shrubs) can invade. The  
629 tolerant equilibrium strategy is then a stable endpoint of evolution, and not a branching point.  
630 However, as the carrying capacity of unfacilitated patches becomes sufficiently low (somewhere  
631 between  $K_{UF} = 100$  and 500 given the parameters tested here, see also Fig. S19), mutants  
632 investing slightly less in stress tolerance become a viable alternative, as they suffer less from the  
633 fecundity cost imposed by stress tolerance, and the propagule pressure from tolerant plants is no  
634 longer enough to prevent them from establishing under the shrubs. The result is two equivalent  
635 strategies coexisting in sympatry, in a so-called protected polymorphism where sensitive plants  
636 are found only underneath the shrubs and tolerant plants are found in both patches (Fig. S17D).

637

638 Note that while a stress-sensitive strategy can branch off from a stress-tolerant one, the re-  
639 verse is not true. Even when the stress-tolerant strategy is a branching point, the stress-sensitive  
640 equilibrium strategy remains a stable attractor of the evolutionary dynamics that is not con-  
641 ducive to branching (Fig. S16A–B). The reason for this is the trade-off between survival and  
642 fecundity — the reproductive output of an established stress-sensitive strategy is higher than  
643 that of an established stress-tolerant one, such that an established sensitive strategy will not  
644 allow the rise of slightly more stress-tolerant mutants in the same way that a tolerant strategy  
645 would have left an opportunity for sensitive plants to invade and coexist. For these reasons, no  
646 branching occurs in our climate change experiment (see Results), where the population always  
647 starts as stress sensitive and not stress tolerant.

648

649 In general, we find that given the parameter values tested, facilitated patches should be able  
650 to host at least around 10 times as many plants as unfacilitated patches per unit area for the  
651 tolerant strategy to be a branching point (Fig. S18). We summarize in Figure S19 the kinds of  
652 evolutionary outcomes (in terms of branching points versus stable attractors) expected across

653 a wide portion of parameter space.

654 **S2 Coexistence analysis**

655 The coexistence of two morphs does not exclusively rely on in situ diversification of the two  
656 strategies from a single one (i.e. on branching points). Under some conditions, environmental  
657 parameters are such that sensitive and tolerant plants can stably coexist, even though they may  
658 not diversify in sympatry. This can happen, for example, in a metapopulation setting (with  
659 multiple demes,  $n_D > 1$ ), where different strategies, evolved in relative geographical separation,  
660 come into secondary contact and are subsequently able to coexist within a site. Figure S20  
661 illustrates this in a simulation where stress-tolerant and stress-sensitive plants are found in the  
662 same sites in a metapopulation with environmental parameters chosen such that divergence in  
663 sympatry is not possible.

664

665 Because coexistence does not rely exclusively on branching points, the scope for the main-  
666 tenance of polymorphism is wider than for sympatric divergence only. By repeating our mutual  
667 invasibility analysis (see Methods) over thousands of parameter combinations, we find that in-  
668 deed, many more parameter combinations allow for the stable coexistence of a sensitive and  
669 a tolerant morph, than would be expected solely based on branching points. This is particu-  
670 larly the case when the carrying capacity in the unfacilitated patches is too high to promote  
671 branching (e.g.  $K_{UF} = 500$ , Fig. S21). We confirmed the predictions of the mutual inva-  
672 sibility analyses by running simulations with two morphs in parts of parameter space where  
673 stable coexistence is predicted to occur, and those simulations remain dimorphic through time  
674 (Fig. S22). Altogether, these results suggest that migration among sites in a metapopulation  
675 is critical to the maintenance of local diversity in a facilitated system, as if diversity is lost lo-  
676 cally, it may not be possible for one morph to re-evolve from the other in small mutational steps.

677

678 We also find that the maintenance of local diversity is sensitive to sexual reproduction and  
679 outcrossing. Indeed, the homogenizing effect of recombination on the gene pool usually breaks  
680 down branching points in the presence of gene flow (i.e. nonzero outcrossing,  $g > 0$ , Fig.  
681 S23). The coexistence of multiple morphs in the presence of gene flow may be rescued through  
682 mechanisms of assortative mating or some other sort of reproductive isolation, but we did not  
683 delve into these in the present study.

684 **Supplementary Figures**

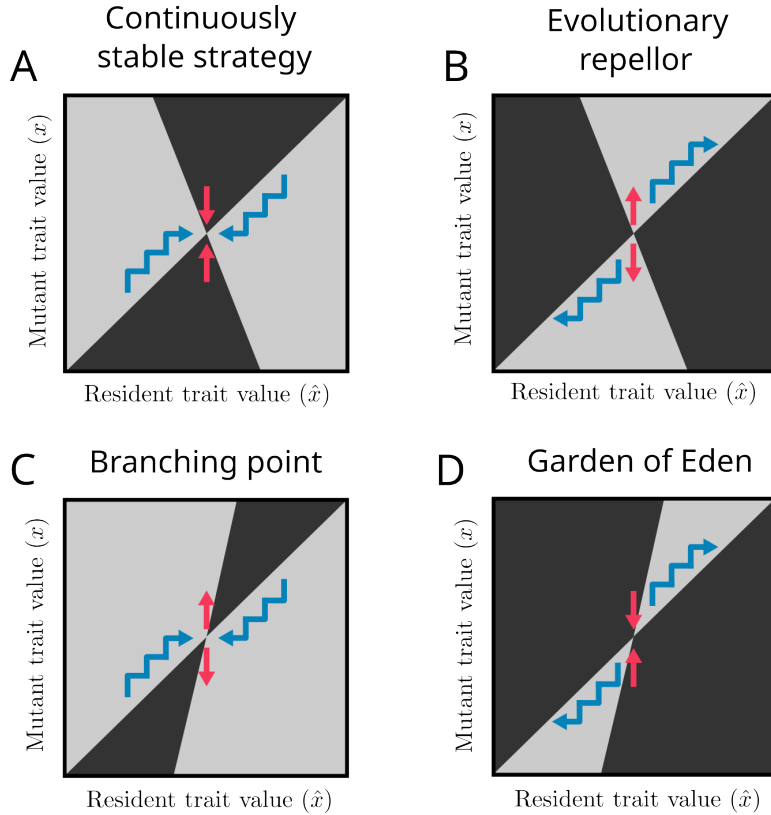


Figure S1: WA pairwise invasibility plot (PIP) is a phase plot showing, for each possible value of a trait fixed in a theoretical (monomorphic) *resident* population (here  $\hat{x}$ ), the range of other values of the same trait that a rare *mutant* arising in a population of residents could have, and what the relative fitness of said mutant (here  $x$ ) would be, compared to the resident. This relative *invasion fitness* determines whether a mutant can invade, and replace, a given resident. A PIP shows, in two different colors, all pairs of mutant and resident strategies where the mutant can invade (light gray here), and all pairs where the mutant cannot (dark gray). The graphical depiction predicts the dynamics of evolution through successive invasions (of mutants becoming the new residents, and so on, blue arrows). Eventually, a so-called *equilibrium* (or *singular*) strategy may be reached, where the direction of evolution changes (i.e. where the *isoclines* delimiting the invasion boundaries cross). Singularities that evolution by selection leads to (blue arrows) are *convergence stable*, but need not be endpoints of the evolutionary dynamics, as once reached they may be *evolutionarily stable* or not (red arrows). (A) Equilibrium strategies that are both convergence and evolutionarily stable are called continuously stable strategies (CSS) — they are stable endpoints of evolution. (B) Repellors are equilibria which are both convergence and evolutionarily unstable — selection leads away from them. (C) Branching points are convergence-stable attractors that are evolutionarily unstable once reached — they promote diversification into two morphs, each with their own trait value. (D) Gardens of Eden are repellors that would be evolutionarily stable if reached but in practice never are. For more information, see Geritz et al. (1998) and Otto and Day (2007).

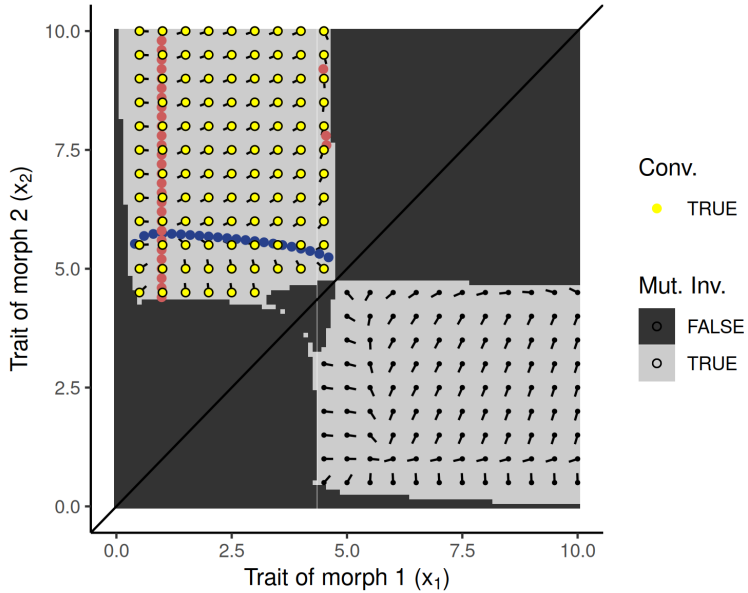


Figure S2: Mutual invasibility plot (MIP) and coexistence analysis. A MIP is a pairwise invasibility plot (PIP, see Figure S1) flipped over its own diagonal (Geritz et al., 1998). It can help understand the conditions under which two strategies can coexist in a population, and/or what happens *after* after a population has split into two groups, each with their own evolving trait (i.e. after a branching point has been reached, in the language of adaptive dynamics, see Appendix). The axes are no longer the mutant and resident strategies, as in a PIP, but the strategies (or traits) of two morphs present in the population. Light gray areas now indicate *mutual invasibility*, where both morphs can invade each other when one is taken as a mutant and the other as resident, and vice versa (the MIP is therefore symmetrical along its diagonal). Dark gray areas in the above figure are pairs of morphs that cannot coexist — one morph overtakes the other in those cases. That two morphs can mutually invade each other does not mean that they will remain in a stable coexistence, however, as evolution may lead to a point where they are no longer able to coexist. For this reason, in our analyses of MIPs we also plot a field of dimorphic *selection gradients* (tick marks), showing the direction in which selection is pushing both morphs to evolve (see Appendix for calculations). Potential endpoints of dimorphic evolution are points in the MIP where selection no longer pushes in any direction. In our study, we graphically find those points by generating null isoclines, i.e. lines in the MIP where the selection gradient is zero in one of its two dimensions (red and blue dots). The crossing points between isoclines are *equilibrium coalitions* of mutually invadable morphs, that is, pairs of strategies that can coexist and will not evolve more once reached. However, similar to the convergence stability problem of PIPs, here we need to know, for a given equilibrium coalition, whether evolution pushes towards or away from it. We determine this by evaluating, for each dimorphic selection gradient (i.e. tick mark) that was computed in the area of mutual invasibility (i.e. the gray zone), the proportion of those gradients pointing towards said equilibrium. The coalitions expected to converge towards the equilibrium coalition (at the crossing of the red and blue isoclines), are labeled in yellow in the plot. The proportion of all tick marks pointing towards a given equilibrium is termed the *basin of attraction* of that equilibrium, and is used as a proxy for the propensity of the system to reach stable coexistence of two morphs in the long term. The example MIP shown here is that of Figure S17B.

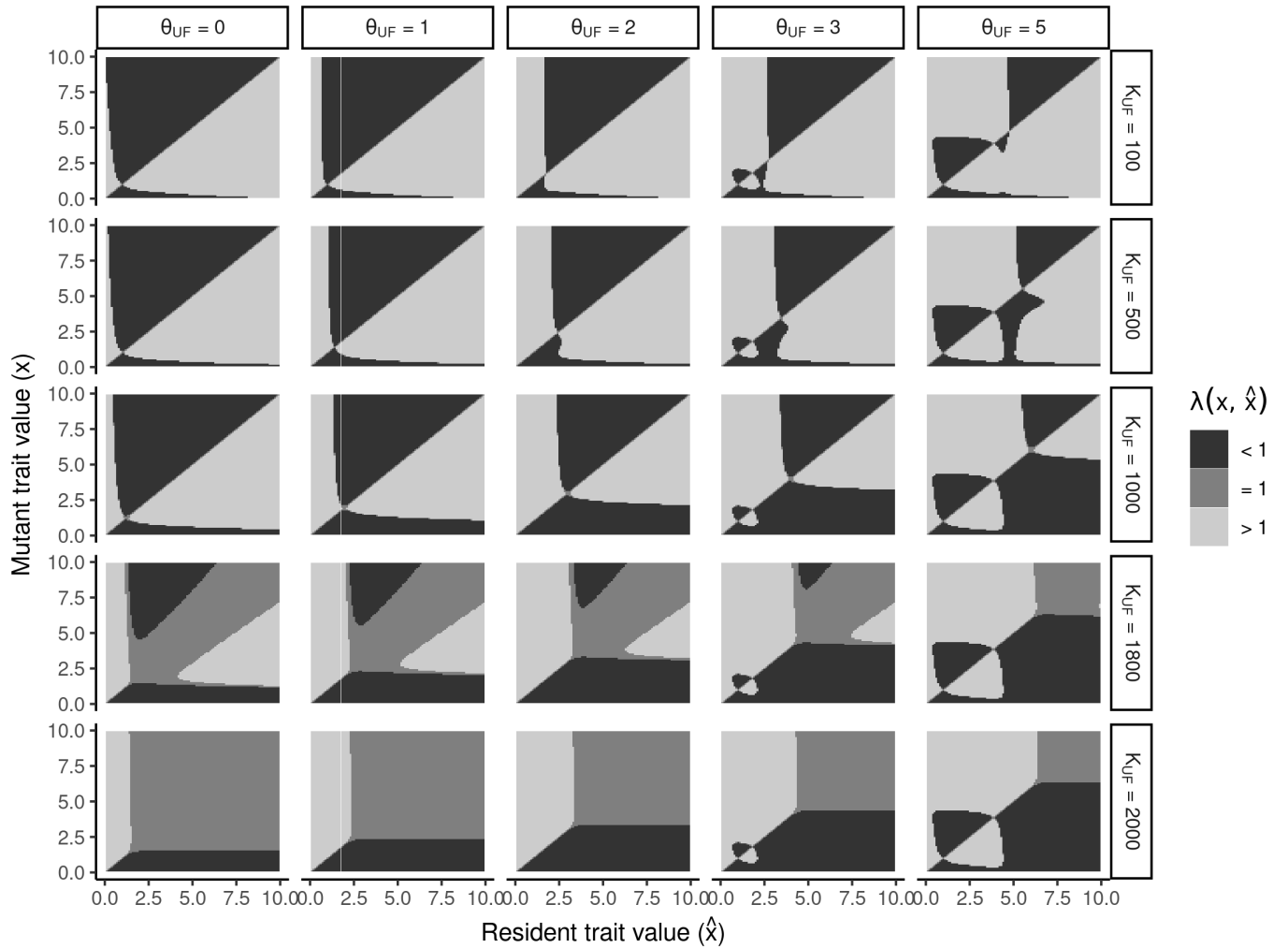


Figure S3: Effects of the level of stress  $\theta_{UF}$  and carrying capacity  $K_{UF}$  of the unfacilitated patches, on the adaptive dynamics of the model. Other parameter values are the same as in Fig. 3. Note: in zones where  $\lambda(x, \hat{x}) = 1$ , mutant and resident have the same fitness.

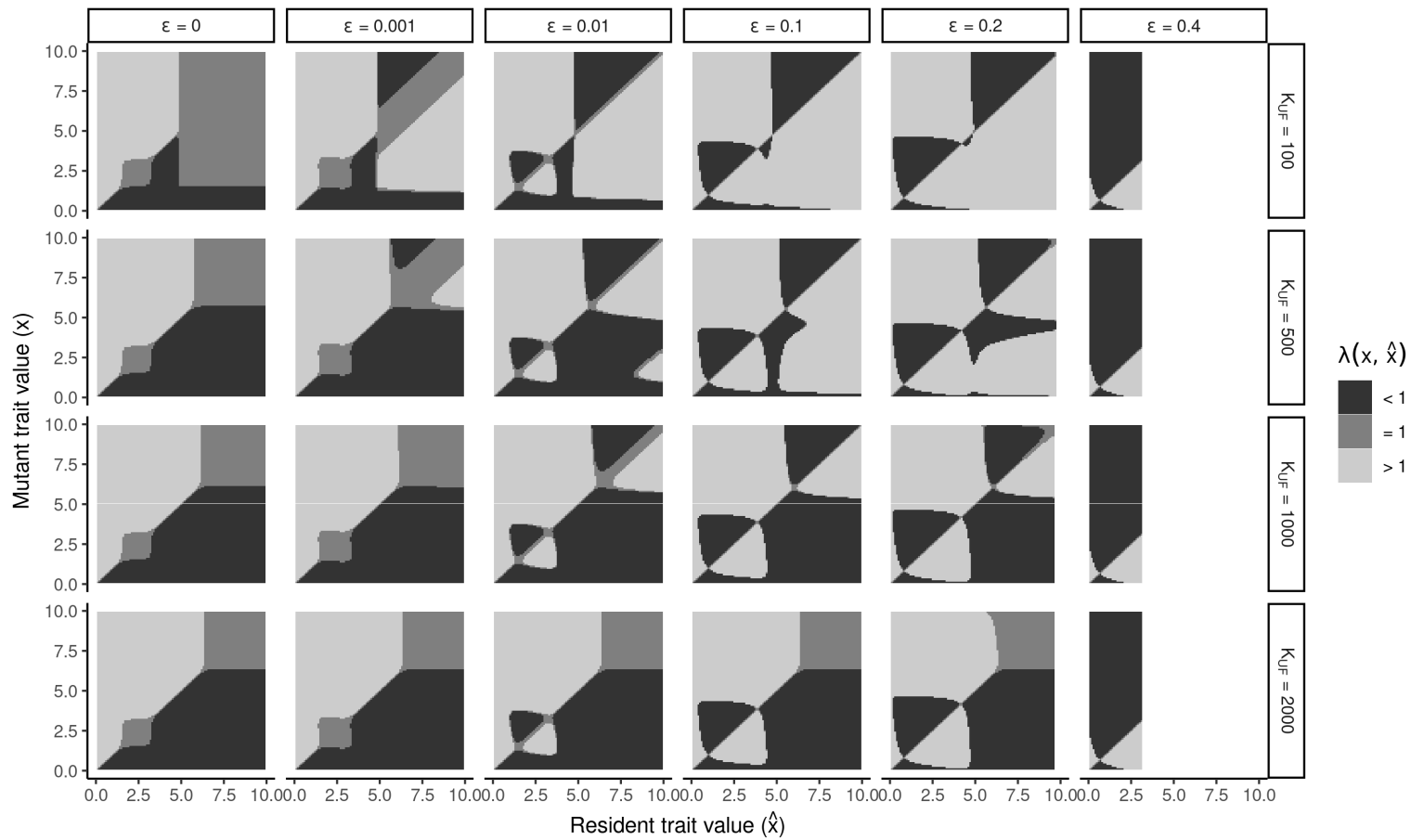


Figure S4: Effects of trade-off strength  $\epsilon$  and carrying capacity  $K_{UF}$  of the unfacilitated patches, on the adaptive dynamics of the model. Other parameters are as per Fig. 3. Note that blank regions of the plot mean that no viable resident population can be sustained for these trait values.

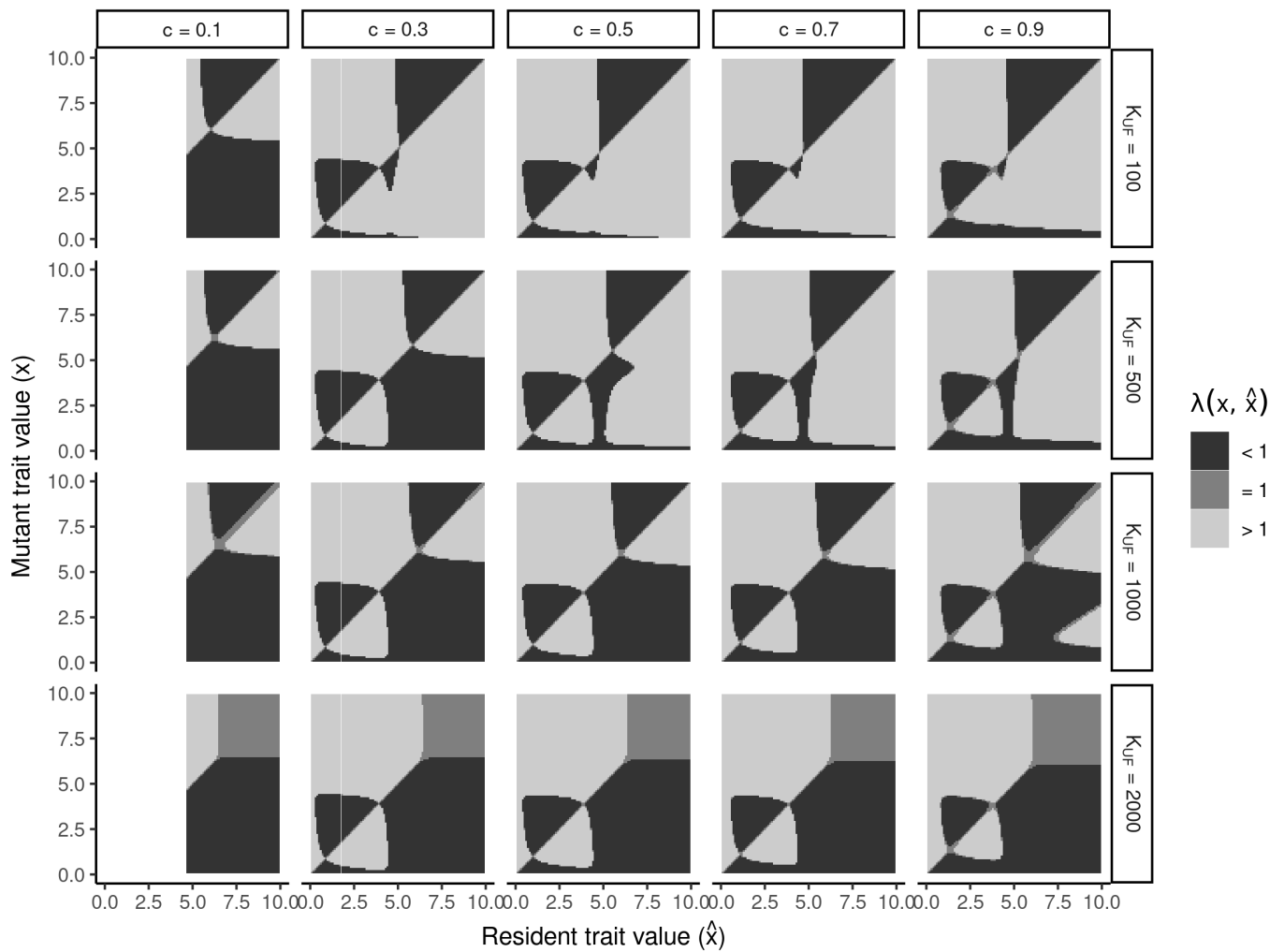


Figure S5: Effects of shrub cover  $c$  and carrying capacity  $K_{UF}$  of the unfacilitated patches, on the adaptive dynamics of the model. Other parameters are as per Fig. 3.

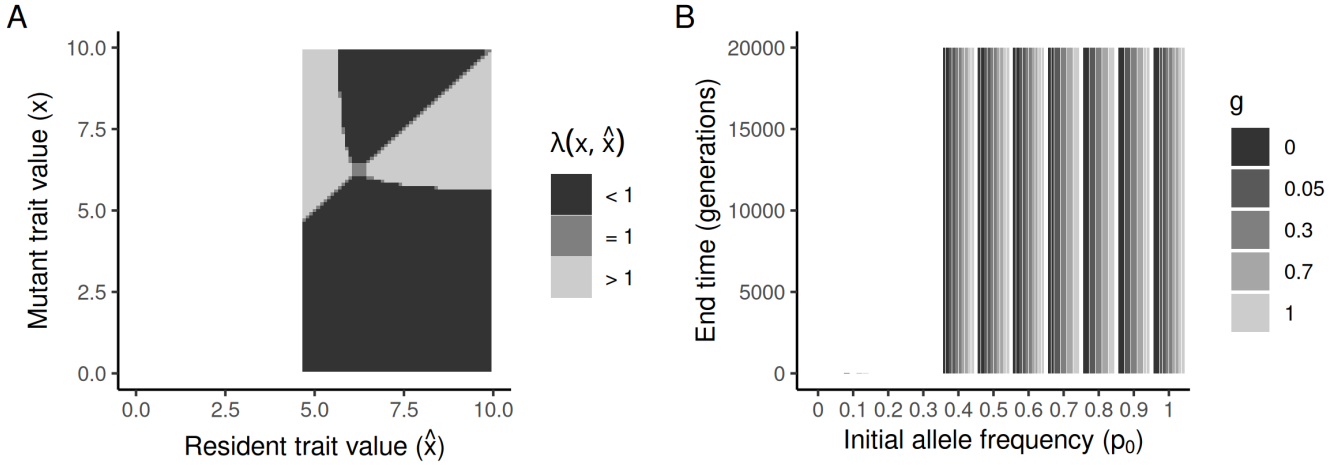


Figure S6: Population extinction in an inhospitable landscape with low shrub cover ( $c = 0.1$ , other parameters as per Fig. 3). (A) Predicted adaptive dynamics under these conditions. The shrub cover is too low for a stress-sensitive strategy to be viable. (B) Simulations are run under different rates of outcrossing  $g$ . Only simulations (bars) with a population starting off with a sufficiently high level of stress tolerance ( $p_0 \geq 0.4$ ) can survive all the way to the end of the simulation time. The ones starting with a too low frequency  $p_0$  of tolerance alleles in their genome go extinct almost immediately.

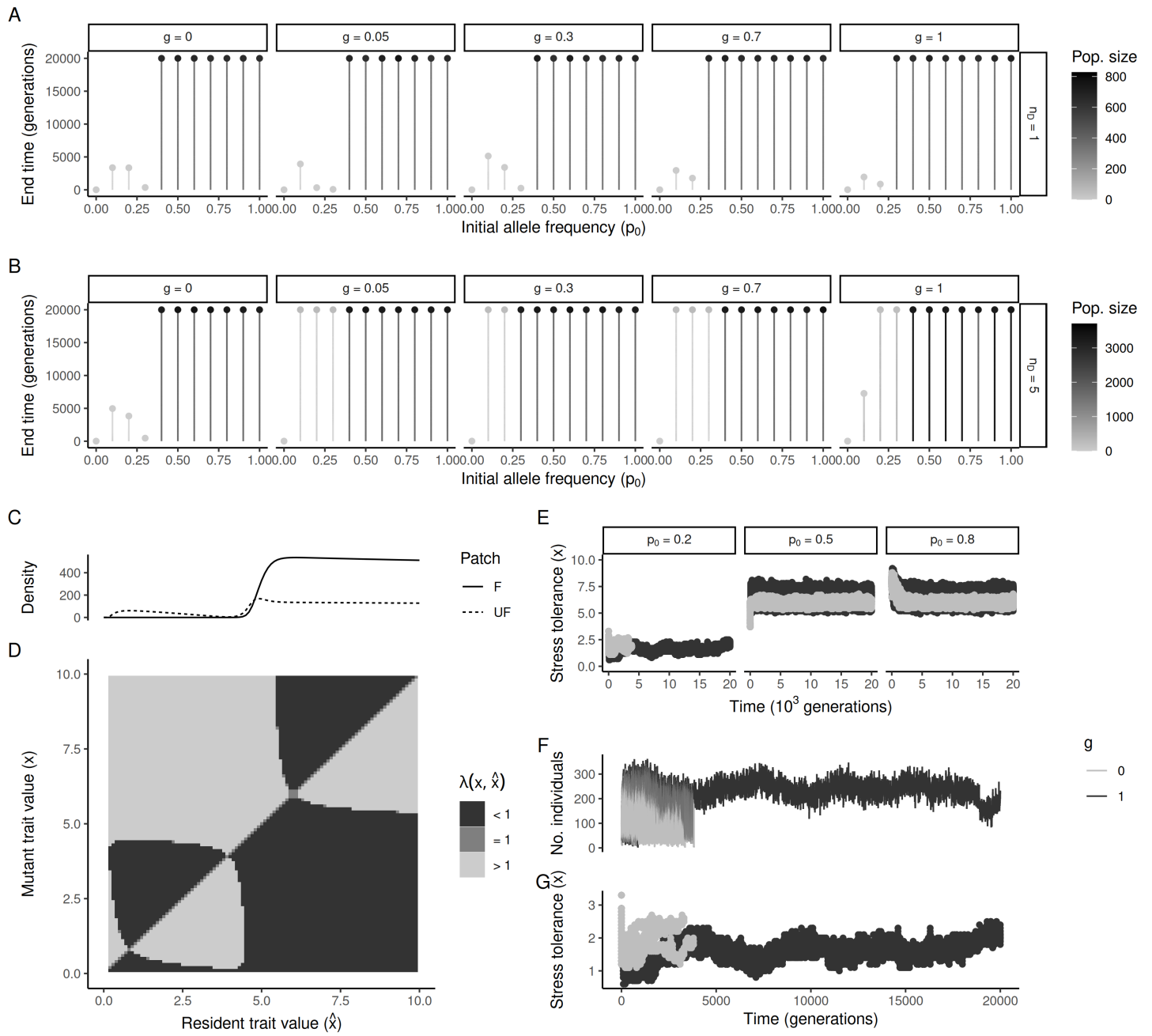
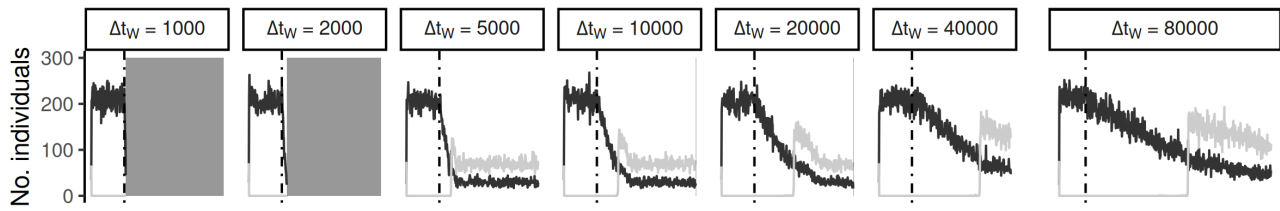


Figure S7: (See next page.)

Figure S7: Outcrossing can protect low-density stress-sensitive populations from stochastic extinction. (A) Simulations run in an environment with one deme ( $n_D = 1$ ), low shrub cover ( $c = 0.2$ ) and across different rates of outcrossing  $g$  (as per Fig. S6B). Similar to  $c = 0.1$  (Fig. S6), stress-sensitive populations rapidly go extinct. (B) With more demes ( $n_D = 5$ ), nonzero levels of outcrossing ( $g > 0$ ) help maintain initially sensitive populations at low densities. Studying the adaptive dynamics of the model reveals why. (C) The predicted equilibrium density of stress sensitive strategies in one deme is above zero in such environments, meaning that they could in theory survive, but at much lower densities than stress tolerant plants. (D) Indeed, the stress sensitive strategy is a reachable, stable evolutionary attractor of the adaptive dynamics under these conditions. (E) Comparison of simulations with  $g = 0$  (pure selfing) and  $g = 1$  (pure outcrossing) across three different starting points taken from B. Besides displaying generally higher phenotypic variation than selfing populations, outcrossed populations typically reach the same evolutionary endpoints, but avoid extinction even when they remain stress-sensitive ( $p_0 = 0.2$ ). (F–G) Zooming in on the leftmost panel in E ( $p_0 = 0.2$ ) and looking at densities (F) and trait evolution (G) reveals that the selfing population ( $g = 0$ ) oscillates more in trait value, probably due to drift. This suggests that outcrossing, by increasing the genetic variance, keeps the population close to its evolutionary equilibrium and prevents it from drifting towards trait values for which the population density that can be sustained is dangerously close to zero (and stochastic demographic fluctuations can easily push the population over that edge).

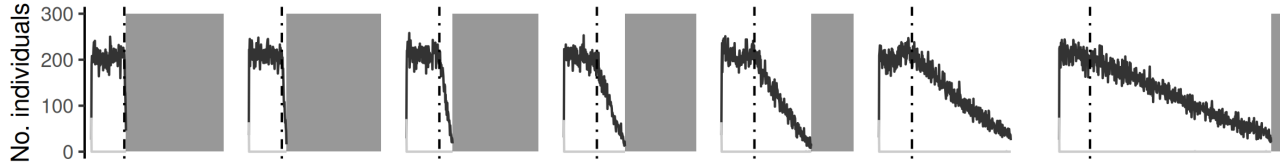
A

## Stress increase under the shrubs



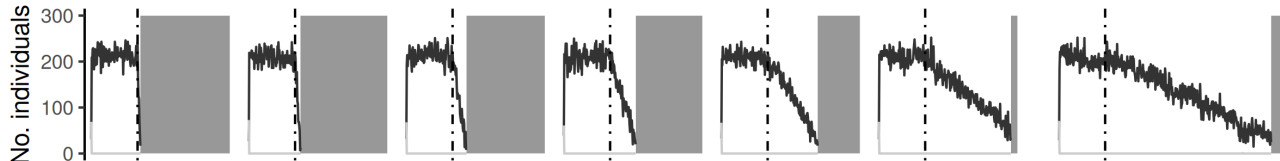
B

## Whole landscape deterioration



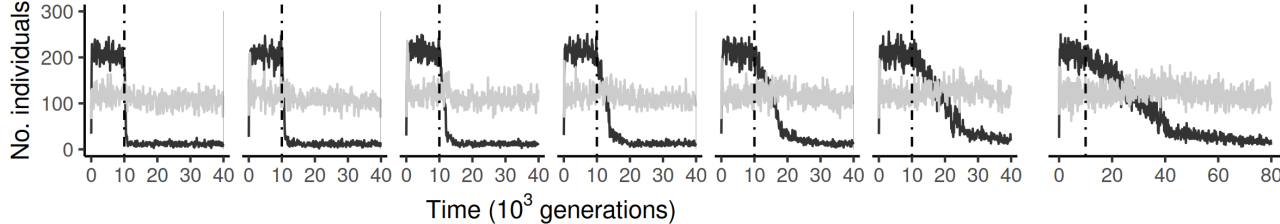
C

## Shrub cover shrinkage



D

## Shrub cover shrinkage with macro-mutations



Patch

— F  
— UF

Figure S8: Densities through time across the three scenarios of our climate change experiment (see Methods and Table 2): (A) stress increase only under the shrubs (parameters  $\theta_F$  and  $K_F$  change from 0 to 5 and from 2000 to 100, respectively); (B) whole-landscape deterioration ( $\theta_F$  changes from 0 to 5,  $K_F$  from 2000 to 100,  $\theta_{UF}$  from 5 to 7, and  $K_{UF}$  from 100 to 50); and (C) shrinkage of the facilitated patches through time (parameter  $c$  changes from 0.3 to 0.1). All other parameters are as per Fig. 2. An extra scenario (D) revisits the shrub-cover shrinkage scenario (C), but with macromutations scattered throughout the genome and allowing large mutational steps during phenotypic evolution (in each simulation 10 loci were sampled at random and their effect size was increased from  $\eta = 0.1$  to  $\eta = 5$ , see Table 1). For each scenario, different durations of environmental change  $\Delta t_W$  are tested. Gray rectangles in the background mean that the population went extinct.

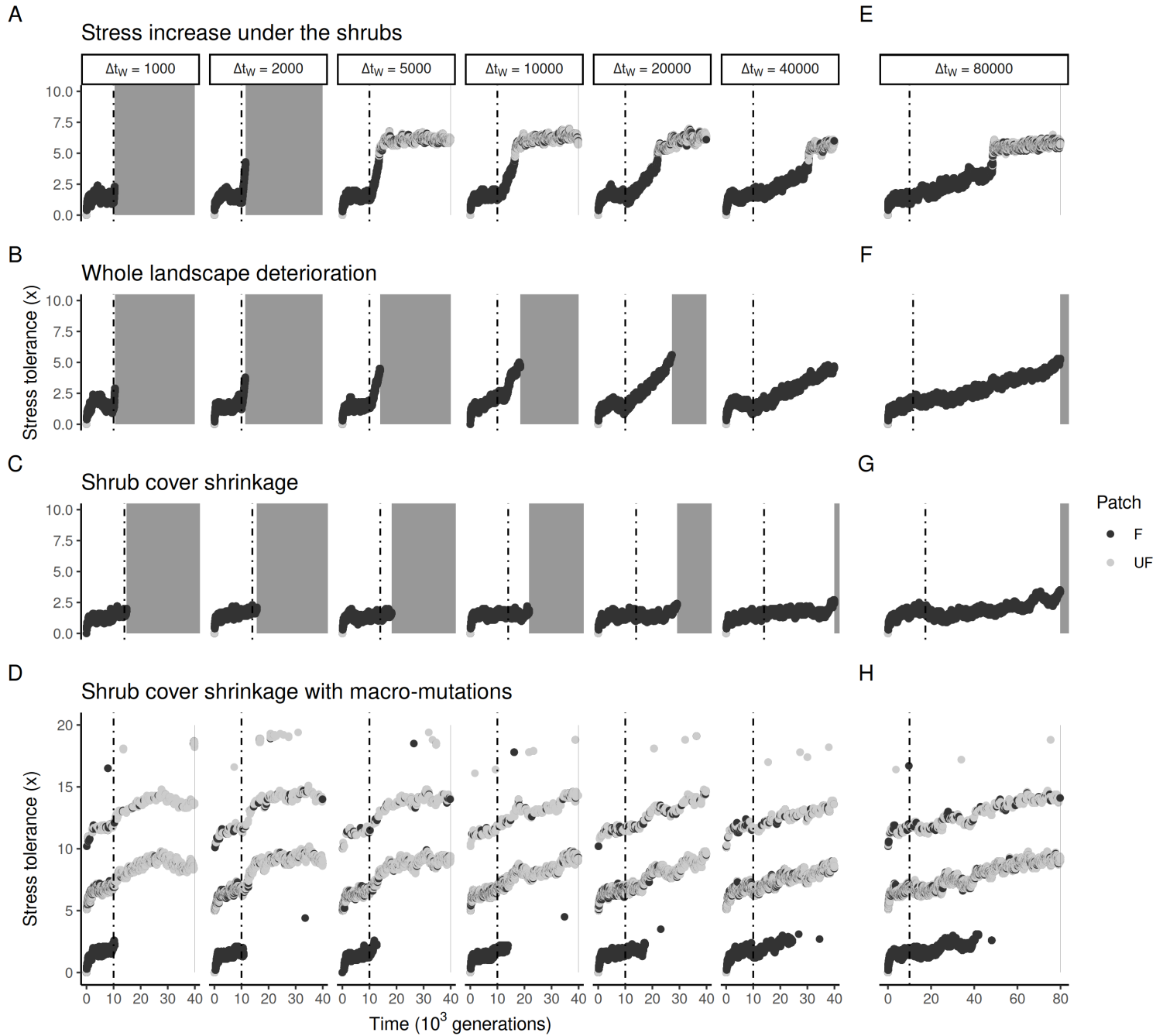


Figure S9: Stress tolerance evolution in our climate change experiment. Each point represents an individual. The simulations are the same as in Figure S8. Note that although scenarios B and C both almost invariably lead to extinction, in the case of the whole-landscape deterioration scenario (B), the population evolves its stress tolerance as the environment changes, while it remains more-or-less constant in the shrub-cover shrinkage scenario (C).

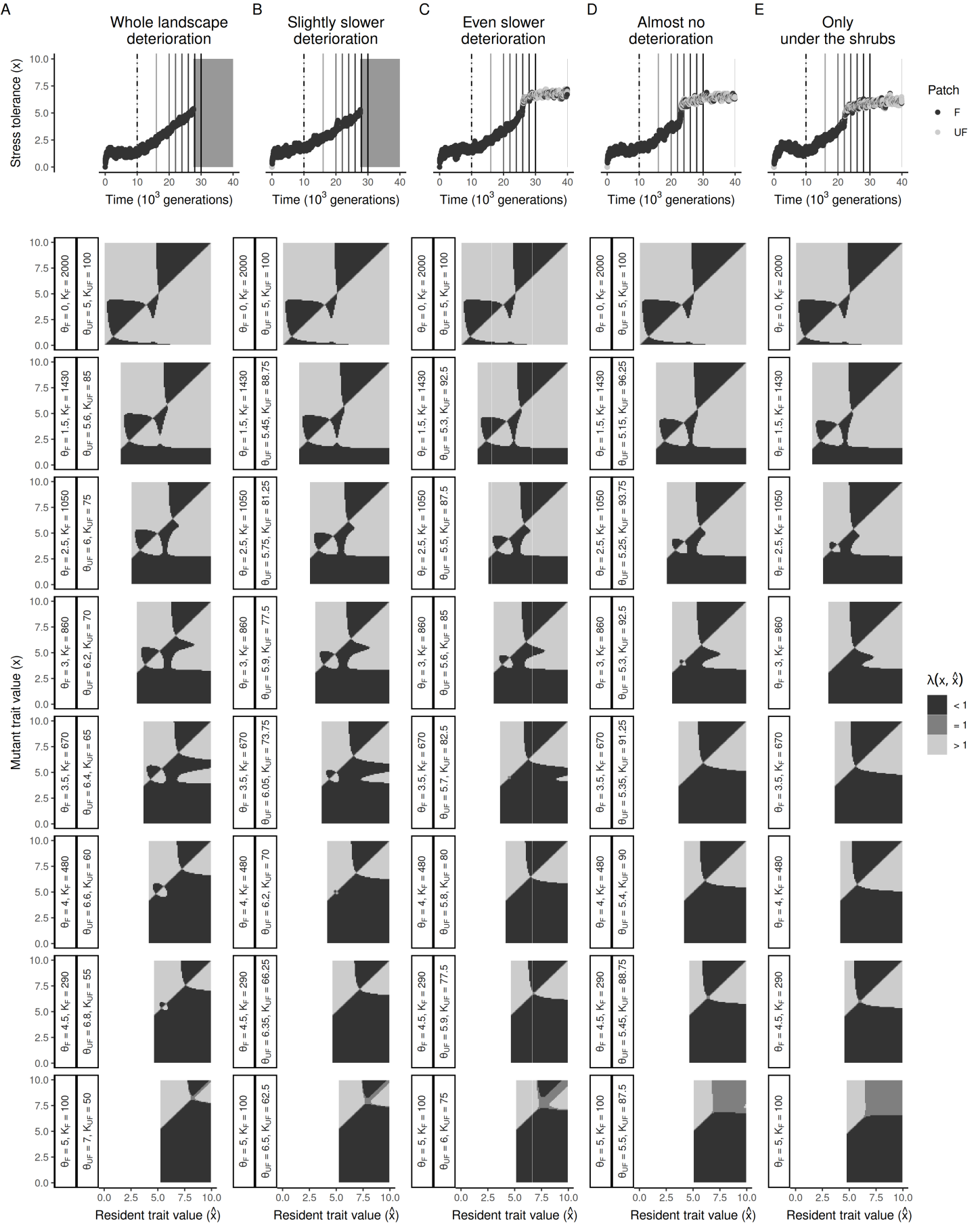


Figure S10: (See next page.)

Figure S10: Adaptive dynamics across paces of landscape deterioration. Legend is as per Fig. 4, except here, the investigate scenarios span a range of rates of deterioration (i.e. increase in stress  $\theta$  and decrease in carrying capacity  $K$ ) of the unfacilitated patches relative to the facilitated patches. In all cases,  $\theta_F$  goes from 0 to 5, and  $K_F$  goes from 2000 to 100 throughout the  $\Delta t_W = 20\,000$  time steps of climate change. However, the magnitude of change of the unfacilitated patches over that time varies, starting from from  $\theta_{UF} = 5$  and  $K_{UF} = 100$ , to (A)  $\theta_{UF} = 7$  and  $K_{UF} = 50$  (the whole-landscape deterioration scenario shown in Fig. 4B), (B)  $\theta_{UF} = 6.5$  and  $K_{UF} = 87.5$ , (C)  $\theta_{UF} = 6$  and  $K_{UF} = 75$ , (D)  $\theta_{UF} = 5.5$  and  $K_{UF} = 62.5$ , or (E) remaining the same throughout (which is the scenario with stress increase only under the shrubs in Fig. 4A).

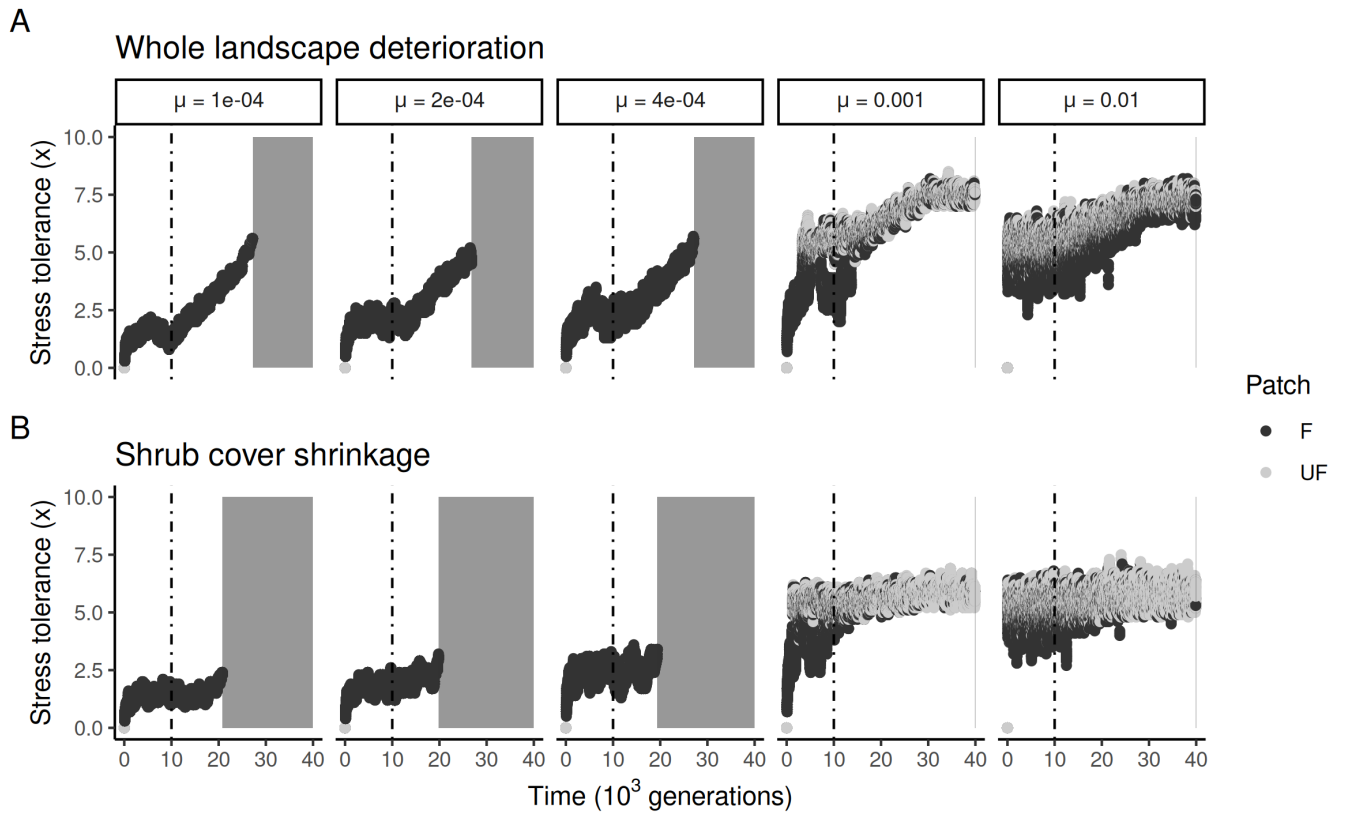


Figure S11: Stress tolerance evolution in climate change simulations across mutation rates  $\mu$ , in (A) the whole-landscape deterioration scenario, and (B) the shrub-cover shrinkage scenario. Parameters are otherwise the same as in Fig. 4 ( $\Delta t_W = 20\,000$ ).

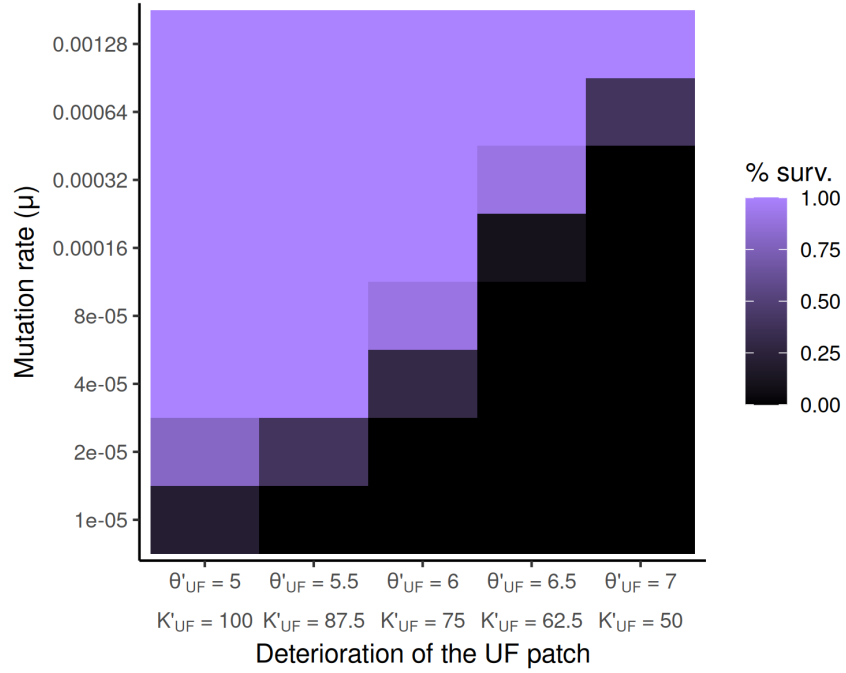


Figure S12: Population rescue across mutation rates  $\mu$  and rates of deterioration of the unfacilitated patches (i.e. final values  $\theta'_{UF}$  and  $K'_{UF}$  of environmental stress and carrying capacity, respectively, after  $\Delta t_W = 20\,000$  time steps of climate change). Parameters are otherwise the same as in Fig. S10. For each combination of parameters, we ran 10 replicate simulations and measured the proportion that survived extinction. Note the non-linear scale of the mutation rate axis.

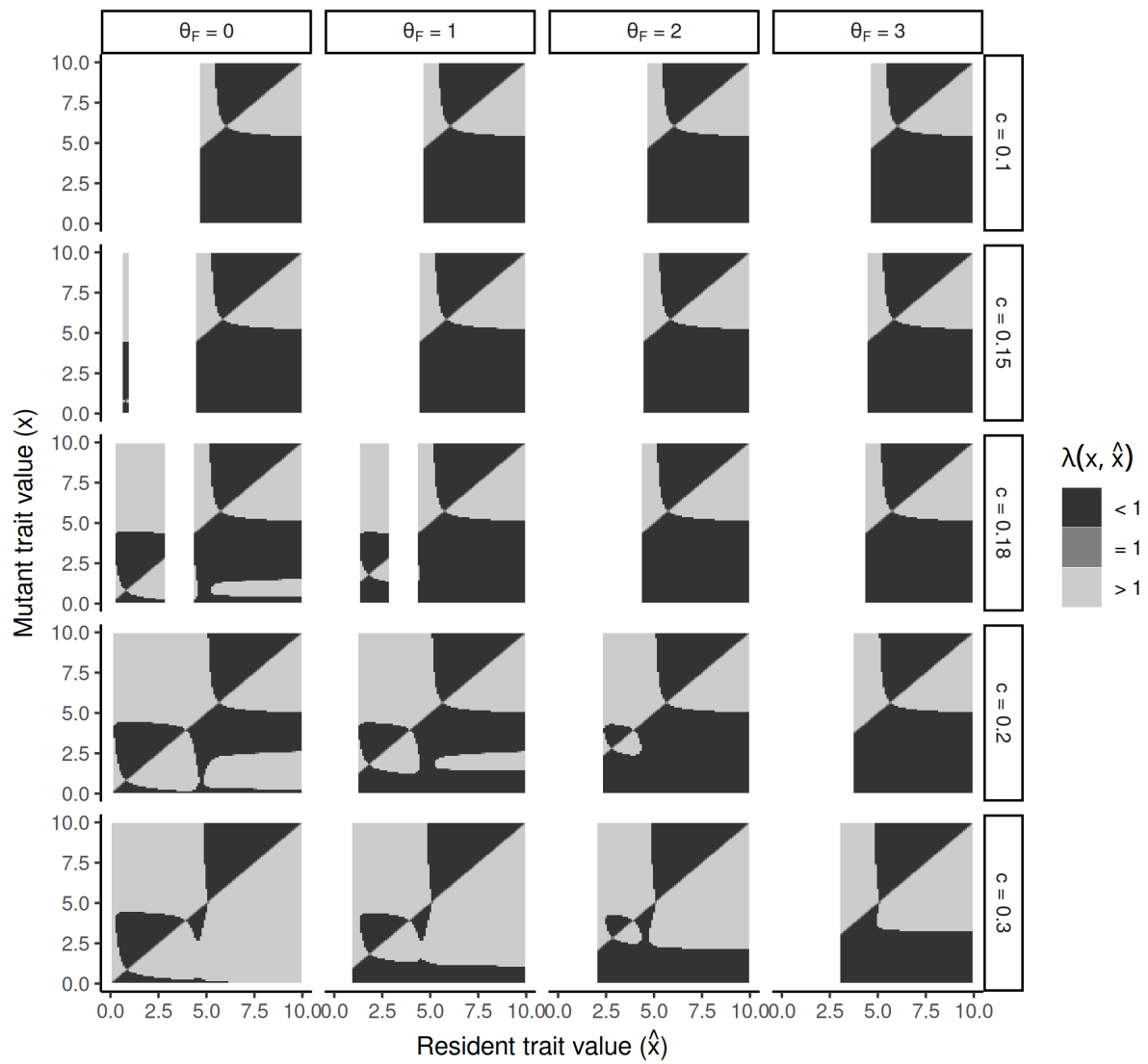


Figure S13: Effects of stress level  $\theta_F$  and cover  $c$  in the facilitated patches on the adaptive dynamics of the model. Parameters otherwise as per Fig. 3.

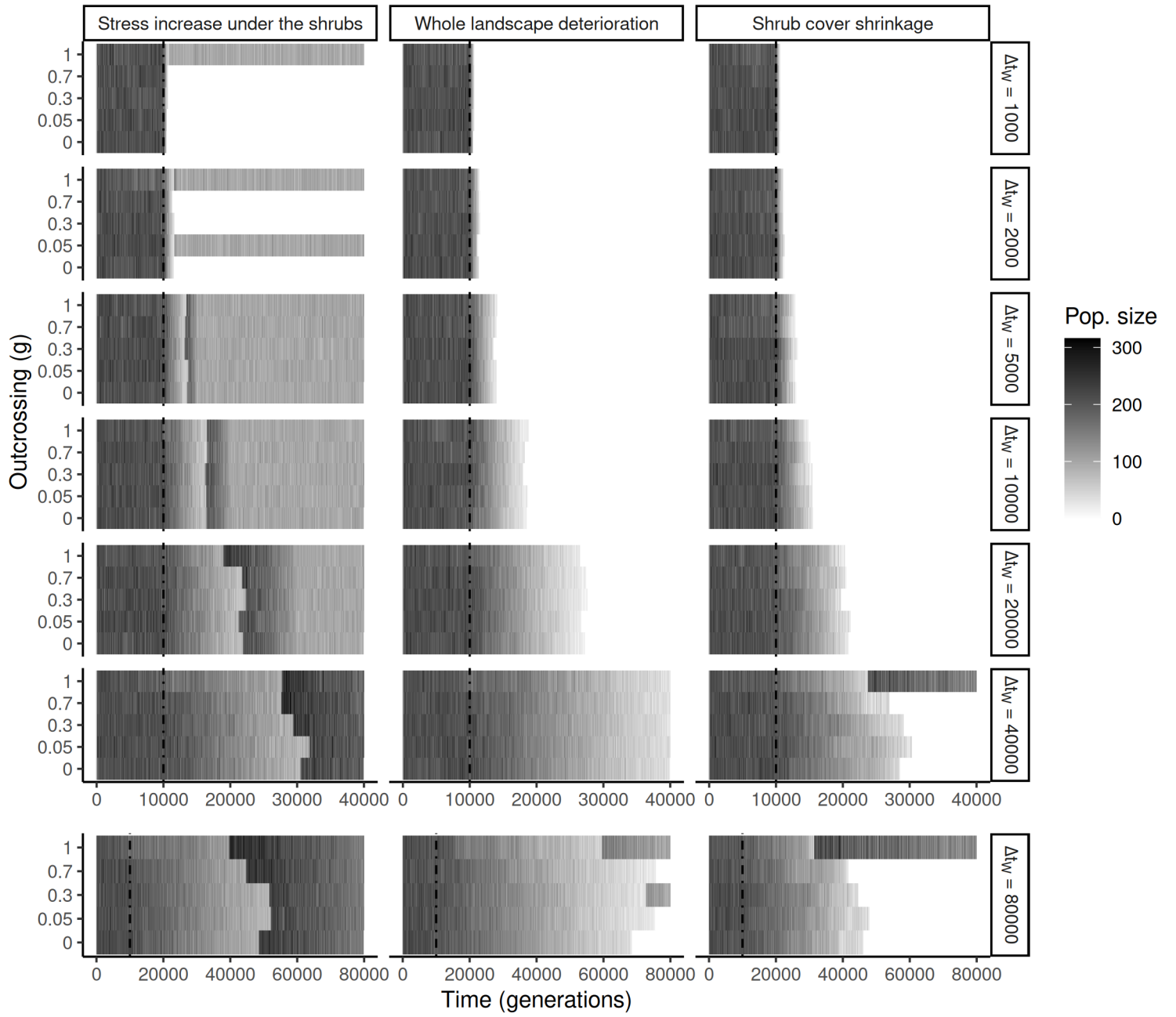


Figure S14: Evolutionary rescue under climate change with outcrossing. Each panel shows the total number of individuals through time in simulations run as per Fig. S8 (same parameters), but with varying rates of outcrossing  $g$ , the probability that a seed is fertilized by a pollen grain (see Methods). Simulations with  $g = 0$  (pure selfing) are those shown in Fig. S8. Vertical dashed lines show the time at which climate starts to change, and blank tiles mean that the population went extinct. Note the difference in time scale between the last row and the rest.

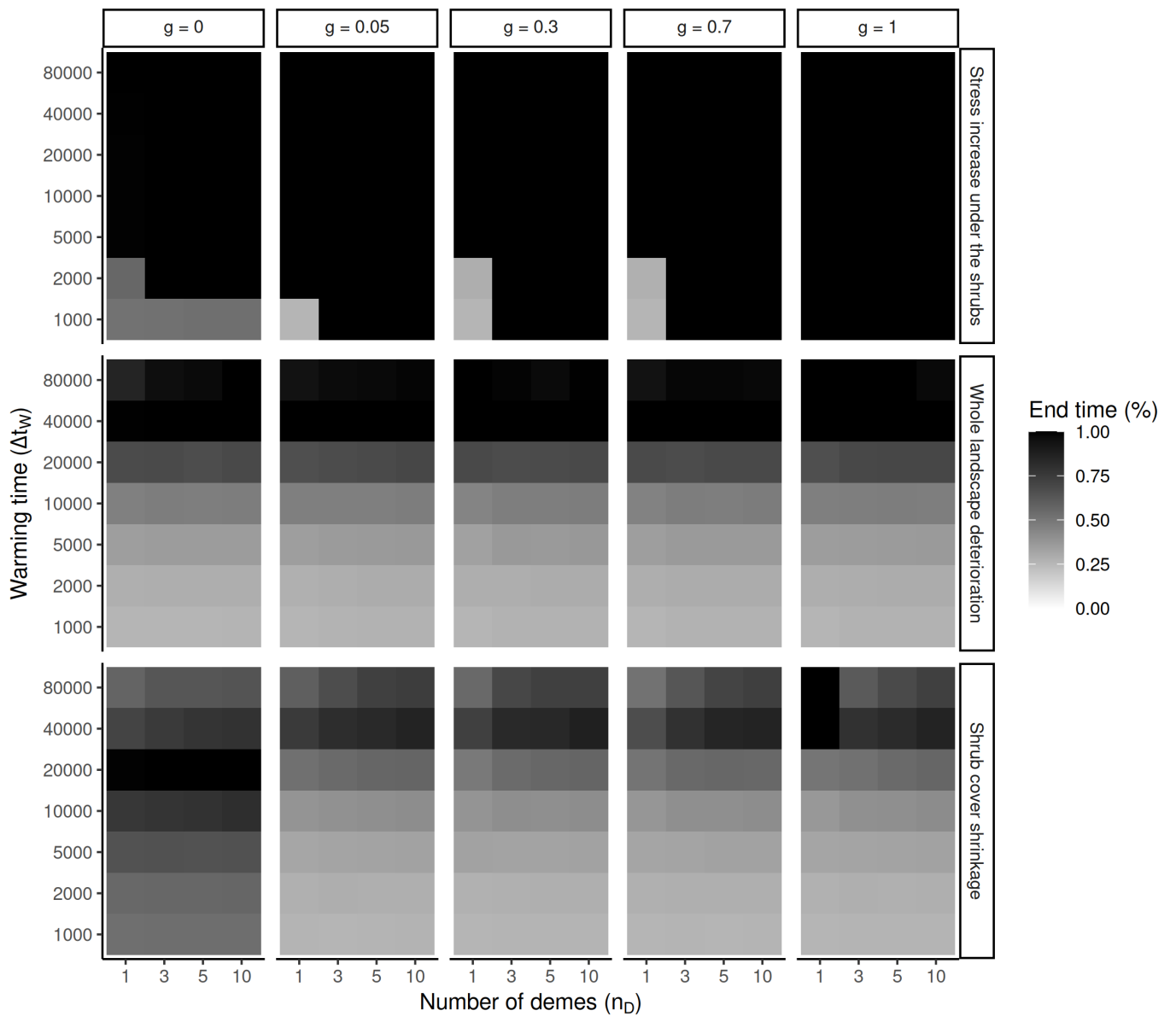


Figure S15: Effect of metapopulation size on evolutionary rescue. The simulations are essentially the same as in Figure S14, but have been extended to different numbers of demes  $n_D$ . Here, end time refers to the proportion of the total allocated time reached by the population (a value of 1 meaning that the population survived all the way to the end).

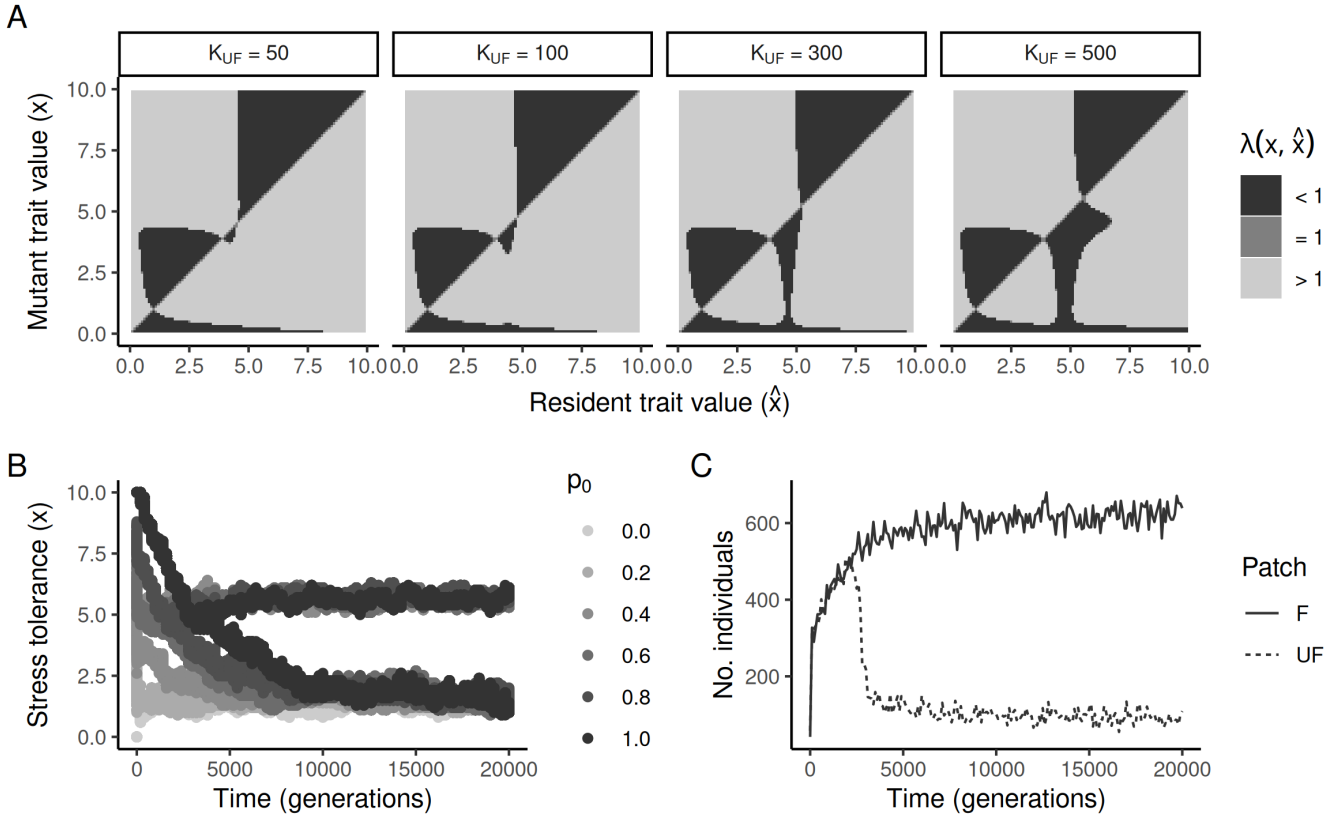


Figure S16: Branching of two stress tolerance strategies in sympatry. Under certain conditions (e.g. unfacilitated patches being particularly inhospitable and having a low carrying capacity  $K_{UF}$ ), a population starting off with a high stress tolerance can split into two groups of individuals — one group maintaining a stress-tolerant strategy and the other evolving a stress-sensitive strategy. (A) Predicted adaptive dynamics across values of the carrying capacity  $K_{UF}$  (all other parameters being as in Fig. 3). Out of the two evolutionary equilibria identified in Fig. 3A, the top one, which is a convergence- and evolutionarily stable strategy (i.e. a continuously stable strategy, CSS) when  $K_{UF}$  is high, turns into a *branching point* (a convergence-stable but evolutionarily unstable strategy) as  $K_{UF}$  goes down ( $K_{UF} \leq 100$ ). (B) Stochastic simulations with  $K_{UF} = 100$  and different starting trait values. The predicted branching occurs in populations starting with a high stress tolerance as they reach the branching point, but not in populations starting with a low stress tolerance ( $p_0 < 0.4$ ), which instead reach the lower, solely stress-sensitive CSS (near  $x \simeq 1$ ). (C) Densities of individuals in the simulation in B with  $p_0 = 1$ , showing a shift in patch occupancy as a stress-sensitive strategy branches off from the stress-tolerant one.

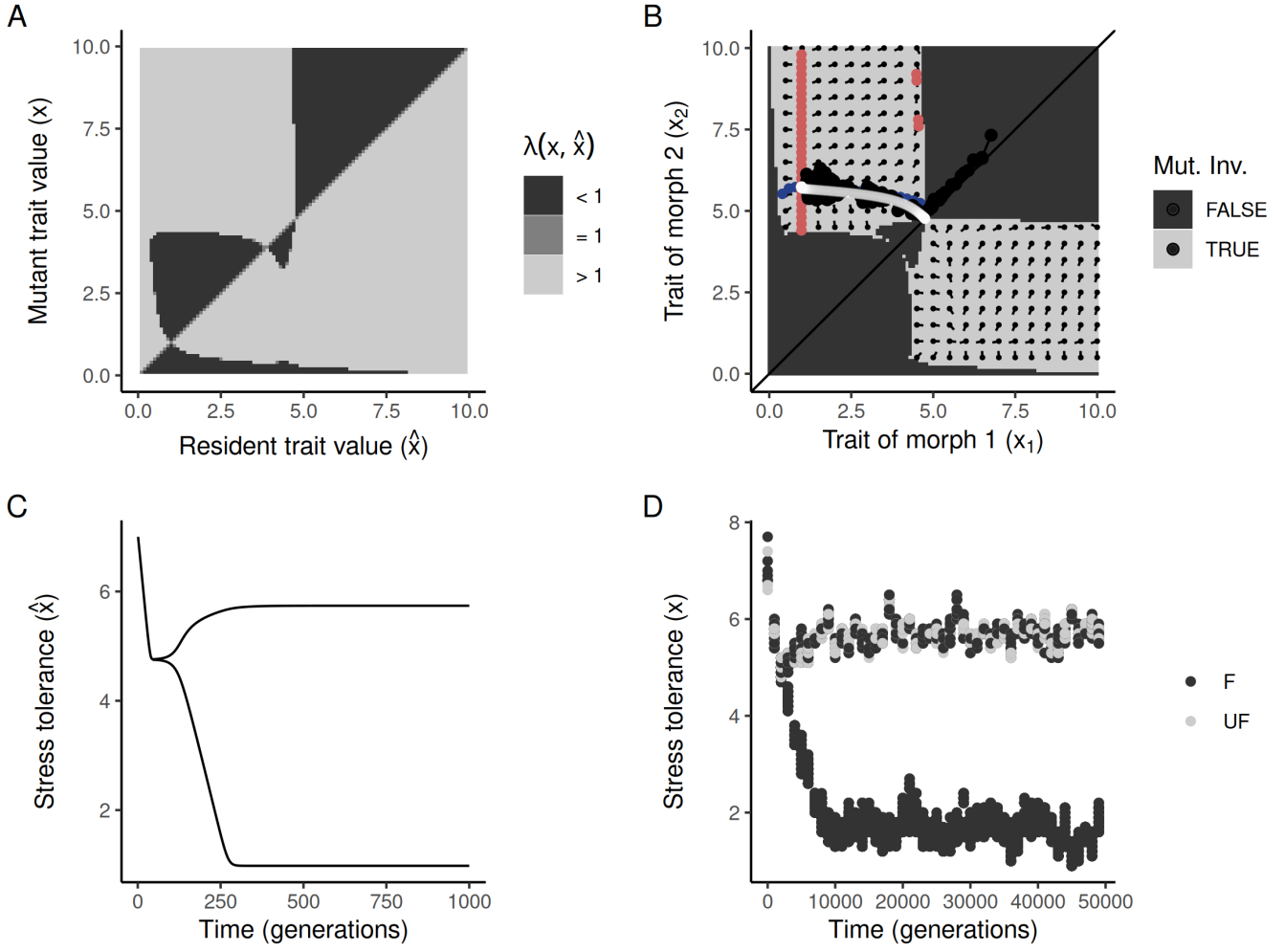


Figure S17: Details of what happens at a branching point in the model. (A) Predicted adaptive dynamics in the case of Figure S16A where  $K_{UF} = 100$ . Under these conditions, the PIP shows a continuously stable strategy (bottom equilibrium strategy near  $x \simeq 1$ ) and a branching point (top equilibrium near  $x \simeq 5$ ), separated by a repellor (see Fig. S1 for the kinds of equilibria possible in adaptive dynamics). (B) By flipping the PIP over its diagonal, we get a mutual invasibility plot (MIP), which shows the predicted adaptive dynamics of the model after the branching point has been reached, with dimorphic fitness isoclines showing in red and blue (see Fig. S2 for details). On top of that, we overlay the trajectories of one particular stochastic simulation (black points) and one particular deterministic simulation (white line), both showing agreement with the predicted adaptive dynamics. (C) Deterministic simulation of evolutionary branching shown in B (see Appendix). (D) Stochastic simulation shown in B. Both simulations are run under the same parameters as panels A and B, albeit with extra parameters  $\mu_x = 0.01$  and  $\sigma_x = 0.5$  proper to the deterministic simulation model, and  $p_0 = 0.7$  and  $g = 0$  proper to the stochastic simulation model (Table 1).

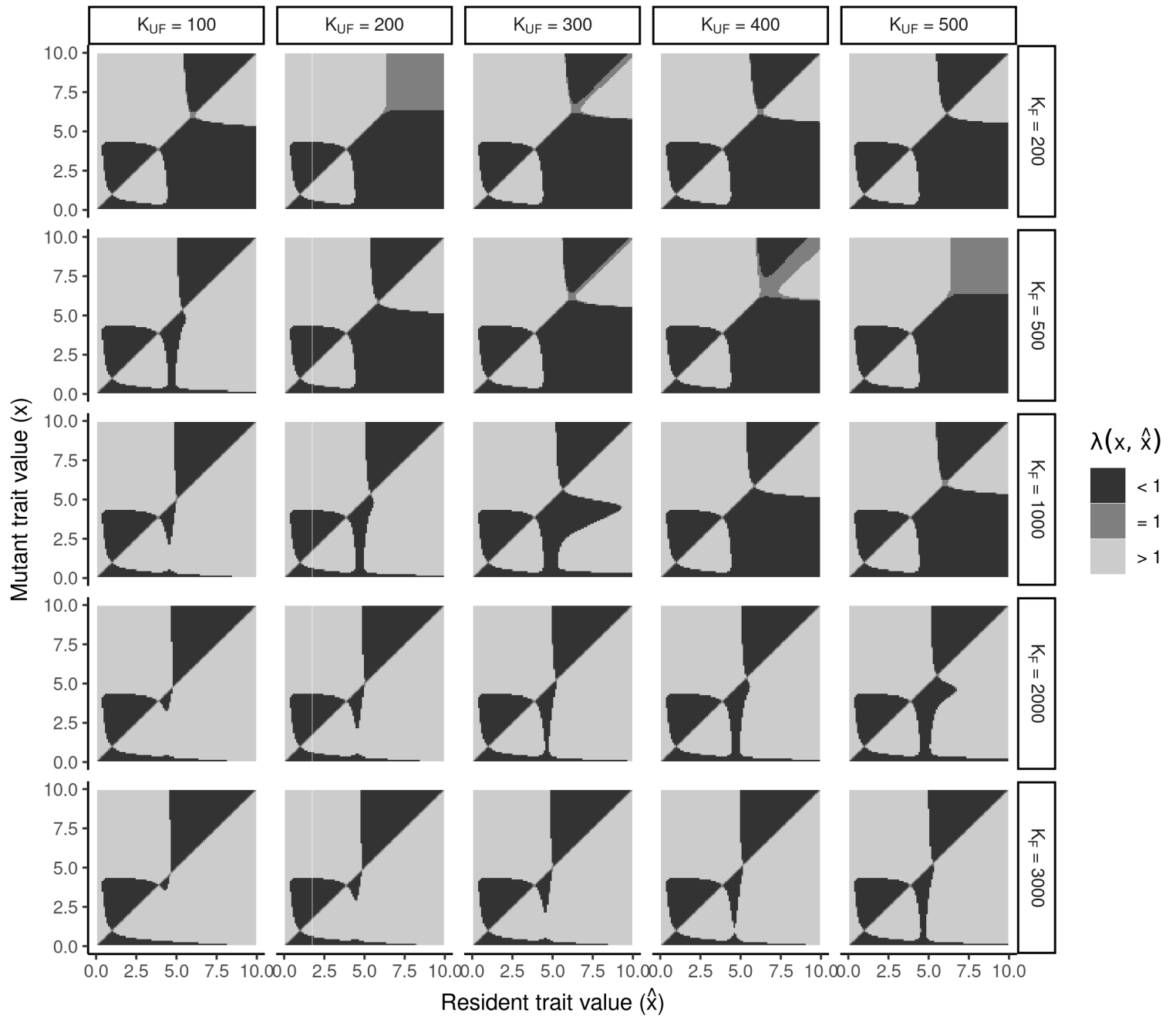


Figure S18: Effects of carrying capacity of the unfacilitated patches  $K_{UF}$ , and of the facilitated patches  $K_F$ , on the adaptive dynamics of the model. Other parameters are as per Fig. 3.

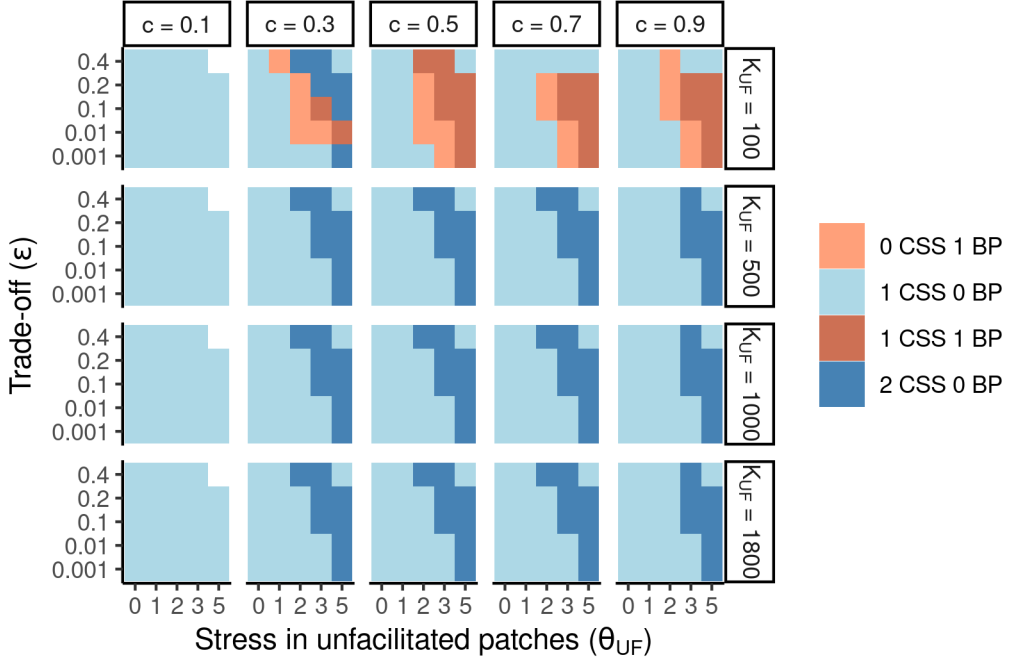


Figure S19: Types of evolutionary equilibria found across parameter space. For each combination of parameters, we used derivations of the invasion fitness function (see Appendix) to compute selection gradients and criteria for evolutionary and convergence stability, which we used to search for evolutionary singularities and evaluate their types (see Fig. S1). In our exploration, we find various combinations of continuously stable strategies (CSS) and branching points (BP) (repellors are not mentioned). Blank tiles indicate that no equilibrium is found. Parameters not mentioned in this figure are as per Fig. 3.

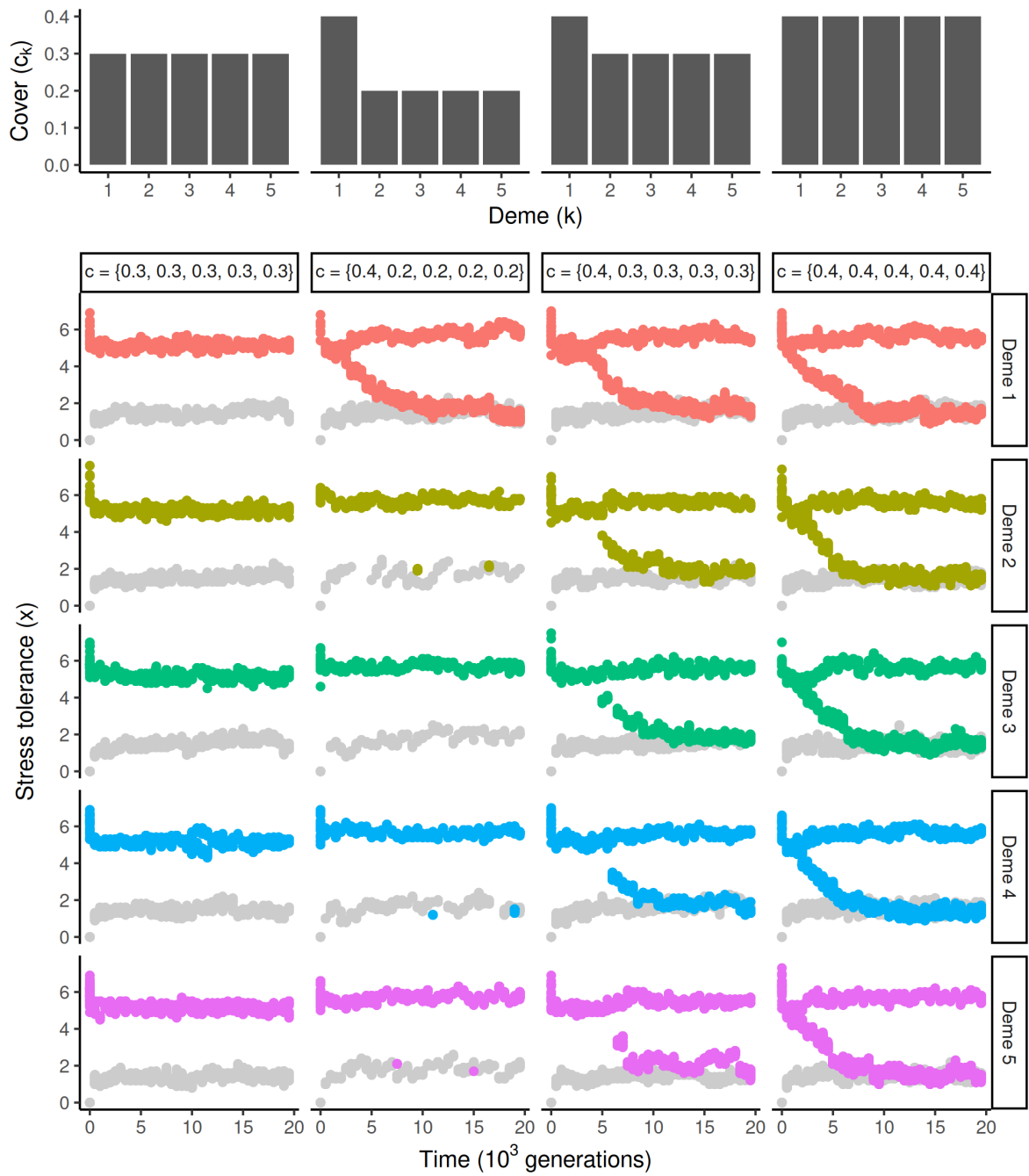


Figure S20: (See next page.)

Figure S20: Coexistence of morphs through secondary contact. In some cases, the stress-tolerant and stress-sensitive strategies can coexist within a deme without having diversified in sympatry (i.e. without the need for a branching point, and as predicted in Fig. S21). To show this, we ran a simulation experiment with five demes ( $n_D = 5$ ), in which two morphs could originate in sympatry in the first deme, but required migration to establish in the other demes. We did so by tuning the shrub cover  $c$  of the different demes (top panel), as we established that a low shrub cover ( $c = 0.2$ ) prevents the establishment of a stress-sensitive strategy, an intermediate shrub cover ( $c = 0.3$ ) allows the stress-sensitive strategy to be viable, and a higher shrub cover ( $c = 0.4$ ) turns the stress-tolerant equilibrium strategy into a branching point (all other parameters being the same as in Fig. 3 except  $K_{UF} = 100$ , see also Fig. S19). We then tested different combinations of shrub covers across the five demes, always starting with a population with an already high stress tolerance (allele frequency  $p_0 = 0.6$ ). The first scenario (column 1) serves as a negative control, where shrub cover ( $c = 0.3$  in all demes) could in theory support stress-sensitive plants, but that equilibrium is not reached because the two equilibrium strategies are exclusive alternative endpoints of the adaptive dynamics, and the stress-tolerant equilibrium is reached instead (e.g. as in Fig. 3). For comparison, we ran simulations under the same conditions but starting with low stress tolerance ( $p_0 = 0$ , gray points in the background) to show that the stress-sensitive equilibrium is reached instead in that case. The second scenario (column 2) allows branching in the first deme ( $c = 0.4$ ) but the stress-sensitive strategy is not viable in the other demes ( $c = 0.2$ ). Hence, we see occasional stress-sensitive migrants appearing in those demes, but never establishing a coexistence with the stress-tolerant plants. Note that in the low-tolerance version of that scenario (gray points) demes 2 to 5 seem more scarcely populated than in other simulations, confirming that they are mostly maintained through migration from deme 1. The third scenario (column 3) allows branching only in the first deme ( $c = 0.4$ ) but allows coexistence of the two morphs in the other demes ( $c = 0.3$ ). After a lag of a few thousand generations, the stress-sensitive strategy eventually colonizes all demes, and both strategies end up coexisting through secondary contact. The last scenario (column 4) serves as a positive control, as shrub cover is high enough ( $c = 0.4$ ) to promote branching in all demes. In that case, the stress-sensitive strategy evolves from the stress-tolerant one multiple times independently (and there is no initial lag). These results confirm the prediction made in Figure S21 that the coexistence of two strategies is promoted by a wider range of conditions than simply those where branching (i.e. divergence in sympatry) occurs.

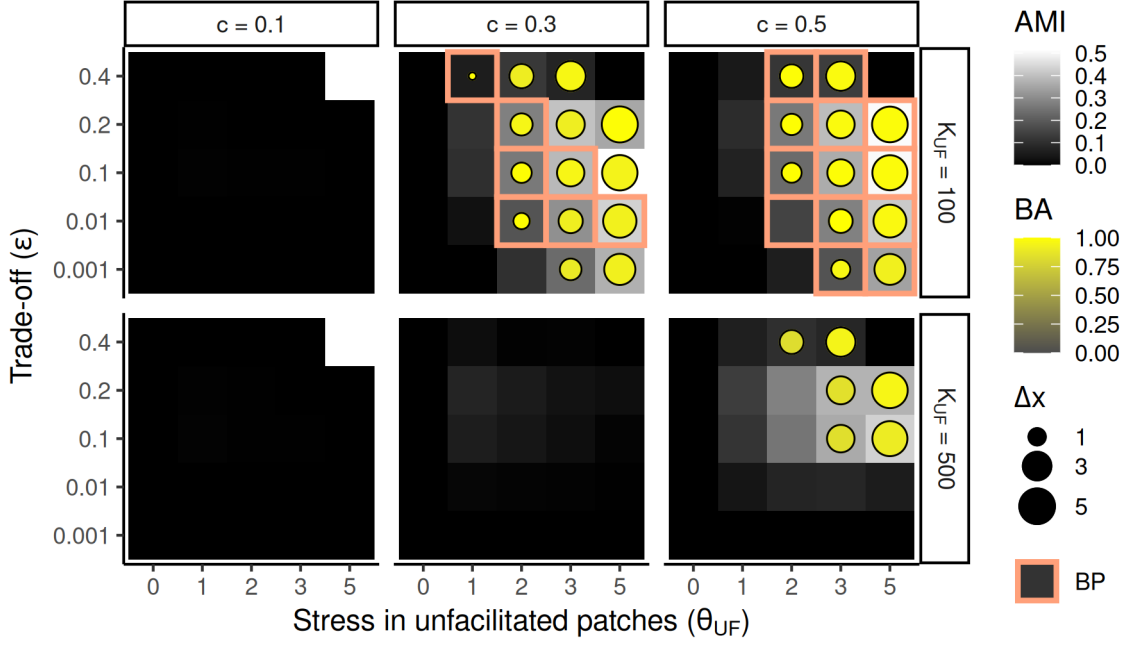


Figure S21: Ability of two morphs to coexist across parameter space. For each combination of parameters, we perform a coexistence analysis as described in Figure S2 (see also Methods). We first determine the *area of mutual invasibility* (AMI), i.e. the proportion of all possible pairs of tolerance strategies, or morphs, that could mutually invade each other in an adaptive dynamics analysis. These are all the pairs of strategies in phenotype space that can in principle coexist, at least on the short term (an AMI of 0 meaning that no coexistence of any two morphs is possible). Following up, we identify stable equilibrium coalitions of morphs, which are pairs of strategies that not only can coexist, but which long-term evolution will also lead to (they are attractors of the dimorphic evolutionary dynamics, see Fig. S2). For each parameter combination where a stable equilibrium coalition is found to exist (circles within tiles), we measure its basin of attraction (BA), the proportion of all pairs of strategies within the AMI that are expected to converge towards that equilibrium coalition during evolution. Tiles where no stable equilibrium coalition is found but still some pairs of strategies are mutually invasible ( $AMI > 0$ ) are cases where coexistence is in theory possible on the short term, but will be lost if morphs are allowed to evolve (as one will end up outcompeting the other). Hence, while the AMI is a proxy for the propensity of the model to allow the coexistence of two morphs on an ecological time scale, given some parameter values, the BA measures how prone selection is to maintain such coexistence over evolutionary time (see Fig. S2 for details about how these metrics are computed). The size of the circles within the tiles indicates the phenotypic distance between the stress tolerance values of the two morphs at the identified equilibrium coalition ( $\Delta x \simeq 5$  being approximately the distance found between the stress-tolerant strategy and the stress-sensitive strategy in Fig. 3A). Finally, orange squares identify parameter combinations where a branching point was found (see Fig. S19), highlighting that branching points are not always needed for transient coexistence ( $AMI > 0$ ) or its long-term maintenance ( $BA > 0$ ) in this model (see Fig. S20). Parameters not mentioned in this figure are as per Fig. 3.

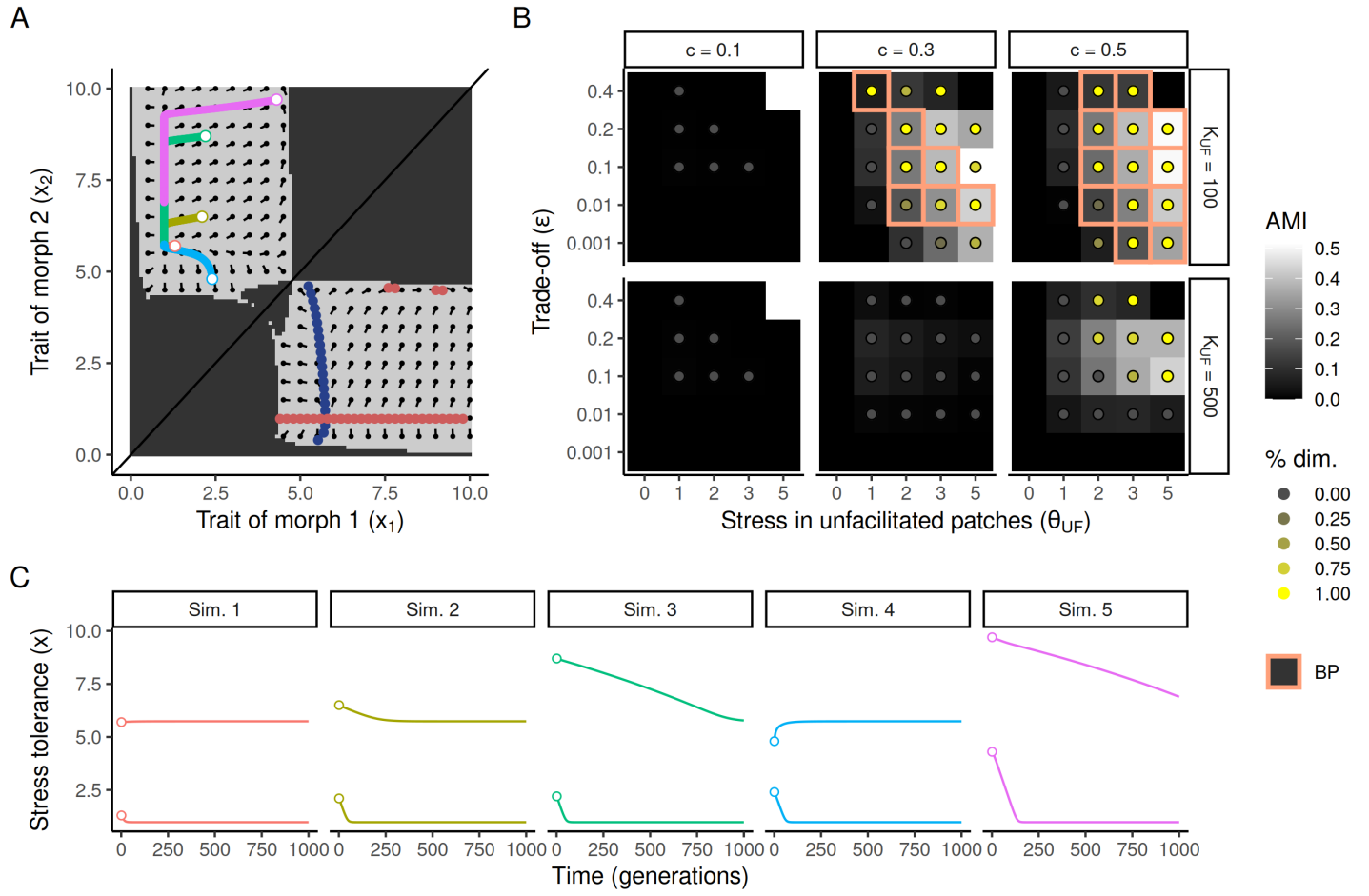


Figure S22: Simulation-based coexistence analysis. In this analysis, we validate the predictions of the adaptive dynamics analysis shown in Fig. S21. (A) For each combination of parameters, we ran five simulations of a deterministic version of our model with two morphs (colored lines above the diagonal, see Appendix for details of the deterministic simulations), starting at randomly sampled points within the area of mutual invasibility (AMI) (white circles within the light gray area, see Fig. S2). The proportion of simulations converging towards a dimorphic, stable equilibrium coalition (such as the crossing between the blue and red isoclines below the diagonal) are shown in B. (B) Results of the analysis, the same as in Fig. S21, but where the potential for coexistence is measured as the proportion of simulations that remained dimorphic rather than using predicted basins of attraction. Simulations that did not remain dimorphic are simulations that went out of the AMI (e.g. into the dark gray zone in A), and one morph outcompeted the other. (C) Trait values of the two morphs in the deterministic simulations shown in A, all converging to the same equilibrium coalition. Parameters specific to the deterministic model:  $\mu_x = 0.01$  and  $\sigma_x = 0.5$ . The mutual invasibility plot (MIP) shown in A is the same as in Fig. S2.

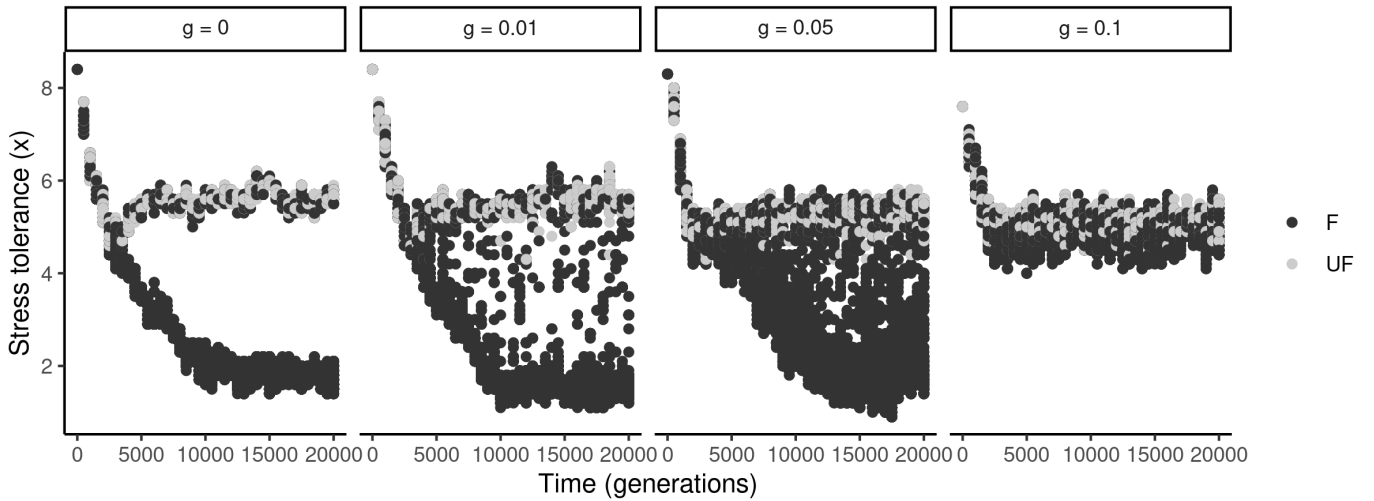


Figure S23: Simulations across levels of outcrossing  $g$ . The parameters were chosen to promote branching of an initially highly tolerant population into a stress-sensitive and a stress-tolerant strategy ( $K_{UF} = 100$ ,  $p_0 = 0.8$ , all other parameters as in Fig. 3). The leftmost panel (pure selfing,  $g = 0$ ) shows that this only holds in the absence of gene flow, as increasing outcrossing even to low levels ( $g$  being the proportion of flowers fecundated by a pollen grain, see Methods) already breaks down diversity and homogenizes the population into one, relatively stress-tolerant, morph.

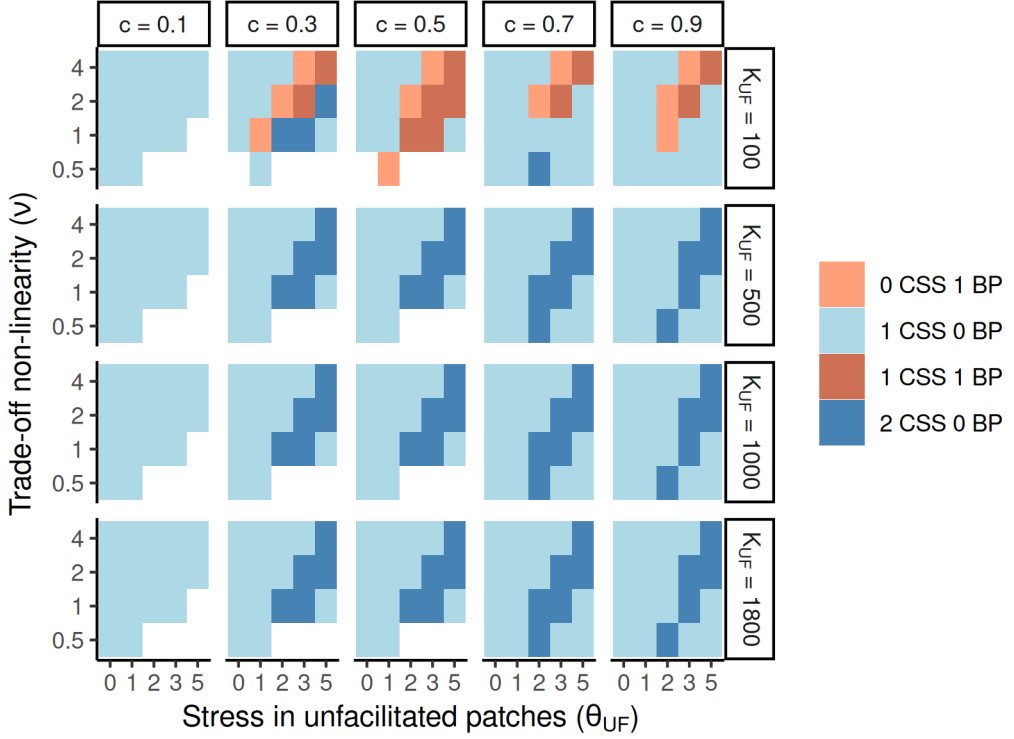


Figure S24: Types of evolutionary equilibria across parameter space when the trade-off between stress tolerance and reproductive output is non-linear. The procedure is the same as in Figure S19, except the trade-off strength parameter is fixed at  $\epsilon = 0.4$ , and the non-linearity parameter  $\nu$  is varied instead (all other parameters as per Fig. 3). The results largely overlap with the linear case (Fig. S19), but note that the image must be flipped to see that, as higher  $\nu$  means a more concave trade-off curve (see Fig. 1C), and so a more shallow decrease in fecundity at low values of stress tolerance (as opposed to higher  $\epsilon$ , which means a steeper decline), and vice versa for lower  $\nu$ .

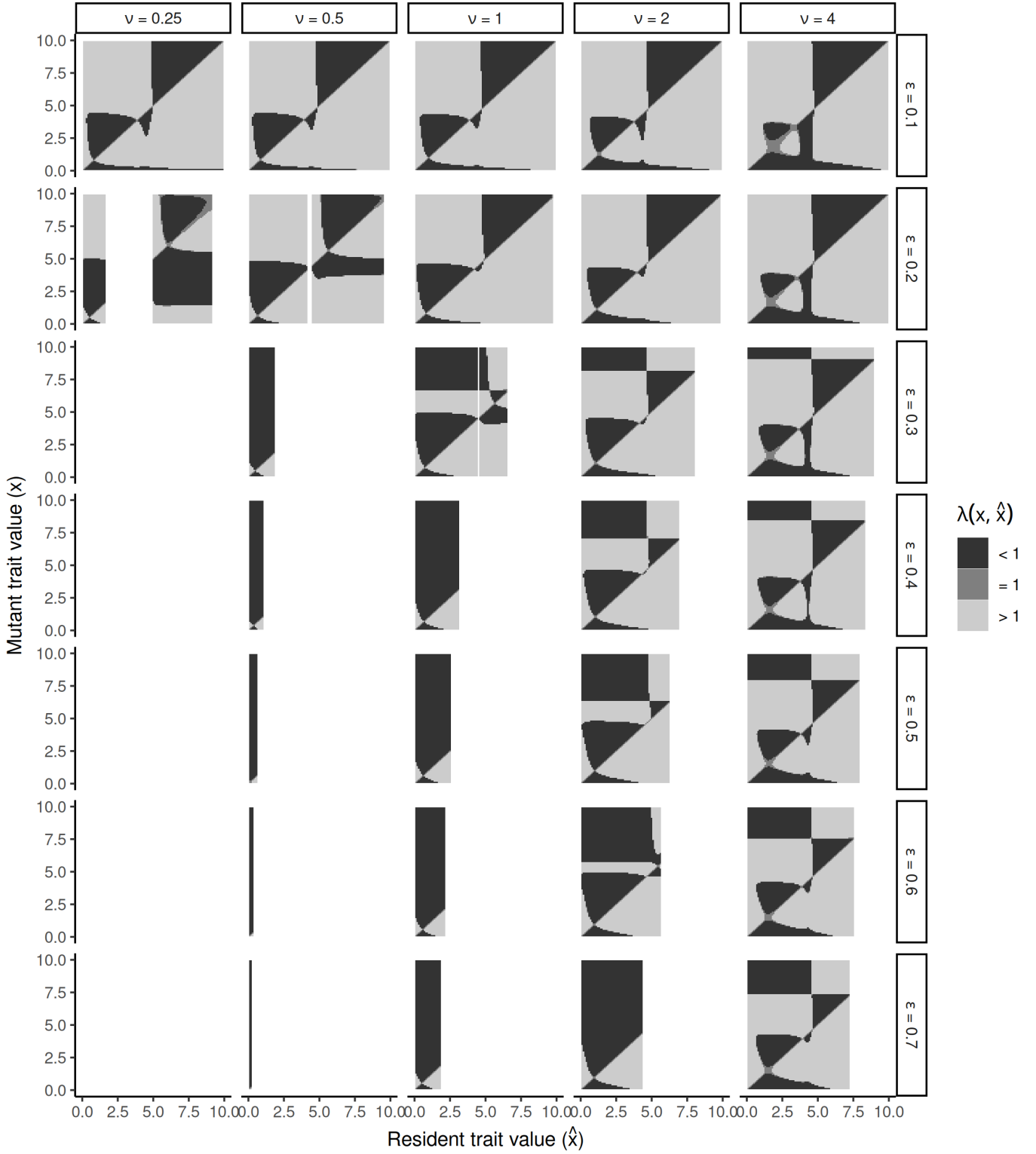


Figure S25: Effects of trade-off non-linearity  $\nu$  and trade-off strength  $\epsilon$  on the adaptive dynamics of the model. Other parameters are as per Fig. 3 (except  $K_{UF} = 100$ ). Note that a higher  $\nu$  (i.e. more concave trade-off) tends to recover the viable trait space that is otherwise lost when  $\epsilon$  increases (i.e. the linear component of the trade-off becomes steeper), by making the decrease in reproductive output with stress tolerance relatively shallow, at least as long as stress tolerance is not too close to its maximum  $x_{\max}$ . In comparison, the effect of  $\nu$  is negligible when the trade-off is weak (e.g.  $\epsilon = 0.1$ ), as the decrease in reproductive output is shallow enough for its convexity or concavity not to matter too much.

685 **Appendix**

686 In this appendix, we go over the approximation model we designed to accompany our stochastic  
 687 simulations (see Methods). We study this deterministic version of the model with adaptive  
 688 dynamics theory, a body of mathematical tools making use of simplifying assumptions (e.g. no  
 689 genetic drift, separation of time scales and monomorphic populations) to get insights into the  
 690 role of selection (in contrast with other factors such as stochasticity or genetic architecture) on  
 691 the evolutionary dynamics of a particular system (Metz et al., 1992; Metz et al., 1996; Geritz  
 692 et al., 1998). The formulas presented here were independently tested using the mathematical  
 693 computing software *Mathematica*, version 12.1 (Wolfram Research, Inc.). Numerical evalua-  
 694 tions of relevant quantities were performed using R 4.3.3 (R Core Team, 2025), with a C++  
 695 backend (integrated into the R environment with Rcpp 1.0.12, Eddelbuettel et al., 2024) for the  
 696 iterative computation of demographic equilibria (see accompanying code).

697 **Demographic model** First, we must determine the demographic dynamics of a rare *mutant*  
 698 with trait value  $x$  (hereafter, the mutant trait value) arising in an otherwise monomorphic  
 699 population of *resident* individuals with trait value  $\hat{x}$  (hereafter, the resident trait value). The  
 700 demographics of the mutant can be described by the deterministic recursion

$$\vec{N}_{t+1} = \boldsymbol{\Lambda}(x, \hat{x}) \vec{N}_t \quad (4)$$

701 where  $\vec{N}_t$  is a vector containing the numbers of mutant individuals in each patch at time  $t$ ,

$$\vec{N}_t = \begin{pmatrix} N_F \\ N_{UF} \end{pmatrix}_t \quad (5)$$

702 (in this simplification we assume only one site,  $n_D = 1$ ), and  $\boldsymbol{\Lambda}$  is a transition matrix from  $t$  to  
 703  $t + 1$ . This transition matrix represents the life cycle of the organism and is given by

$$\boldsymbol{\Lambda}(x, \hat{x}) = \boldsymbol{S}(x) \boldsymbol{M} \boldsymbol{R}(x, \hat{x}) \quad (6)$$

704 where  $\boldsymbol{R}$  is the reproduction matrix,  $\boldsymbol{M}$  is the (between-patch) migration matrix, and  $\boldsymbol{S}$  is the  
 705 survival matrix. These matrices are the steps of the life cycle and are multiplied with the  
 706 population vector  $\vec{N}_t$ , from right to left. Hence, the life cycle starts with the generation of  
 707 seeds, determined by the reproduction matrix,

$$\boldsymbol{R}(x, \hat{x}) = \begin{pmatrix} r_F(x, \hat{x}) & 0 \\ 0 & r_{UF}(x, \hat{x}) \end{pmatrix} \quad (7)$$

708 where  $r_j(x)$  is the reproductive output of an individual from patch  $j$  (F or UF) with trait value  
 709  $x$ , given by

$$r_j(x, \hat{x}) = \exp \left[ y(x) \left( 1 - \frac{\hat{N}_j^*(\hat{x})}{C_j K_j} \right) \right] \quad (8)$$

710 where

$$y(x) = r_{\max} - \epsilon x (x/x_{\max})^{\nu-1}, \quad (9)$$

711 just as in Equations ?? and ?? (see Methods), except that here  $\hat{N}_j^*$  represents the equilibrium  
 712 population density of a resident with trait value  $\hat{x}$  (we assume that the density of mutants  $N_j$   
 713 is negligible). Same as in the stochastic version of our model, we have  $C_F = c$  and  $C_{UF} = 1 - c$ ,  
 714 where  $c$  is the shrub cover in the environment. Other parameters and variables are as explained  
 715 in the Methods.

716

717 Reproduction is followed by dispersal between the (F and UF) patches, according to the  
 718 migration matrix,

$$\mathbf{M} = \begin{pmatrix} c & c \\ 1 - c & 1 - c \end{pmatrix} \quad (10)$$

719 which corresponds to free dispersal of seeds within the site (the seeds join a common pool and  
 720 are then distributed into the two patches proportionally to their relative cover,  $c$  or  $1 - c$ , irre-  
 721 spective of patch of origin).

722

723 Once landed, successful seed germination is determined by the survival matrix,

$$\mathbf{S}(x) = \begin{pmatrix} s_F(x) & 0 \\ 0 & s_{UF}(x) \end{pmatrix} \quad (11)$$

724 where  $s_j(x)$  is the probability of survival of an individual with trait value  $x$  in patch  $j$ , given  
 725 by

$$s_j(x) = \frac{1}{1 + \exp[a(\theta_j - x)]} \quad (12)$$

726 (just like in Eq. ??).

727 **Invasion fitness** Next, we conduct an *invasion analysis* to know whether a given mutant  $x$   
 728 will invade, and replace, its resident competitor  $\hat{x}$ , or disappear, before the next mutant enters  
 729 the scene — adaptive dynamics assumes a separation of time scales between ecological and  
 730 evolutionary processes, such that the demographics reach their equilibrium fast relative to the  
 731 appearance of new mutations. This is done by calculating the so-called *invasion fitness*  $\lambda$  of the  
 732 mutant given the resident. Following Otto and Day (2007), the invasion fitness can be derived  
 733 as the leading eigenvalue of the transition matrix  $\mathbf{A}$  of the mutant, which in this case is

$$\lambda(x, \hat{x}) = c r_F(x, \hat{x}) s_F(x) + (1 - c) r_{UF}(x, \hat{x}) s_{UF}(x). \quad (13)$$

734 The mutant will invade and become the new resident if its invasion fitness is above one ( $\lambda > 1$ ).

735 **Resident equilibrium density** The separation of time scales also means that  $\hat{N}_j^*(\hat{x})$  is the  
 736 equilibrium population density reached by the resident population before the introduction of a

737 new mutant. This equilibrium density must be known in order to compute the invasion fitness.  
 738 It can be found by solving the system of equations

$$\vec{\hat{N}}_t = \mathbf{\Lambda}(\hat{x}, \hat{x}) \vec{\hat{N}}_t, \quad (14)$$

739 that is, finding the steady state at which the density of the resident no longer changes through  
 740 ecological time. However, because  $\mathbf{\Lambda}(\hat{x}, \hat{x})$  is not independent of  $\hat{N}_F$  and  $\hat{N}_{UF}$  (the components  
 741 of  $\vec{\hat{N}}$ ), we did not find this solution analytically. Instead, we computed the equilibrium density  
 742 vector using long-term iteration of the demographic dynamics, starting with low initial densities  
 743 (see accompanying code for details).

744

745 Once the invasion fitness computed, it can be used to visualize which mutant strategies can  
 746 invade which resident ones. Such graphical representations, called *pairwise invasibility plots*, can  
 747 help identify evolutionary steady states, or *singularities*, which in some cases are the predicted  
 748 endpoints of evolution through successive invasions (see Fig. S1).

749 **Selection gradient** It is also possible to derive a *selection gradient* from the invasion fitness  
 750 function. The selection gradient represents the direction and magnitude of selection operating  
 751 on the evolving trait during evolution through successive invasions. This means that evolu-  
 752 tionary singularities are resident strategies where the selection gradient is zero — solving this  
 753 equation can therefore help find singularities without having to calculate invasion fitness for  
 754 thousands of mutant-resident pairs. The selection gradient can also be used to run evolutionary  
 755 simulations according to the deterministic version of the model, and compare them to stochastic  
 756 individual-based simulations.

757

758 Mathematically, the selection gradient  $G(\hat{x})$  is the derivative of the invasion fitness  $\lambda$  with  
 759 respect to the mutant trait value  $x$ , evaluated at the resident strategy  $\hat{x}$  (i.e. when the mutant  
 760 has the same trait value as the resident,  $x = \hat{x}$ ). For our model, this corresponds to

$$G(\hat{x}) = \frac{\partial \lambda}{\partial x} \Big|_{x=\hat{x}} = c \left( \hat{r}'_F(\hat{x}) s_F(\hat{x}) + \hat{r}_F(\hat{x}) \hat{s}'_F(\hat{x}) \right) + (1 - c) \left( \hat{r}'_{UF}(\hat{x}) s_{UF}(\hat{x}) + \hat{r}_{UF}(\hat{x}) \hat{s}'_{UF}(\hat{x}) \right) \quad (15)$$

761 where  $\hat{r}_j(\hat{x}) = r_j(\hat{x}, \hat{x})$ ,  $\hat{r}'_j(\hat{x}) = \partial r_j / \partial x|_{x=\hat{x}}$  and  $\hat{s}'_j(\hat{x}) = \partial s_j / \partial x|_{x=\hat{x}}$ , with

$$\frac{\partial s_j}{\partial x} = a s_j(x) (1 - s_j(x)) \quad (16)$$

762 and

$$\frac{\partial r_j}{\partial x} = \left( 1 - \frac{N_j^*(\hat{x})}{C_j K_j} \right) \frac{\partial y}{\partial x} r_j(x, \hat{x}) \quad (17)$$

763 where

$$\frac{\partial y}{\partial x} = -\epsilon \nu x_{\max}^{1-\nu} x^{\nu-1}. \quad (18)$$

764 **Numerical simulations** Because the selection gradient  $G(\hat{x})$  is a function of the resident  
765 trait  $\hat{x}$  and not of the mutant trait  $x$  anymore, we can use it to simulate the expected change in  
766 resident trait value through evolutionary time given some parameter values, without explicitly  
767 modeling the mutants. In our deterministic evolutionary simulations, the change in trait from  
768 one (evolutionary) time point to the next is given by

$$\hat{x}_{t+1} = \hat{x}_t + 1/2 N_t \mu_x \sigma_x^2 G(\hat{x}_t) \quad (19)$$

769 where  $N_t$  is the total population size at time  $t$ ,  $\mu_x$  is the trait-wide mutation rate of trait  $x$  (as  
770 opposed to a locus-specific mutation rate  $\mu$  used in the individual-based model, see Methods)  
771 and  $\sigma_x$  is the mutational standard deviation, which controls the magnitude of phenotypic change  
772 brought about by mutations (see Table ?? for the default values of these parameters). Note that  
773 models studied with adaptive dynamics are phenotypic models, which must assume a simple  
774 genetic basis of traits in order to be mathematically tractable (Metz et al., 1996; Geritz et al.,  
775 1998). Here, the phenotype is assumed to be encoded by a single haploid locus with an infinite  
776 continuum of quantitative alleles, where the phenotypic effects of mutations occurring at rate  
777  $\mu_x$  are normally distributed with standard deviation  $\sigma_x$ .

778 **Evolutionary stability** It is possible to determine the evolutionary stability of a singular  
779 strategy (i.e. whether once reached, no mutants can invade) by studying the sign of the cur-  
780 vature of the invasion fitness function, evaluated at that singular strategy. If the curvature is  
781 negative, the singularity is a fitness ‘peak’ — no mutant in close phenotypic proximity can in-  
782 vade, and the strategy is evolutionarily stable. If the curvature is positive, the singular strategy  
783 is an unstable evolutionary equilibrium.

784

785 The fitness curvature  $F$  at a singularity  $x^*$  is the second derivative of the fitness function  
786 evaluated at that resident strategy, i.e.,

$$F(x^*) = \frac{\partial^2 \lambda}{\partial x^2} \Big|_{x=\hat{x}=x^*} = c \left( \hat{r}_F''(x^*) s_F(x^*) + 2 \hat{r}_F'(x^*) \hat{s}_F'(x^*) + \hat{r}_F(x^*) \hat{s}_F''(x^*) \right) \\ + (1 - c) \left( \hat{r}_{UF}''(x^*) s_{UF}(x^*) + 2 \hat{r}_{UF}'(x^*) \hat{s}_{UF}'(x^*) + r_{UF}(x^*) \hat{s}_{UF}''(x^*) \right) \quad (20)$$

787 where  $\hat{r}_j''(x^*) = \partial^2 r_j / \partial x^2|_{x=x^*}$  and  $\hat{s}_j''(x^*) = \partial^2 s_j / \partial x^2|_{x=x^*}$ , with

$$\frac{\partial^2 s_j}{\partial x^2} = a (1 - 2 s_j(x)) \frac{\partial s_j}{\partial x} \quad (21)$$

788 and

$$\frac{\partial^2 r_j}{\partial x^2} = \epsilon \left( 1 - \frac{\hat{N}_j^*(\hat{x})}{C_j K_j} \right) \left( \frac{\partial y}{\partial x} \frac{\partial r_j}{\partial x} + r_j(x, \hat{x}) \frac{\partial^2 y}{\partial x^2} \right) \quad (22)$$

789 where

$$\frac{\partial y}{\partial x} = -\epsilon \nu x_{\max}^{1-\nu} x^{\nu-1} \quad (23)$$

790 and

$$\frac{\partial^2 y}{\partial x^2} = -\epsilon \nu (\nu - 1) x_{\max}^{1-\nu} x^{\nu-2}. \quad (24)$$

791 **Convergence stability** The convergence stability of a singular strategy, i.e. whether evolution  
 792 leads towards it (independently of whether it is evolutionarily stable once reached, see  
 793 above), can be determined by looking at whether the selection gradient points towards that  
 794 singularity from nearby resident strategies. This is equivalent to studying how the sign of the  
 795 selection gradient  $G(\hat{x})$  changes as the resident strategy  $\hat{x}$  varies and goes through the putative  
 796 equilibrium strategy that the singularity  $x^*$  represents, which is given by the sign of

$$H(x^*) = \left. \frac{\partial G}{\partial \hat{x}} \right|_{\hat{x}=x^*}. \quad (25)$$

797 If  $H$  is negative, the selection gradient is positive for  $\hat{x} < x^*$  and negative for  $\hat{x} > x^*$ , meaning  
 798 that the singular strategy  $x^*$  is a local attractor of the adaptive dynamics — it is convergence  
 799 stable. If  $H$  is positive, selection leads away from  $x^*$ , and  $x^*$  is convergence unstable.

800

801 Because calculating  $H$  involves differentiating  $\hat{N}_j$  with respect to  $\hat{x}$ , we could not find it analytically,  
 802 for the same reason that we had to compute  $\hat{N}_j$  numerically (see section on equilibrium  
 803 resident density above). Instead, we measured  $H$  numerically, by computing the selection gradient  
 804  $G$  on each side of the equilibrium and looking at the sign of the difference (details available  
 805 in the accompanying code).

806 **Dimorphic evolution** Some types of evolutionary singularities are convergence stable but  
 807 evolutionarily unstable. These are called *branching points* (see Fig. S1), and can cause a  
 808 monomorphic population to split into two coevolving morphs, each with their own adaptive  
 809 dynamics. Once such branching happens, the monomorphic model no longer describes the  
 810 dynamics of the system, and must be updated to keep track of the adaptive dynamics of the  
 811 two morphs. In the updated model, each morph  $k$  with mutant trait value  $x_k$  and resident trait  
 812 values  $\hat{x}_k$  and  $\hat{x}_l$  ( $l$  referring to the other morph) has its own transition matrix  $\mathbf{\Lambda}_{\text{dim}}(x_k, \hat{x}_k, \hat{x}_l) =$   
 813  $\mathbf{S}(x_k) \mathbf{M} \mathbf{R}_{\text{dim}}(x_k, \hat{x}_k, \hat{x}_l)$ , where the migration matrix  $\mathbf{M}$  and the survival matrix  $\mathbf{S}$  have not  
 814 changed, but where the (dimorphic) reproduction matrix is now

$$\mathbf{R}_{\text{dim}}(x_k, \hat{x}_k, \hat{x}_l) = \begin{pmatrix} r_{\text{F}}^{\text{dim}}(x_k, \hat{x}_k, \hat{x}_l) & 0 \\ 0 & r_{\text{F}}^{\text{dim}}(x_k, \hat{x}_k, \hat{x}_l) \end{pmatrix} \quad (26)$$

815 where

$$r_j^{\text{dim}}(x_k, \hat{x}_k, \hat{x}_l) = \exp \left[ y(x_k) \left( 1 - \frac{\hat{N}_{jk}^*(\hat{x}_k, \hat{x}_l) + \hat{N}_{jl}^*(\hat{x}_k, \hat{x}_l)}{C_j K_j} \right) \right] \quad (27)$$

816 where

$$y = r_{\max} - \epsilon x \left( x/x_{\max} \right)^{\nu-1} \quad (28)$$

817 where  $\hat{N}_{jk}^*(\hat{x}_k, \hat{x}_l) + \hat{N}_{jl}^*(\hat{x}_k, \hat{x}_l)$  symbolizes the fact that any individual experiences density de-  
818 pendence from both morphs in its local patch  $j$ .

819

820 The invasion fitness of a mutant is now given by

$$\lambda_{\text{dim}}(x_k, \hat{x}_k, \hat{x}_l) = c r_F^{\text{dim}}(x_k, \hat{x}_k, \hat{x}_l) s_F(x_k) + (1 - c) r_{UF}^{\text{dim}}(x_k, \hat{x}_k, \hat{x}_l) s_{UF}(x_k) \quad (29)$$

821 and the morph-specific selection gradient (obtained, for each morph  $k$ , by differentiating the  
822 invasion fitness while keeping the other morph constant) becomes

$$G_k(\hat{x}_k, \hat{x}_l) = \frac{\partial \lambda_k}{\partial x_k} \Big|_{x_k=\hat{x}_k} = c \left( \hat{r}_F^{\text{dim}}(\hat{x}_k, \hat{x}_l) s_F(\hat{x}_k) + \hat{r}_{UF}^{\text{dim}}(\hat{x}_k, \hat{x}_l) \hat{s}_F'(\hat{x}_k) \right) + (1 - c) \left( \hat{r}_{UF}^{\text{dim}}(\hat{x}_k, \hat{x}_l) s_{UF}(\hat{x}_k) + \hat{r}_{UF}^{\text{dim}}(\hat{x}_k, \hat{x}_l) \hat{s}_{UF}'(\hat{x}_k) \right) \quad (30)$$

823 where  $\hat{r}_j^{\text{dim}}(\hat{x}_k, \hat{x}_l) = \partial r_j^{\text{dim}} / \partial x_k|_{x_k=\hat{x}_k}$ . The two-dimensional dimorphic selection gradient vec-  
824 tor is then given by

$$\vec{G}_{\text{dim}}(\hat{x}_k, \hat{x}_l) = \begin{pmatrix} G_k(\hat{x}_k, \hat{x}_l) \\ G_l(\hat{x}_l, \hat{x}_k) \end{pmatrix} . \quad (31)$$

## 825 References

826 Adler, P. B., Smull, D., Beard, K. H., Choi, R. T., Furniss, T., Kulmatiski, A., Meiners, J. M.,  
827 Tredennick, A. T., & Veblen, K. E. (2018). Competition and coexistence in plant com-  
828 munities: Intraspecific competition is stronger than interspecific competition. *Ecology*  
829 *Letters*, 21(9), 1319–1329. <https://doi.org/10.1111/ele.13098>

830 Aguilée, R., Raoul, G., Rousset, F., & Ronce, O. (2016). Pollen dispersal slows geographical  
831 range shift and accelerates ecological niche shift under climate change. *Proceedings of*  
832 *the National Academy of Sciences*, 113(39), E5741–E5748. <https://doi.org/10.1073/pnas.1607612113>

833 Aguilera, M. A., Valdivia, N., & Broitman, B. R. (2015). Facilitative effect of a generalist  
834 herbivore on the recovery of a perennial alga: Consequences for persistence at the edge  
835 of their geographic range. *PLOS ONE*, 10(12), e0146069. <https://doi.org/10.1371/journal.pone.0146069>

836 Alfaro, M., Berestycki, H., & Raoul, G. (2017). The effect of climate shift on a species sub-  
837 mitted to dispersion, evolution, growth, and nonlocal competition. *SIAM Journal on*  
838 *Mathematical Analysis*, 49(1), 562–596. <https://doi.org/10.1137/16M1075934>

839 Alleaume-Benharira, M., Pen, I. R., & Ronce, O. (2006). Geographical patterns of adaptation  
840 within a species' range: Interactions between drift and gene flow. *Journal of Evolutionary*  
841 *Biology*, 19(1), 203–215. <https://doi.org/10.1111/j.1420-9101.2005.00976.x>

842 Angert, A. L., Bontrager, M. G., & Ågren, J. (2020). What do we really know about adaptation  
843 at range edges? *Annual Review of Ecology, Evolution, and Systematics*, 51 (Volume 51,  
844 2020), 341–361. <https://doi.org/10.1146/annurev-ecolsys-012120-091002>

845 Arenas, M., Ray, N., Currat, M., & Excoffier, L. (2012). Consequences of range contractions and  
846 range shifts on molecular diversity. *Molecular Biology and Evolution*, 29(1), 207–218.  
847 <https://doi.org/10.1093/molbev/msr187>

848 Armas, C., Pugnaire, F. I., & Sala, O. E. (2008). Patch structure dynamics and mechanisms of  
849 cyclical succession in a Patagonian steppe (Argentina). *Journal of Arid Environments*,  
850 72(9), 1552–1561. <https://doi.org/10.1016/j.jaridenv.2008.03.002>

851 Armas, C., & Pugnaire, F. I. (2005). Plant interactions govern population dynamics in a semi-  
852 arid plant community. *Journal of Ecology*, 93(5), 978–989. <https://doi.org/10.1111/j.1365-2745.2005.01033.x>

853 Armas, C., Rodríguez-Echeverría, S., & Pugnaire, F. I. (2011). A field test of the stress-gradient  
854 hypothesis along an aridity gradient. *Journal of Vegetation Science*, 22(5), 818–827.  
855 <https://doi.org/10.1111/j.1654-1103.2011.01301.x>

856 Badyaev, A. V. (2005). Stress-induced variation in evolution: From behavioural plasticity to  
857 genetic assimilation. *Proceedings of the Royal Society B: Biological Sciences*, 272(1566),  
858 877–886. <https://doi.org/10.1098/rspb.2004.3045>

859 Barton, N. H. (2001). Adaptation at the edge of a species' range. In *Integrating ecology and*  
860 *evolution in a spatial context* (pp. 365–392). Blackwell.

861 Bell, G. (2017). Evolutionary rescue. *Annual Review of Ecology, Evolution, and Systematics*,  
862 48 (Volume 48, 2017), 605–627. <https://doi.org/10.1146/annurev-ecolsys-110316-023011>

866 Bell, G., & Collins, S. (2008). Adaptation, extinction and global change. *Evolutionary Applications*, 1(1), 3–16. <https://doi.org/10.1111/j.1752-4571.2007.00011.x>

867

868 Bertness, M. D., & Callaway, R. (1994). Positive interactions in communities. *Trends in Ecology & Evolution*, 9(5), 191–193.

869

870 Boulding, E. G., & Hay, T. (2001). Genetic and demographic parameters determining population persistence after a discrete change in the environment. *Heredity*, 86(3), 313–324. <https://doi.org/10.1046/j.1365-2540.2001.00829.x>

871

872

873 Bridle, J. R., Polechová, J., Kawata, M., & Butlin, R. K. (2010). Why is adaptation prevented at ecological margins? New insights from individual-based simulations. *Ecology Letters*, 13(4), 485–494. <https://doi.org/10.1111/j.1461-0248.2010.01442.x>

874

875 Bridle, J. R., & Vines, T. H. (2007). Limits to evolution at range margins: When and why does adaptation fail? *Trends in Ecology & Evolution*, 22(3), 140–147. <https://doi.org/10.1016/j.tree.2006.11.002>

876

877

878 Brooker, R. W. (2006). Plant–plant interactions and environmental change. *New Phytologist*, 171(2), 271–284. <https://doi.org/10.1111/j.1469-8137.2006.01752.x>

879

880 Brown, J. S., & Pavlovic, N. B. (1992). Evolution in heterogeneous environments: Effects of migration on habitat specialization. *Evolutionary Ecology*, 6(5), 360–382. <https://doi.org/10.1007/BF02270698>

881

882 Bruno, J. F., Stachowicz, J. J., & Bertness, M. D. (2003). Inclusion of facilitation into ecological theory. *Trends in Ecology & Evolution*, 18(3), 119–125. [https://doi.org/10.1016/S0169-5347\(02\)00045-9](https://doi.org/10.1016/S0169-5347(02)00045-9)

883

884 Bulleri, F. (2009). Facilitation research in marine systems: State of the art, emerging patterns and insights for future developments. *Journal of Ecology*, 97(6), 1121–1130. <https://doi.org/10.1111/j.1365-2745.2009.01567.x>

885

886 Bürger, R., & Lynch, M. (1995). Evolution and extinction in a changing environment: A quantitative-genetic analysis. *Evolution*, 49(1), 151–163. <https://doi.org/10.1111/j.1558-5646.1995.tb05967.x>

887

888 Callaway, R. M. (2007a). Interaction between competition and facilitation. In *Positive interactions and interdependence in plant communities* (pp. 179–254). Springer.

889

890 Callaway, R. M. (2007b). *Positive interactions and interdependence in plant communities*. Springer.

891

892 Case, T. J., Holt, R. D., McPeek, M. A., & Keitt, T. H. (2005). The community context of species' borders: Ecological and evolutionary perspectives. *Oikos*, 108(1), 28–46. <https://doi.org/10.1111/j.0030-1299.2005.13148.x>

893

894 Case, T. J., & Taper, M. L. (2000). Interspecific competition, environmental gradients, gene flow, and the coevolution of species' borders. *The American Naturalist*, 155(5), 583–605. <https://doi.org/10.1086/303351>

895

896 Chevin, L.-M., & Lande, R. (2011). Adaptation to marginal habitats by evolution of increased phenotypic plasticity. *Journal of Evolutionary Biology*, 24(7), 1462–1476. <https://doi.org/10.1111/j.1420-9101.2011.02279.x>

897

898

899

900

901

902

903

904

905

906 Chevin, L.-M., & Hoffmann, A. A. (2017). Evolution of phenotypic plasticity in extreme en-  
907 vironments. *Philosophical Transactions of the Royal Society B: Biological Sciences*,  
908 372(1723), 20160138. <https://doi.org/10.1098/rstb.2016.0138>

909 Chevin, L.-M., Lande, R., & Mace, G. M. (2010). Adaptation, plasticity, and extinction in  
910 a changing environment: Towards a predictive theory. *PLOS Biology*, 8(4), e1000357.  
911 <https://doi.org/10.1371/journal.pbio.1000357>

912 Crombach, A., & Hogeweg, P. (2008). Evolution of evolvability in gene regulatory networks  
913 (H. M. Sauro, Ed.). *PLOS Computational Biology*, 4(7), e1000112. <https://doi.org/10.1371/journal.pcbi.1000112>

915 Day, R. L., Laland, K. N., & Odling-Smee, F. J. (2003). Rethinking adaptation: The niche-  
916 construction perspective. *Perspectives in Biology and Medicine*, 46(1), 80–95.

917 de Mazancourt, C., & Dieckmann, U. (2004). Trade-off geometries and frequency-dependent  
918 selection. *The American Naturalist*, 164(6), 765–778. <https://doi.org/10.1086/424762>

919 D'Odorico, P., Bhattachan, A., Davis, K. F., Ravi, S., & Runyan, C. W. (2013). Global de-  
920 sertification: Drivers and feedbacks. *Advances in Water Resources*, 51, 326–344. <https://doi.org/10.1016/j.advwatres.2012.01.013>

922 Duputié, A., Massol, F., Chuine, I., Kirkpatrick, M., & Ronce, O. (2012). How do genetic  
923 correlations affect species range shifts in a changing environment? *Ecology Letters*, 15(3),  
924 251–259. <https://doi.org/10.1111/j.1461-0248.2011.01734.x>

925 Eddelbuettel, D., François, R., Allaire, J., Ushey, K., Kou, Q., Russel, N., Ucar, I., Bates, D.,  
926 & Chambers, J. (2024). Rcpp: Seamless R and C++ integration.

927 Filin, I., Holt, R. D., & Barfield, M. (2008). The relation of density regulation to habitat  
928 specialization, evolution of a species' range, and the dynamics of biological invasions.  
929 *The American Naturalist*, 172(2), 233–247. <https://doi.org/10.1086/589459>

930 Flatt, T. (2005). The evolutionary genetics of canalization. *The Quarterly Review of Biology*,  
931 80(3), 287–316. <https://doi.org/10.1086/432265>

932 Franklin, J., Serra-Diaz, J. M., Syphard, A. D., & Regan, H. M. (2016). Global change and  
933 terrestrial plant community dynamics. *Proceedings of the National Academy of Sciences*,  
934 113(14), 3725–3734. <https://doi.org/10.1073/pnas.1519911113>

935 Gandon, S., & Michalakis, Y. (2002). Local adaptation, evolutionary potential and host–parasite  
936 coevolution: Interactions between migration, mutation, population size and generation  
937 time. *Journal of Evolutionary Biology*, 15(3), 451–462. <https://doi.org/10.1046/j.1420-9101.2002.00402.x>

939 García-Ramos, G., & Huang, Y. (2013). Competition and evolution along environmental gradients:  
940 Patterns, boundaries and sympatric divergence. *Evolutionary Ecology*, 27(3), 489–  
941 504. <https://doi.org/10.1007/s10682-012-9614-y>

942 García-Ramos, G., & Kirkpatrick, M. (1997). Genetic models of adaptation and gene flow in  
943 peripheral populations. *Evolution*, 51(1), 21–28. <https://doi.org/10.1111/j.1558-5646.1997.tb02384.x>

945 Geritz, S. A. H., Kisdi, É., Meszéna, G., & Metz, J. A. J. (1998). Evolutionarily singular  
946 strategies and the adaptive growth and branching of the evolutionary tree. *Evolutionary  
947 Ecology*, 12(1), 35–57. <https://doi.org/10.1023/A:1006554906681>

948 Gibson, G., & Dworkin, I. (2004). Uncovering cryptic genetic variation. *Nature Reviews Genetics*, 5(9), 681–690. <https://doi.org/10.1038/nrg1426>

949

950 Gilbert, K. J., & Whitlock, M. C. (2017). The genetics of adaptation to discrete heterogeneous  
951 environments: Frequent mutation or large-effect alleles can allow range expansion. *Journal  
952 of Evolutionary Biology*, 30(3), 591–602. <https://doi.org/10.1111/jeb.13029>

953 Glémin, S., Ronfort, J., & Bataillon, T. (2003). Patterns of inbreeding depression and architec-  
954 ture of the load in subdivided populations. *Genetics*, 165(4), 2193–2212. <https://doi.org/10.1093/genetics/165.4.2193>

955

956 Gomulkiewicz, R., & Holt, R. D. (1995). When does evolution by natural selection prevent  
957 extinction? *Evolution*, 49(1), 201–207. <https://doi.org/10.1111/j.1558-5646.1995.tb05971.x>

958

959 Gomulkiewicz, R., Holt, R. D., & Barfield, M. (1999). The effects of density dependence and  
960 immigration on local adaptation and niche evolution in a black-hole sink environment.  
961 *Theoretical Population Biology*, 55(3), 283–296. <https://doi.org/10.1006/tpbi.1998.1405>

962 Gomulkiewicz, R., Holt, R. D., Barfield, M., & Nuismer, S. L. (2010). Genetics, adaptation,  
963 and invasion in harsh environments. *Evolutionary Applications*, 3(2), 97–108. <https://doi.org/10.1111/j.1752-4571.2009.00117.x>

964

965 Gomulkiewicz, R., & Houle, D. (2009). Demographic and genetic constraints on evolution. *The  
966 American Naturalist*, 174(6), E218–E229. <https://doi.org/10.1086/645086>

967 Gonzalez, A., Ronce, O., Ferriere, R., & Hochberg, M. E. (2013). Evolutionary rescue: An emerg-  
968 ing focus at the intersection between ecology and evolution. *Philosophical Transactions of the Royal Society B: Biological Sciences*, 368(1610), 20120404. <https://doi.org/10.1098/rstb.2012.0404>

969

970

971 Hampe, A., & Jump, A. S. (2011). Climate relicts: Past, present, future. *Annual Review of  
972 Ecology, Evolution, and Systematics*, 42(Volume 42, 2011), 313–333. <https://doi.org/10.1146/annurev-ecolsys-102710-145015>

972

973

974 Hannah, L., Flint, L., Syphard, A. D., Moritz, M. A., Buckley, L. B., & McCullough, I. M.  
975 (2014). Fine-grain modeling of species' response to climate change: Holdouts, stepping-  
976 stones, and microrefugia. *Trends in Ecology & Evolution*, 29(7), 390–397. <https://doi.org/10.1016/j.tree.2014.04.006>

977

978 Hendry, A. P. (2017). *Eco-evolutionary dynamics*. Princeton University Press.

979 Holt, R. D., Gomulkiewicz, R., & Barfield, M. (2003). The phenomenology of niche evolution via  
980 quantitative traits in a 'black-hole' sink. *Proceedings of the Royal Society B: Biological  
981 Sciences*, 270(1511), 215–224. <https://doi.org/10.1098/rspb.2002.2219>

982 Holt, R. D. (1985). Population dynamics in two-patch environments: Some anomalous conse-  
983 quences of an optimal habitat distribution. *Theoretical Population Biology*, 28(2), 181–  
984 208. [https://doi.org/10.1016/0040-5809\(85\)90027-9](https://doi.org/10.1016/0040-5809(85)90027-9)

985 Holt, R. D. (1990). The microevolutionary consequences of climate change. *Trends in Ecology  
986 & Evolution*, 5(9), 311–315. [https://doi.org/10.1016/0169-5347\(90\)90088-U](https://doi.org/10.1016/0169-5347(90)90088-U)

987 Holt, R. D. (1996). Demographic constraints in evolution: Towards unifying the evolutionary  
988 theories of senescence and niche conservatism. *Evolutionary Ecology*, 10(1), 1–11. <https://doi.org/10.1007/BF01239342>

989

990 Holt, R. D. (1997). On the evolutionary stability of sink populations. *Evolutionary Ecology*,  
991 11(6), 723–731. <https://doi.org/10.1023/A:1018438403047>

992 Holt, R. D. (2003). On the evolutionary ecology of species' ranges. *Evolutionary Ecology Re-*  
993 *search*, 5(2), 159–178.

994 Holt, R. D., & Barfield, M. (2011). Theoretical perspectives on the statics and dynamics of  
995 species' borders in patchy environments. *The American Naturalist*, 178(S1), S6–S25.  
996 <https://doi.org/10.1086/661784>

997 Holt, R. D., & Gaines, M. S. (1992). Analysis of adaptation in heterogeneous landscapes: Im-  
998 plications for the evolution of fundamental niches. *Evolutionary Ecology*, 6(5), 433–447.  
999 <https://doi.org/10.1007/BF02270702>

1000 Holt, R. D., Keitt, T. H., Lewis, M. A., Maurer, B. A., & Taper, M. L. (2005). Theoretical  
1001 models of species' borders: Single species approaches. *Oikos*, 108(1), 18–27. <https://doi.org/10.1111/j.0030-1299.2005.13147.x>

1003 IPCC. (2014). *Climate change 2014 : Mitigation of climate change. Working group III: Contri-  
1004 bution to the fifth assessment report of the intergovernmental panel on climate change*  
1005 (tech. rep.). New York, NY  
1006 Cambridge University Press.

1007 Kawecki, T. J. (1995). Demography of source—sink populations and the evolution of ecological  
1008 niches. *Evolutionary Ecology*, 9(1), 38–44. <https://doi.org/10.1007/BF01237695>

1009 Kawecki, T. J. (2000). Adaptation to marginal habitats: Contrasting influence of the dispersal  
1010 rate on the fate of alleles with small and large effects. *Proceedings of the Royal Society  
1011 B: Biological Sciences*, 267(1450), 1315–1320. <https://doi.org/10.1098/rspb.2000.1144>

1012 Kawecki, T. J. (2003). Sex-biased dispersal and adaptation to marginal habitats. *The American  
1013 Naturalist*, 162(4), 415–426. <https://doi.org/10.1086/378048>

1014 Kawecki, T. J. (2004). Ecological and evolutionary consequences of source-sink population dy-  
1015 namics. In I. Hanski & O. E. Gaggiotti (Eds.), *Ecology, genetics, and evolution of  
1016 metapopulations* (pp. 387–414). Academic Press. <https://doi.org/10.1016/B978-012323448-3/50018-0>

1018 Kawecki, T. J. (2008). Adaptation to marginal habitats. *Annual Review of Ecology, Evolution,  
1019 and Systematics*, 39, 321–342. <https://doi.org/10.1146/annurev.ecolsys.38.091206.095622>

1021 Kawecki, T. J., & Holt, R. D. (2002). Evolutionary consequences of asymmetric dispersal rates.  
1022 *The American Naturalist*, 160(3), 333–347. <https://doi.org/10.1086/341519>

1023 Kéfi, S., Baalen, M. v., Rietkerk, M., & Loreau, M. (2008). Evolution of local facilitation in arid  
1024 ecosystems. *The American Naturalist*, 172(1), E1–E17. <https://doi.org/10.1086/588066>

1025 Kimbrell, T., & Holt, R. D. (2007). Canalization breakdown and evolution in a source-sink  
1026 system. *The American Naturalist*, 169(3), 370–382. <https://doi.org/10.1086/511314>

1027 Kinnison, M. T., & Hairston, N. G. (2007). Eco-evolutionary conservation biology: Contempo-  
1028 rary evolution and the dynamics of persistence. *Functional Ecology*, 21(3), 444–454.

1029 Kirkpatrick, M., & Barton, N. H. (1997). Evolution of a species' range. *The American Naturalist*,  
1030 150(1), 1–23. <https://doi.org/10.1086/286054>

1031 Korte, M. K. (2024). *The angle of response: Facilitation and its effect on the Brachypodium*  
1032 *distachyon grass complex* (Doctoral dissertation). University of Groningen.

1033 Korte, M. K., Manzaneda, A. J., Martinez, L. M., Patterson, T. A., Etienne, R. S., van de  
1034 Zande, L., & Smit, C. (2025). The effect of local perennial plants on the occurrence and  
1035 traits of the *Brachypodium distachyon* complex along an aridity gradient. *Plant Ecology*,  
1036 226(5), 485–495. <https://doi.org/10.1007/s11258-025-01508-y>

1037 Laland, K., Matthews, B., & Feldman, M. W. (2016). An introduction to niche construction  
1038 theory. *Evolutionary Ecology*, 30(2), 191–202. [https://doi.org/10.1007/s10682-016-9821-z](https://doi.org/10.1007/s10682-016-<br/>1039 9821-z)

1040 Lande, R., & Shannon, S. (1996). The role of genetic variation in adaptation and population  
1041 persistence in a changing environment. *Evolution*, 50(1), 434–437. [https://doi.org/10.1111/j.1558-5646.1996.tb04504.x](https://doi.org/10.<br/>1042 1111/j.1558-5646.1996.tb04504.x)

1043 Ledón-Rettig, C. C., Pfennig, D. W., Chunco, A. J., & Dworkin, I. (2014). Cryptic genetic  
1044 variation in natural populations: A predictive framework. *Integrative and Comparative  
1045 Biology*, 54(5), 783–793. <https://doi.org/10.1093/icb/icu077>

1046 Lenormand, T. (2002). Gene flow and the limits to natural selection. *Trends in Ecology &  
1047 Evolution*, 17(4), 183–189. [https://doi.org/10.1016/S0169-5347\(02\)02497-7](https://doi.org/10.1016/S0169-5347(02)02497-7)

1048 Levins, R. A. (1974). *Evolution in changing environments: Some theoretical explorations* (3.  
1049 printing). Princeton University Press.

1050 Liancourt, P., Choler, P., Gross, N., Thibert-Plante, X., & Tielbörger, K. (2012). How facilita-  
1051 tion may interfere with ecological speciation. *International Journal of Ecology*, 2012(1),  
1052 725487. <https://doi.org/10.1155/2012/725487>

1053 Lopez, S., Rousset, F., Shaw, F. H., Shaw, R. G., & Ronce, O. (2009). Joint effects of inbreeding  
1054 and local adaptation on the evolution of genetic load after fragmentation. *Conservation  
1055 Biology*, 23(6), 1618–1627. <https://doi.org/10.1111/j.1523-1739.2009.01326.x>

1056 Lortie, C. J., Filazzola, A., Westphal, M., & Butterfield, H. S. (2022). Foundation plant species  
1057 provide resilience and microclimatic heterogeneity in drylands. *Scientific Reports*, 12(1),  
1058 18005. <https://doi.org/10.1038/s41598-022-22579-1>

1059 Mellard, J. P., de Mazancourt, C., & Loreau, M. (2015). Evolutionary responses to environmen-  
1060 tal change: Trophic interactions affect adaptation and persistence. *Proceedings of the  
1061 Royal Society B: Biological Sciences*, 282(1805), 20141351. [https://doi.org/10.1098/rspb.2014.1351](https://doi.org/10.1098/<br/>1062 rspb.2014.1351)

1063 Metz, J. A. J., Geritz, S. A. H., Meszena, G., Jacobs, F. J. A., & van Heerwaarden, J. S.  
1064 (1996). Adaptive dynamics: A geometrical study of the consequences of nearly faithful  
1065 reproduction. In S. J. van Strien & S. M. Verduyn Lunel (Eds.), *Stochastic and spatial  
1066 structures of dynamical systems* (pp. 183–231).

1067 Metz, J. A. J., Nisbet, R. M., & Geritz, S. A. H. (1992). How should we define ‘fitness’ for  
1068 general ecological scenarios? *Trends in Ecology & Evolution*, 7(6), 198–202. [https://doi.org/10.1016/0169-5347\(92\)90073-K](https://doi.<br/>1069 org/10.1016/0169-5347(92)90073-K)

1070 Michalet, R., Xiao, S., Touzard, B., Smith, D. S., Cavieres, L. A., Callaway, R. M., & Whitham,  
1071 T. G. (2011). Phenotypic variation in nurse traits and community feedbacks define an

1072 alpine community. *Ecology Letters*, 14(5), 433–443. <https://doi.org/10.1111/j.1461-0248.2011.01605.x>

1073

1074 Nuismer, S. L. (2006). Parasite local adaptation in a geographic mosaic. *Evolution*, 60(1), 24–30. <https://doi.org/10.1111/j.0014-3820.2006.tb01078.x>

1075

1076 Nuismer, S. L., & Kirkpatrick, M. (2003). Gene flow and the coevolution of parasite range. *Evolution*, 57(4), 746–754. <https://doi.org/10.1111/j.0014-3820.2003.tb00286.x>

1077

1078 O'Brien, M. J., Carbonell, E. P., Losapio, G., Schlüter, P. M., & Schöb, C. (2020). Foundation species promote local adaptation and fine-scale distribution of herbaceous plants. *Journal of Ecology*, 109(1), 191–203. <https://doi.org/10.1111/1365-2745.13461>

1079

1080

1081 Orr, H. A., & Unckless, R. L. (2008). Population extinction and the genetics of adaptation. *The American Naturalist*, 172(2), 160–169. <https://doi.org/10.1086/589460>

1082

1083 Otto, S. P., & Day, T. (2007). Evolutionary invasion analysis. In *A biologist's guide to mathematical modeling in ecology and evolution* (pp. 454–512). Princeton University Press.

1084

1085 Paaby, A. B., & Rockman, M. V. (2014). Cryptic genetic variation: Evolution's hidden substrate. *Nature Reviews Genetics*, 15(4), 247–258. <https://doi.org/10.1038/nrg3688>

1086

1087 Pannell, J. R. (2016). Evolution of the mating system in colonizing plants. In *Invasion genetics* (pp. 57–80). <https://doi.org/10.1002/9781119072799.ch4>

1088

1089 Pease, C. M., Lande, R., & Bull, J. J. (1989). A model of population growth, dispersal and evolution in a changing environment. *Ecology*, 70(6), 1657–1664. <https://doi.org/10.2307/1938100>

1090

1091

1092 Polechová, J. (2018). Is the sky the limit? On the expansion threshold of a species' range. *PLOS Biology*, 16(6), e2005372. <https://doi.org/10.1371/journal.pbio.2005372>

1093

1094 Polechová, J., & Barton, N. H. (2015). Limits to adaptation along environmental gradients. *Proceedings of the National Academy of Sciences*, 112(20), 6401–6406. <https://doi.org/10.1073/pnas.1421515112>

1095

1096

1097 Prieto, I., Kikvidze, Z., & Pugnaire, F. I. (2010). Hydraulic lift: Soil processes and transpiration in the Mediterranean leguminous shrub *Retama sphaerocarpa* (L.) Boiss. *Plant and Soil*, 329(1), 447–456. <https://doi.org/10.1007/s11104-009-0170-3>

1098

1099

1100 Proulx, S. R. (2002). Niche shifts and expansion due to sexual selection. *Evolutionary Ecology Research*, 4(3), 351–369.

1101

1102 Pugnaire, F. I., Armas, C., & Maestre, F. T. (2011). Positive plant interactions in the Iberian Southeast: Mechanisms, environmental gradients, and ecosystem function. *Journal of Arid Environments*, 75(12), 1310–1320. <https://doi.org/10.1016/j.jaridenv.2011.01.016>

1103

1104

1105 R Core Team. (2025). R: A language and environment for statistical computing.

1106

1107 Raath-Krüger, M. J., Schöb, C., McGeoch, M. A., & le Roux, P. C. (2021). Interspecific facilitation mediates the outcome of intraspecific interactions across an elevational gradient. *Ecology*, 102(1), e03200. <https://doi.org/10.1002/ecy.3200>

1108

1109 Richardson, J. L., Urban, M. C., Bolnick, D. I., & Skelly, D. K. (2014). Microgeographic adaptation and the spatial scale of evolution. *Trends in Ecology & Evolution*, 29(3), 165–176. <https://doi.org/10.1016/j.tree.2014.01.002>

1110

1111

1112 Ronce, O. (2007). How does it feel to be like a rolling stone? Ten questions about dispersal  
1113 evolution. *Annual Review of Ecology, Evolution, and Systematics*, 38, 231–253. <https://doi.org/10.1146/annurev.ecolsys.38.091206.095611>

1115 Ronce, O., & Kirkpatrick, M. (2001). When sources become sinks: Migrational meltdown in  
1116 heterogeneous habitats. *Evolution*, 55(8), 1520–1531. <https://doi.org/10.1111/j.0014-3820.2001.tb00672.x>

1118 Sasaki, A., & de Jong, G. (1999). Density dependence and unpredictable selection in a het-  
1119 erogeneous environment: Compromise and polymorphism in the ESS reaction norm.  
1120 *Evolution*, 53(5), 1329–1342. <https://doi.org/10.1111/j.1558-5646.1999.tb05398.x>

1121 Schiffers, K., Schurr, F. M., Travis, J. M. J., Duputié, A., Eckhart, V. M., Lavergne, S., McIn-  
1122 ery, G., Moore, K. A., Pearman, P. B., Thuiller, W., Wüest, R. O., & Holt, R. D.  
1123 (2014). Landscape structure and genetic architecture jointly impact rates of niche evo-  
1124 lution. *Ecography*, 37(12), 1218–1229. <https://doi.org/10.1111/ecog.00768>

1125 Soliveres, S., Eldridge, D. J., Maestre, F. T., Bowker, M. A., Tighe, M., & Escudero, A. (2011).  
1126 Microhabitat amelioration and reduced competition among understorey plants as drivers  
1127 of facilitation across environmental gradients: Towards a unifying framework. *Perspec-  
1128 tives in Plant Ecology, Evolution and Systematics*, 13(4), 247–258. <https://doi.org/10.1016/j.ppees.2011.06.001>

1130 Suggitt, A. J., Wilson, R. J., Isaac, N. J. B., Beale, C. M., Auffret, A. G., August, T., Bennie,  
1131 J. J., Crick, H. Q. P., Duffield, S., Fox, R., Hopkins, J. J., Macgregor, N. A., Morecroft,  
1132 M. D., Walker, K. J., & Maclean, I. M. D. (2018). Extinction risk from climate change  
1133 is reduced by microclimatic buffering. *Nature Climate Change*, 8(8), 713–717. <https://doi.org/10.1038/s41558-018-0231-9>

1135 Tirado, R., & Pugnaire, F. I. (2003). Shrub spatial aggregation and consequences for reproduc-  
1136 tive success. *Oecologia*, 136(2), 296–301. <https://doi.org/10.1007/s00442-003-1264-x>

1137 Tufto, J. (2001). Effects of releasing maladapted individuals: A demographic-evolutionary model.  
1138 *The American Naturalist*, 158(4), 331–340. <https://doi.org/10.1086/321987>

1139 Uecker, H., & Hermisson, J. (2016). The role of recombination in evolutionary rescue. *Genetics*,  
1140 202(2), 721–732. <https://doi.org/10.1534/genetics.115.180299>

1141 Urban, M. C., Scarpa, A., Travis, J. M. J., & Bocedi, G. (2019). Maladapted prey subsidize  
1142 predators and facilitate range expansion. *The American Naturalist*, 194(4), 590–612.  
1143 <https://doi.org/10.1086/704780>

1144 Valiente-Banuet, A., Rumebe, A. V., Verdú, M., & Callaway, R. M. (2006). Modern quaternary  
1145 plant lineages promote diversity through facilitation of ancient tertiary lineages. *Pro-  
1146 ceedings of the National Academy of Sciences*, 103(45), 16812–16817. <https://doi.org/10.1073/pnas.0604933103>

1148 Valiente-Banuet, A., & Verdú, M. (2007). Facilitation can increase the phylogenetic diversity of  
1149 plant communities. *Ecology Letters*, 10(11), 1029–1036. <https://doi.org/10.1111/j.1461-0248.2007.01100.x>

1151 van der Heijden, M. G. A., & Horton, T. R. (2009). Socialism in soil? The importance of  
1152 mycorrhizal fungal networks for facilitation in natural ecosystems. *Journal of Ecology*,  
1153 97(6), 1139–1150. <https://doi.org/10.1111/j.1365-2745.2009.01570.x>

1154 Verdú, M., Gómez, J. M., Valiente-Banuet, A., & Schöb, C. (2021). Facilitation and plant  
1155 phenotypic evolution. *Trends in Plant Science*, 26(9), 913–923. <https://doi.org/10.1016/j.tplants.2021.04.005>

1156

1157 Vicente-Serrano, S. M., Lopez-Moreno, J.-I., Beguería, S., Lorenzo-Lacruz, J., Sanchez-Lorenzo,  
1158 A., García-Ruiz, J. M., Azorin-Molina, C., Morán-Tejeda, E., Revuelto, J., Trigo, R.,  
1159 Coelho, F., & Espejo, F. (2014). Evidence of increasing drought severity caused by  
1160 temperature rise in southern Europe. *Environmental Research Letters*, 9(4), 044001.  
1161 <https://doi.org/10.1088/1748-9326/9/4/044001>

1162 Vogel, J. P., Tuna, M., Budak, H., Huo, N., Gu, Y. Q., & Steinwand, M. A. (2009). Development  
1163 of SSR markers and analysis of diversity in Turkish populations of *Brachypodium*  
1164 *distachyon*. *BMC Plant Biology*, 9(1), 88. <https://doi.org/10.1186/1471-2229-9-88>

1165 Willi, Y., & Hoffmann, A. A. (2009). Demographic factors and genetic variation influence popu-  
1166 lation persistence under environmental change. *Journal of Evolutionary Biology*, 22(1),  
1167 124–133. <https://doi.org/10.1111/j.1420-9101.2008.01631.x>

1168 Wright, I. J., Reich, P. B., Cornelissen, J. H. C., Falster, D. S., Garnier, E., Hikosaka, K.,  
1169 Lamont, B. B., Lee, W., Oleksyn, J., Osada, N., Poorter, H., Villar, R., Warton, D. I.,  
1170 & Westoby, M. (2005). Assessing the generality of global leaf trait relationships. *New  
1171 Phytologist*, 166(2), 485–496. <https://doi.org/10.1111/j.1469-8137.2005.01349.x>